

**PHYTOCHEMICAL STUDY AND BIOLOGICAL ACTIVITIES OF THE
CHEMICAL CONSTITUENTS OF HELICHRYSUM PANDURIFOLIUM
SCHRANK**

BY:

JUSTIN JOHN MOSER

Maser of Applied Science: Chemistry
in Faculty of Applied sciences
at the Cape Peninsula University of Technology

Supervisor: Prof Ahmed Mohammed

Bellville

November 2021

CPUT copyright information

RESEARCH SUBMITTED IN PART FULFILLMENT OF THE REQUIREMENT OF THE
MASTER'S DEGREE AWARD WITHIN THE APPLIED SCIENCES FACULTY AND
DEPARTMENT OF CHEMISTRY WITHIN CPUT.

DECLARATION:

I, Justin John Moser hereby declare that "Phytochemical Study and Biological Activities Of The Chemical Constituents Of *Helichrysum pandurifolium* Schrank" is my original work and to the best my knowledge, that it has not been submitted before for any degree or assessment in any other University, and that all the sources I have used or quoted have been indicated and acknowledged by means of complete references.

DATE: 18/10/2020.....

SIGNED: Justin John Moser.....

ABSTRACT:

The Cape Floral Kingdom in South Africa is one of six recognised floral kingdoms in the world containing one of the largest concentrates of high density endemic plant species. Over 40 % of the world's *Helichrysum* species are found in Southern Africa, many of which have not yet been chemically categorised, and offers a potential resource for new bioactive phytochemicals. *Helichrysum* plays an important role within many of the South African traditions, historically used as medicine by the native amaXhosa and isiZulu communities.

Chemical investigation of *Helichrysum pandurifolium* Schrank resulted in the isolation of four flavonoids (C1-C4). Chemical structures were elucidated based on their spectroscopic data, the compounds were identified as 5-hydroxy-3,7-dimethoxyflavone (C1), 3,5-dihydroxy-6,7,8-trimethoxyflavone (C2), 3',4',7-trihydroxy-3-methoxyflavone (C3) and 5,7-dihydroxy-3-methoxyflavone (C4).

In vitro assays used to determine the antioxidant activities for the isolated compounds as well as the total extract include the Ferric ion reducing antioxidant power (FRAP) and Trolox equivalent absorbance capacity (TEAC) assays. The total phenolic content (TPC) of the total extract was also quantified. Anti-diabetic activities were determined via the *in vitro* inhibition of key digestive enzymes α -glucosidase and α -amylase.

Compounds C2-C4 revealed FRAP total antioxidant capacities of IC₅₀ equal to 272.8 ± 7.1; 1183.6 ± 69.7 and 17.6 ± 2.8 μ mol AAE/g respectively. Compounds C1-C4 measured TEAC antioxidant activities as 246.8 ± 2.9; 799.8 ± 8.6; 952.9 ± 1.5 and 486.6 ± 3.7 μ mol TE/g respectively. Compounds C1-C3 showed α -glucosidase inhibitions of 18.7 ± 2.4; 40.5 ± 11.6 and 3.3 ± 0.4 μ g/mL respectively, where compound C3 was found to have an α -amylase inhibition of 116.2 ± 5.8 μ g/mL. The total phenolic content of the total extract was quantified to be 108.3 ± 18.9 mg GAE/g and resulted in FRAP, TEAC and α -glucosidase inhibition of 248.2 ± 0.1 μ mol AAE/g; 722.4 ± 16.6 μ mol TE/g and 126.5 ± 14.3 μ g/mL respectively.

This is the first report on the isolation and identification of methoxyflavanoids from *H. pandurifolium* and their biological activities. Results suggest that the isolated phytochemicals may be used as a natural source of anti-diabetic medication by reducing the risk of hyperglycaemia and as preventative medication related to various chronic diseases, however further *in-vivo* studies will be required.

Keywords: *Helichrysum*, *H. pandurifolium* Schrank, phytochemical, methoxyflavonoids, biological activity, anti-diabetic, antioxidant, South Africa.

ACKNOWLEDGMENTS:

I would first like to acknowledge my supervisor **Professor Ahmed Mohammed (Ahmed. A. Hussein)**, for without you this research would not be possible. Thank you for enriching my learning experience with intriguing knowledge, allowing me the opportunity to study under your guidance, and above all teaching me the true meaning of hard work and perseverance.

I would secondly like to acknowledge **Dr. Rajan Sharma** for making such a great addition to our laboratories. Thank you for grounding our work group, always making yourself available for myself and my colleagues in the natural product laboratories, and for your tremendous the help in the editing of my thesis.

I would like to share great thanks to **Eloge Lwamba**, for being such an incredible colleague. You have to be one of the most genuine people I have ever met, always helping others, always supporting those around you, and no matter how much pressure you find yourself under, you always make time for anyone and everyone in need. God bless you.

A special thanks must also be awarded to **Dr. Umar M. Badeggi**, whom I cannot express enough gratitude to for keeping my head up during the gruelling hours of laboratory work, often lasting into the early hours of the morning. For those of you who have never experienced the labour-intensive task of separating natural products using column chromatography, let me tell you that such a task is enough to make you constantly rethink your degree. Working alongside Umar provided me with the determination, encouragement and support I needed to complete my research. So, I thank you again.

I must to also acknowledge **Prof Jeanine Marenwick, Dr. Jelili A. Badmus** and **Fanie Rautenbach**, for all their help at the Oxidative Stress Research Centre in the determination of my antioxidant and biological activity studies.

To all of my fellow laboratory colleagues, **Akeem Omolaja Akinfenwa, Aliwa Maelsand, Dr. Ninon G. E. R. Etsassala, Dr. Abubakar Saleh Ibrakaw, Bara`a Jad, Selena Orango Adewinogo, Bongiwé Msebele, Khady (Kadidiatou Ndjoubi Ossamy)**, and **Charnice Mouton, Sulafa Suliman** and **Dr. Enas**. It has been a pleasure working with all of you, thank you for creating with me all the greatest of memories, with which I will carry for the rest of my life.

Thank you **Zandile Mthembu** for being such a great mother to our laboratories, and **Gillian Fennessy-Yon**, for ensuring our laboratories were always equipped with the chemicals and equipment we need to complete our research.

I'd like to also thank **Timothy H. Lesch** (University of the Western Cape) for the field work adventures of harvesting plants for study, and also for your aid regarding GC/MS analysis at UWC.

Thank you to the **CPUT Centre for Postgraduate Studies** for awarding me the **Mauerberger Foundation Scholarship**, and to **Professor Ahmed Mohammed** for your combined financial assistance during my stay at CPUT.

I would also like to express my gratitude to **Professor Nikoletta Báthori**, who ultimately inspired me to persue a career in research from a younger age.

Thank you to all of my closest friends, there are too many to name, and you have all had a significant influence on my life.

Thank you **Amy Beukes** for all the love and support you have given me.

Last but not least, I'd would like to express my gratitude to my family. My uncle, **Tony Chicken**, thank you for the additional financial support when I needed it most, and providing me with the boost of confidence to pursue my Masters. Thanks mom (**Leona Chicken**), for always believing in me, teaching and encouraging me to always do my best. Thank you to my immediate brothers, **Jeremy** and **Matthew Moser**, for being awesome, and to **Thomas Dufour**, for being such a supportive brother to me over the years. To all of my fathers - **Derek Gardner**, **Mark Riordan**, **Theo Moser**, **Olivier Dufour** and of course **Arnold van Der Merwe**, thank you for teaching me the values of life, and I am honoured to have had the opportunity to experience and gain so much perspective from so many different mentors. To my cousins, aunts and uncles, grandparents, nieces and nephews, thank you for all of your positive addition to my life.

I love you all.

DEDICATION:

I wish to dedicate this research to my old friend:

Chad Gillis Webber.

TABLE OF CONTENTS

DECLARATION:.....	II
ABSTRACT:.....	III
ACKNOWLEDGMENTS:.....	IV
DEDICATION:.....	VI
TABLE OF CONTENTS.....	VII
LIST OF ABBREVIATIONS AND ACRONYMS.....	X
LIST OF FIGURES:.....	XII
LIST OF TABLES:.....	XV
LIST OF EQUATIONS:.....	XVII
LIST OF APPENDICES:.....	XVIII
LIST OF ISOLATED COMPOUNDS:.....	XIX
CHAPTER 1 : INTRODUCTION.....	1
1.1 CHAPTER OVERVIEW.....	1
1.2 MEDICINAL PLANTS AND MODERN-DAY MEDICINE.....	1
1.3 THE CAPE FLORAL KINGDOM AND THE HISTORY OF TRADITIONAL MEDICINE IN SOUTH AFRICA.....	2
1.4 SOUTH AFRICAN HELICHRYSUM (IMPEPHO).....	3
1.5 ANTIOXIDANTS AND OXIDATIVE STRESS.....	3
1.5.1 THE AGEING PROCESS.....	4
1.5.2 OXIDATIVE STRESS AND THE INCREASED RISK OF CHRONIC DISEASE.....	4
1.5.3 ANTIOXIDANTS.....	5
1.5.4 THE USE OF NATURAL PRODUCTS AS OXIDATIVE STRESS INHIBITORS.....	5
1.6 DIABETES MELLITUS.....	5
1.6.1 α -AMYLASE.....	7
1.6.2 α -GLUCOSIDASE.....	8
1.6.3 THE USE OF NATURAL PRODUCTS AS SUGAR REGULATORS FOR DIABETICS.....	9
1.7 THESIS STATEMENT.....	9
1.8 RATIONALE OF THE STUDY.....	9
1.9 AIMS & OBJECTIVES OF STUDY.....	10
1.10 RESEARCH QUESTIONS.....	11
1.11 SCOPE AND DELIMITATIONS OF STUDY.....	11
1.12 THESIS CHAPTERS OUTLINES.....	12
CHAPTER 2: LITERATURE REVIEW.....	13
2.1 CHAPTER OVERVIEW.....	13
2.2 THE ASTERACEAE FAMILY (SUNFLOWER FAMILY).....	13

2.3 THE GENUS OF HELICHRYSUM	13
2.4 TRADITIONAL USES OF SOUTH AFRICAN HELICHRYSUM	14
2.5 HELICHRYSUM PANDURIFOLIUM SCHRANK.....	16
2.6 CHEMISTRY OF HELICHRYSUM.....	18
2.6.1 THE GENERAL CHEMISTRY OF HELICHRYSUM	18
2.6.2 FLAVONOIDS	20
2.6.3 THE ANTIOXIDANT ACTIVITY OF HELICHRYSUM	21
2.6.4 ANTIOXIDANT PROPERTIES OF FLAVONOIDS.....	22
2.6.5 ANTI-DIABETIC PROPERTIES OF HELICHRYSUM.....	23
2.6.6 ANTI-DIABETIC PROPERTIES OF FLAVONOIDS.....	24
2.7 CONCLUSION	25
CHAPTER 3: MATERIALS AND METHODS	33
3.1 CHAPTER OVERVIEW.....	33
3.2 COLLECTION AND IDENTIFICATION OF PLANT MATERIAL	33
3.3 GENERAL EXPERIMENTAL PROCEDURES FOR PHYTOCHEMICAL IDENTIFICATION.....	33
3.3.1 REAGENTS AND SOLVENTS.....	33
3.3.2 CHROMATOGRAPHY	33
3.3.2.1 THIN LAYER CHROMATOGRAPHY (TLC).....	34
3.3.2.2 COLUMN CHROMATOGRAPHY	34
3.3.3 SPECTROSCOPY	34
3.3.3.1 NUCLEAR MAGNETIC RESONANCE (NMR) SPECTROSCOPY.....	34
3.3.3.2 GAS CHROMATOGRAPHY/MASS SPECTROSCOPY (GC/MS).....	35
3.3.3.3 ULTRAVIOLET (UV) SPECTROSCOPY	35
3.4 GENERAL EXPERIMENTAL PROCEDURES FOR THE ANTIOXIDANT AND BIOLOGICAL ASSAYS.....	36
3.4.1 REAGENTS AND SOLVENTS.....	36
3.4.2 ANTIOXIDANT ASSAYS.....	36
3.4.2.1 TOTAL POLYPHENOLIC CONTENT DETERMINATION (FOLIN-CIOCALTEU ASSAY).....	36
3.4.2.2 FERRIC-ION REDUCING ANTIOXIDANT POWER (FRAP) ASSAY	37
3.4.2.3 TROLOX EQUIVALENT ABSORBANCE CAPACITY (TEAC) ASSAY.....	37
3.4.3 ANTI-DIABETIC STUDIES.....	38
3.4.3.1 α -GLUCOSIDASE INHIBITION	38
3.4.3.2 α -AMYLASE INHIBITION	39
3.5 STATISTICAL ANALYSIS.....	40
CHAPTER 4: CHEMICAL CHARACTERISATION OF HELICHRYSUM PANDURIFOLIUM AND STRUCTURE ELUCIDATION OF CONSTITUENTS.....	41
4.1 CHAPTER OVERVIEW.....	41
4.2 EXTRACTION AND FRACTIONATION OF TOTAL EXTRACT.....	41

4.3 ISOLATION OF PURE COMPOUNDS	43
4.3.1 ISOLATION OF COMPOUND C1 - COLUMN CHROMATOGRAPHY OF MAIN FRACTION III.....	43
4.3.2 ISOLATION OF COMPOUND C2 - COLUMN CHROMATOGRAPHY OF MAIN FRACTION IV	45
4.3.3 ISOLATION OF COMPOUNDS C3 AND C4 - COLUMN CHROMATOGRAPHY OF MAIN FRACTION VI.....	49
4.4 CHEMICAL EVALUATIONS: RESULTS AND DISCUSSION.....	52
4.4.1 SUMMARY OF THE ISOLATED COMPOUNDS	53
4.4.2 SUMMARY OF SPECTRAL DATA OF ISOLATED FLAVONOIDS	54
4.4.2.1 UV SPECTRUMS OF ISOLATED FLAVONOIDS.....	54
4.4.2.2. NMR SPECTRAL DATA OF ISOLATED COMPOUNDS.....	55
4.5.1 STRUCTURE ELUCIDATION OF COMPOUND C1.....	56
4.5.2 STRUCTURE ELUCIDATION OF COMPOUND C2.....	60
4.5.3 STRUCTURE ELUCIDATION OF COMPOUND C3.....	67
4.5.4 STRUCTURE ELUCIDATION OF COMPOUND C4.....	73
4.6 CONCLUSION	77
CHAPTER 5: BIOLOGICAL CHARACTERIZATION OF HELICHRYSUM PANDURIFOLIUM CONSTITUENTS	78
5.1 CHAPTER OVERVIEW.....	78
5.2 BIOLOGICAL EVALUATIONS: RESULTS AND DISCUSSION.....	78
5.2.1 EVALUATING THE TOTAL POLYPHENOLIC CONTENT OF H. PANDURIFOLIUM (FOLIN-CIOCALTEU ASSAY)...	78
5.2.2 EVALUATING THE FRAP AND TEAC ACTIVITY OF THE ISOLATED COMPOUNDS	79
5.2.3 EVALUATING THE α -GLUCOSIDASE INHIBITION OF ISOLATED COMPOUNDS.....	81
5.2.4 EVALUATING THE α -AMYLASE INHIBITION OF THE ISOLATED COMPOUNDS.....	83
5.3 CONCLUSION	84
CHAPTER 6: GENERAL DISCUSSION, CONCLUSION AND RECOMMENDATIONS.....	85
CONCLUSION	90
RECOMMENDATIONS.....	90
REFERENCES.....	91
APPENDIX.....	103

LIST OF ABBREVIATIONS AND ACRONYMS

^{13}C NMR:	Carbon-13 nuclear magnetic resonance
^1H NMR:	Proton nuclear magnetic resonance
AAE/g:	Ascorbic acid equivalence per gram
CDCl_3 :	Deuterated chloroform
COSY	^1H - ^1H Correlation Spectroscopy (NMR)
COX-1:	Cyclooxygenase-1
COX-2 :	Cyclooxygenase-2
CPUT:	Cape Peninsula University of Technology
DCM:	Dichloromethane
DMSO:	Dimethyl sulfoxide
DPPH:	α,α -diphenyl- β -picrylhydrazyl free radical scavenging assay
EGCG	Epigallocatechingallate
EtOAc:	Ethyl Acetate
EtOH:	Ethanol
FRAP:	Ferric-ion reducing antioxidant power
H_2SO_4 :	Sulphuric acid
HCl:	Hydrochloric acid
HMBC	^1H - ^{13}C Heteronuclear Multiple Bond Correlation (NMR) Spectroscopy
HQSC	^1H - ^{13}C Heteronuclear Single Quantum Coherence (NMR) Spectroscopy
HSV:	Herpes Simplex Virus

HIV:	Human Immunodeficiency Virus
HPLC:	High Performance Liquid Chromatography
IC ₅₀ :	Half maximal inhibitory concentration
KCl:	Potassium chloride
IR:	Infra-Red
MeOH:	Methanol
MS:	Mass Spectrometry
NADH:	Nicotinamide adenine dinucleotide phosphate
NHS:	National Healthcare System
NMR:	Nuclear Magnetic Resonance
ORAC:	Oxygen radical absorbance capacity
ROS:	Reactive oxygen species
SD:	Standard deviation
Spp.:	Species
TE/g:	Trolox equivalent per gram
TEAC:	Trolox equivalent absorbance capacity
TLC:	Thin Layer Chromatography
TPTZ:	2,4,6-Tri(2-pyridyl)-s-triazine
Trolox:	6 -Hydroxyl-2,5,7,8-tetramethylchroman-2-carboxylic acid

LIST OF FIGURES:

Figure 1.1: The role of α -amylase and α -glucosidase in starch digestion and metabolism	8
Figure 2.1: <i>H. Pandurifolium</i>	17
Figure 2.2: Common flavonoid backbone structures	19
Figure 2.3: The flavonoid backbone (flavan) and its numbering system	23
Figure 2.4: Metal chelation of flavonoids	23
Figure 2.5: Flavonoid substitution patterns for increased α -glucosidase activity	25
Figure 2.6: Flavonoid substitution patterns for increased α -amylase activity	25
Figure 4.1: TLC profile of main fractions under UV	43
Figure 4.2: TLC profile of the sub-fractions of main fraction III under UV	45
Figure 4.3: Pure crystals of compound C1	45
Figure 4.4: TLC profile of the sub-fractions of main fraction IV under UV	47
Figure 4.5: Pure crystals of compound C2	47
Figure 4.6: TLC profile of the sub-fraction III-9 after silica gel column chromatography under UV	48
Figure 4.7: TLC profile of the sub-fraction III-9-7/8 after silica gel column chromatography under UV	49
Figure 4.8: TLC profile of the sub-fractions of main fraction VI	50
Figure 4.9: TLC profile of the sub-fractions of VI-18	51
Figure 4.10: Prep TLC plates of subfractions 13-22	52
Figure 4.11: TLC profile of the band 3 after sephadex separation	52
Figure 4.12: Flow diagram summarising the isolation procedure of phytochemicals from <i>H. pandurifolium</i>	53
Figure 4.13: Bands observed in the UV spectrum of flavonoids	54

Figure 4.14: UV spectrums of compound C1 after addition of various reagents	56
Figure 4.15: Structure of 5-hydroxy-3,7-dimethoxyflavone	57
Figure 4.16: ¹ H NMR spectrum of compound C1	57
<i>Figure 4.17: ¹³C spectrum of compound C1</i>	58
<i>Figure 4.18: DEPT spectrum for compound C1</i>	58
Figure 4.19: UV spectrums of compound C2 after addition of various reagents	60
<i>Figure 4.20: Structure of 3,5-dihydroxy-6,7,8-trimethoxyflavone</i>	61
<i>Figure 4.21: ¹H NMR spectrum of compound C2</i>	61
<i>Figure 4.22: ¹³C NMR spectrum for compound C2</i>	62
<i>Figure 4.23: DEPT spectra for compound C2</i>	62
<i>Figure 4.24: COSY spectra for compound C2</i>	63
<i>Figure 4.25: COSY spectra for compound C2 (zoomed)</i>	64
<i>Figure 4.26: HSQC spectrum for compound C2</i>	64
<i>Figure 4.27: HSQC spectrum for compound C2 (zoomed)</i>	65
<i>Figure 4.28: HMBC spectrum for compound C2</i>	65
Figure 4.29: UV spectrums of compound C3 after addition of various reagents	67
<i>Figure 4.30: Structure of 3',4',5,7-tetrahydroxy-3-methoxyflavone</i>	68
<i>Figure 4.31: ¹H NMR peaks for compound C3</i>	68
<i>Figure 4.32: ¹H NMR spectrum of compound C3</i>	69
<i>Figure 4.33: ¹³C NMR spectrum of compound C3</i>	70

Figure 4.34: DEPT spectrum for compound C3	70
Figure 4.35: HSQC spectrum for compound C3	71
Figure 4.36: HMBC spectrum for compound C3	71
Figure 4.37: UV spectrums of compound C4 after addition of various reagents	73
Figure 4.38: Structure of 5,7-dihydroxy-3-methoxyflavone	74
Figure 4.39: ¹ H NMR spectrum of compound C4	74
Figure 4.40: ¹³ C NMR of compound C4	75
Figure 4.41: HSQC spectrum of C4	76
Figure 4.42: HMBC spectrum for compound C4	76
Figure 5.1: Visual comparison of FRAP antioxidant assay results	81
Figure 5.2: Visual comparison of ABTS (TEAC) antioxidant assay results	81
Figure 5.3: Graphical comparison of IC ₅₀ values from α-glucosidase inhibition assay	83
Figure 6.1: Comparison of TPC and FRAP results of <i>H. pandurifolium</i> with other <i>Helichrysum</i> species	89

LIST OF TABLES:

Table 2.1: Reported traditional uses of <i>Helichrysum</i> in South Africa	15
Table 2.2: Antioxidant activities of 16 methanolic <i>Helichrysum</i> extracts	21
Table 2.3: Terpenoids found in <i>Helichrysum</i>	26
Table 2.4: Phloroglucinols and derivatives found in <i>Helichrysum</i>	27
Table 2.5: Coumarins found in <i>Helichrysum</i>	28
Table 2.6: Flavones found in <i>Helichrysum</i>	28
Table 2.7: Flavonols found in <i>Helichrysum</i>	29
Table 2.8: Flavanones found in <i>Helichrysum</i>	30
Table 2.9: Chalcones found in <i>Helichrysum</i>	31
Table 3.1: TLC plate solvent systems	34
Table 4.1: Fractionation of the <i>H. pandurifolium</i> methanol extract	42
Table 4.2: Main fractions from <i>H. pandurifolium</i> total extract	42
Table 4.3: Fractionation of the main fraction III	44
Table 4.4: Sub-fractions obtained from main fraction III	44
Table 4.5: Fractionation of the main fraction IV	46
Table 4.6: Sub-fractions obtained from the main fraction IV	46
Table 4.7: Fractionation of the main fraction VI	49
Table 4.8: Sub-fractions from main fraction VI	50
Table 4.9: UV spectral analysis of pure compounds (λ_{\max} for each band)	54

Table 4.10: NMR spectral data for of pure compounds C1-C4	55
Table 5.1: Total antioxidant capacities of isolated flavonoids and total extract of <i>H. pandurifolium</i>	80
Table 5.2: α -Glucosidase inhibition (IC_{50}) for isolated flavonoids and total extract	81
Table 5.3: α -Amylase inhibition for isolated flavonoids and total extract (IC_{50})	84
Table 6.1: Isolated flavonoids from <i>H. pandurifolium</i>	87
Table 6.2: Summary of biological activities of isolated flavonoids and total extract from <i>H. pandurifolium</i>	87

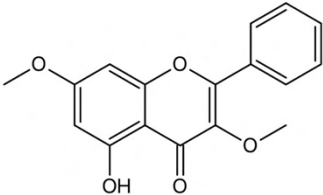
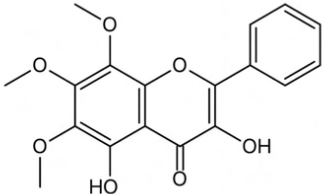
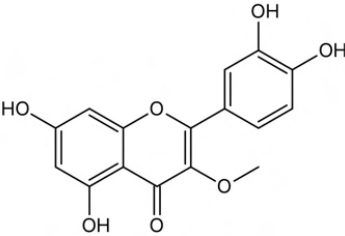
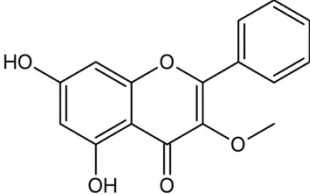
LIST OF EQUATIONS:

Equation 2.1: Hydroxyl radical generation by iron and copper	22
Equation 2.2: Free radical neutralization by flavonoids	22
Equation 3.1: Percent inhibition equation	39
Equation 3.2: General straight-line formula	39
Equation 3.3: Standard deviation formula	39
Equation 5.1: Free radical scavenging mechanism	79

LIST OF APPENDICES:

Appendix 1: Standard calibration curve - Polyphenols (Folin-Ciocalteu assay)	103
Appendix 2: Standard calibration curve - FRAP assay	103
Appendix 3: Standard calibration curve - ABTS (TEAC) assay	103
Appendix 4: α -Glucosidase inhibition curve of C1	104
Appendix 5: α -Glucosidase inhibition curve of C2	104
Appendix 6: α -Glucosidase inhibition curve of C3	104
Appendix 7: α -Glucosidase inhibition curve of C4	104
Appendix 9: α -Glucosidase inhibition curve of total extract	104
Appendix 10: α -Amylase inhibition curve of C2	105
Appendix 11: α -Amylase inhibition curve of C3	105
Appendix 12: α -Amylase inhibition curve of total extract	105

LIST OF ISOLATED COMPOUNDS:

Compound	Compound structure	IUPAC name
C1	 <p>The structure shows a flavone core with a hydroxyl group at position 5, a methoxy group at position 3, and a phenyl ring at position 7.</p>	5-Hydroxy-3,7-dimethoxyflavone
C2	 <p>The structure shows a flavone core with hydroxyl groups at positions 3 and 5, and methoxy groups at positions 6, 7, and 8. A phenyl ring is attached at position 7.</p>	3,5-Dihydroxy-6,7,8-trimethoxyflavone
C3	 <p>The structure shows a flavone core with hydroxyl groups at positions 3, 4, 5, and 7, and a methoxy group at position 3. A 3,4,5-trihydroxyphenyl ring is attached at position 7.</p>	3',4',5,7-Tetrahydroxy-3-methoxyflavone (3-O-Methylquercetin)
C4	 <p>The structure shows a flavone core with hydroxyl groups at positions 5 and 7, and a methoxy group at position 3. A phenyl ring is attached at position 7.</p>	5,7-Dihydroxy-3-methoxyflavone

CHAPTER 1 : INTRODUCTION

“Education is the most powerful weapon which you can use to change the world.”

– Nelson Mandela

1.1 Chapter Overview

In this chapter, a brief overview of the Cape Floral Kingdom and the historical background of traditional medicine in South Africa is described, which is where this investigation was based/completed. South African *Helichrysum* or “Impepho” (isiXhosa) has been used medicinally to treat a multitude of different diseases and disorders, and the chapter discusses the varying species of *Helichrysum* classified under the broad local classification “Impepho”, suggesting that there are many local species of *Helichrysum* that have not yet been chemically investigated. The necessary definitions and explanations of antioxidants and oxidative stress are explained, which includes how natural products have proven to be inhibitors of oxidative stress. An overview of diabetes is then provided followed by the rationale, aims, and objectives of this research study. Finally, the research approach as well as the scope and delimitations in the research process are explained.

1.2 Medicinal Plants and Modern-day Medicine

Medicinal plants provide us with a range of phytochemicals, such as flavonoids, terpenoids, alkaloids, phloroglucinols, glycosides and phenolics in the form of secondary metabolites (Velu et al., 2018). These secondary metabolites possess valuable bioactivities within the human body such as antibacterial, antioxidant, anti-inflammatory, anti-carcinogenic, antitumor, and antimutagenic activities (Jain et al., 2019). Many chemists and biochemists are turning to medicinal plants as a source of new drug discovery which do not possess the many side effects that come with modern-day synthetic drugs but still exhibit equivalent bioactive potency (Maridass & De Britto, 2008). Today, about 80 percent of the world population depends primarily on herbal remedies for their needs, as they do not have access to modern medicine (Bhat, 2014). Furthermore, in 1991, an evidence supported study revealed the importance of natural products when findings showed that almost half of the top-selling pharmaceuticals in the U.S. were either natural products themselves or derivatives of such (Cragg et al., 1997). In more recent times, the formulations of new drugs derived from natural plant sources have

become increasingly popular as many natural products themselves serve as lead compounds to new drug discoveries (Balunas & Kinghorn, 2005).

1.3 The Cape Floral Kingdom and the History of Traditional Medicine in South Africa

The Cape Floral Kingdom is one of six recognised floral kingdoms in the world (Odendaal et al., 2008). Covering an area that stretches from the Western Cape and extends up to the Eastern Cape, the Cape Floral Kingdom is the smallest floral kingdom in the world (Cowling et al., 1996). Although small, the area has one of the largest concentrates of high density endemic species – known as a `biodiversity hotspot` (Cowling et al., 1996). According to Goldblatt and Manning (2002), the kingdom yields over 9,000 vascular plants, of which over 6,000 are endemic (Goldblatt & Manning, 2002). Here, more than 30,000 species of higher plants have been identified, of which about 3, 000 (10%) are used in traditional medicines throughout the country (Van Wyk et al., 1997).

Historically within the South African Cape Floral Kingdom, one of the first major groups of inhabitants was the amaXhosa who settled in the area that later became known as the Eastern Cape (former Transkei). Symbiotically, traditional medicinal practices proliferated in harmony with the flourishing endemic plant life in the richly biodiverse Cape Floral Kingdom region. As such, prior to the introduction and imposition of westernised medicine that accompanied the colonisation of Southern Africa, the amaXhosa relied solely on their traditional knowledge of natural medicinal remedies to treat disease and illness.

In the contemporary context, although modern biomedicine has become the dominant model of medical treatment, a large proportion of people still choose to seek treatment through traditional remedies (Bhat, 2014). What this emphasises is how even in the contemporary, modern, biomedical context, there remains a continued importance and centrality of traditional healing remedies. Put differently, this highlights a kind of naturalised, endemic dependence of traditional medicine in South Africa.

The importance of traditional medicine in South Africa has culminated in the introduction of many new laws and regulations. This began in 1996, when the National Drug Policy (NDP) was passed, which became one of the first legal documents that truly recognised the potential benefits and role of traditional medicines in the South African national healthcare system (Mmamoshedi & Sibanda, 2016). This propelled investigations into the efficiency, safety, and quality of traditional medicines, which could be incorporated into the National Healthcare System (NHS). In 2007, the Act of Traditional Health Practitioners (Act no. 22 of 2007) authorised the registration of all traditional healers in South Africa. This includes healers from all diverse categories, such as sangomas, herbalists, diviners, traditional surgeons, and

traditional midwives, allowing them to legally and safely prescribe natural remedies such as the infamous South African traditional medicine – *Helichrysum*.

1.4 South African *Helichrysum* (Impepho)

The genus *Helichrysum* Mill. belongs to the Asteraceae family. It consists of 500-600 different species throughout the world, of which around 250 species are found in South Africa alone (Lourens et al., 2008a). *Helichrysum* (also commonly referred to as *Impepho*) plays an important role within many of the South African traditions. The lead into chemical research regarding South African *Helichrysum* species stems almost directly from the medicinal data received by the native amaXhosa and isiZulu communities who still use the plant for medicinal purposes (Mhlongo & Van Wyk, 2019).

Traditionally *Impepho* is used to treat a multitude of different diseases and disorders. This includes, but is not limited to diarrhoea, coughs, colds, skin infections, and other conditions involving the respiratory and gastrointestinal tracts. Amongst its many fascinating traditional uses, the *Helichrysum* plant is commonly dried and then burnt in the form of smudge sticks by sangomas to invoke the goodwill of their ancestors and bridge a connection of themselves to the spirit world (Maroyi, 2019).

Although the various uses and biological activities of many of the *Helichrysum* species have been well documented in the past, the renaming of various species over recent years has caused much confusion within the medical and the scientific community (Lourens et al., 2008a). For example, *Impepho* is referred to as a wide variety of different *Helichrysum* species, such as *H. cymosum*, *H. nudifolium*, *H. odoratissimum* and *H. petiolare*, all of which have variations in chemical and medicinal properties. This is confirmed in another study regarding isiZulu traditional medicines, where in Amandawe it was found that a single species of medicinal plant may have several praise names, used as synonyms or alternate names by traders and healers to conceal the identity of the plant materials they were dealing with (Mhlongo & Van Wyk, 2019). *H. luteoalbum* for example was found to have eight different vernacular names alone, supporting the idea that medicinal ethnobotany is still not completely documented in South Africa. It is not uncommon to find that these plant species and common names are being used interchangeably by the locals (Van Wyk & Gericke, 2000), and of the somewhat 250 local species of *Helichrysum*, there are still many which have not yet been chemically investigated, such as *H. pandurifolium* Shrank.

1.5 Antioxidants and Oxidative Stress

Antioxidants are classified as substances which can inhibit/prevent oxidative stress, which is often associated with an increased risk of chronic diseases. In this section, the definition of

oxidative stress and antioxidants are defined, as well as a brief overview as to how natural products can be used to prevent oxidative stress.

1.5.1 The Ageing Process

An essential part of aerobic life and human metabolism involves the transfer of electrons from one atom to another, an electron flow system that produces energy in the form of ATP. This simple, yet renowned process, is chemically referred to as oxidation (Davies, 1995). Higher eukaryotic aerobic organisms cannot live without oxygen, yet a paradox exists whereby oxygen is also inherently dangerous to their wellbeing. The problem occurs when the electron flow becomes uncoupled resulting in the formation of free radicals or reactive oxygen species (ROS) such as super oxides, peroxy, alkoxy, hydroxy, and nitric oxides. Some of these free radicals are highly reactive and attack the molecules of nearby cells causing somewhat unavoidable damage. This is the process of ageing (Reeg & Grune, 2015). The “free radical theory of ageing” was first postulated by Harman in 1956 and still holds firm today (Harman, 1956), basically stating that the cause of ageing is the accumulation of oxidatively damaged macromolecules by free radicals.

The process of ageing in its entirety is complicated, and what it comes down to is the continuous oxidation process your body performs to produce energy, the damage such oxidation does to neighbouring macromolecules and cells, and the repair process performed to reverse such damage.

1.5.2 Oxidative Stress and the Increased Risk of Chronic Disease

Oxidative stress is the result of the excess accumulation of bioactive oxidative products, free radicals and reactive oxygen species within the body such that they overwhelm the capacity of the cellular antioxidant defence system (Basu, 2010; Schrader & Fahimi, 2006). When these free radicals react with cellular biological molecules there is an increased risk of chronic disease and can lead to the progression of degenerative diseases, damage to cells and organs, DNA (deoxyribonucleic acid) damage, carcinogenesis, ageing, inflammation, diabetes, and atherosclerosis (Carocho & Ferreira, 2013; Rufino et al., 2009; Adom & Liu, 2002). In addition, research confirmed that diabetic patients show a postprandial concentration increase of free radicals (Anderson et al., 2001). Thus, it is important that the human body is able to detoxify itself from reactive oxygen species and free radicals, especially in those who suffer from diabetes. Under normal human physiological conditions, the body produces reactive oxygen species in low concentrations which act as secondary messengers to regulate key cellular responses. When an increase in these free radicals occurs under nonphysiological concentration conditions (an imbalance between the number of reactive oxygen species and

antioxidants within the body), cell dysfunction occurs leading to oxidative alterations to lipids, DNA and proteins (Chabert et al., 2014).

1.5.3 Antioxidants

Antioxidants are substances that can prevent or slow the damage to cells caused by free radicals or reactive oxygen species. They are often referred to as “free-radical scavengers” and have been shown to exert protective effects against oxidative damages which are commonly associated with the increased risk of chronic diseases (Adom & Liu, 2002). These substances can be of natural or artificial origin and apply to both the internal and external human body environments. Antioxidants can have many modes of action, such as acting as free radical acceptors, chelating with metals to form complexes or breaking chain reactions caused by oxidative stress (Pratt, 1992).

1.5.4 The Use of Natural Products as Oxidative Stress Inhibitors

Plants, especially dietary fruits and vegetables, are known to be a rich source of antioxidants and most plants possess compounds that show antioxidant activity (Szymanska et al., 2018). These compounds are polyphenolics that are found to occur in all parts of the plant and the most common natural antioxidants are flavonoids, carotenoids, coumarins, cinnamic acid derivatives, tocopherols, anthocyanins, lignans, stilbenes, vitamins and polyfunctional organic acids (Pratt, 1992). The efficient extraction and scientific investigation of antioxidants from natural sources are of great interest to food science and nutrition as they promote the application in pharmaceuticals, functional foods, and food additives (Xu et al., 2017). Different evaluation assays have been developed for the assessment of natural products and their extracts to determine their antioxidant capabilities such as the Trolox equivalence antioxidant capacity (TEAC) and the ferric ion reducing antioxidant power (FRAP) assay. These will be utilized in the later sections to determine the antioxidant potential of *H. pandurifolium*.

1.6 Diabetes Mellitus

Diabetes mellitus is a metabolic disorder associated with chronic hyperglycaemia (high blood sugar) and is characterised by either total or relatively high deficiency of pancreatic insulin secretion (Duckworth, 2001). Persistent hyperglycaemia is due to an impairment of insulin secretion/synthesis from pancreatic β -cells and/or insulin resistance on target tissues and results in an increase of ROS which is linked to major diabetic complications and other chronic diseases (Giacco & Brownlee, 2010; Turner et al., 1979). Diabetes is categorised into two major types; namely Type-1 Diabetes Mellitus (T1DM) and Type-2 Diabetes Mellitus (T2DM), with a third minor category involving pregnant women without previously diagnosed diabetes commonly known as gestational diabetes mellitus (Szmuiłowicz et al., 2019).

Type-1 diabetes is the consequence/outcome of insulin-producing pancreatic β cells being destroyed by an autoimmune β cell-specific process (Yoon & Jun, 2005). Insulin dependency in this condition is undoubtedly unavoidable, and T1DM patients will always require an external source to obtain insulin to survive and live an improved quality of life (Delli & Lernmark, 2015). In contrast, Type-2 diabetes, which is associated with defective insulin action or secretion, are not insulin-dependent but rather they suffer from insulin resistance – whereby their target cells do not use insulin the way they normally should (Chatterjee et al., 2017).

In 2017, it was estimated that there were 451 million people with diabetes worldwide and an expected 693 million people to have diabetes by 2045. During 2017, there were approximately 5 million deaths worldwide attributed to diabetes, and an estimated 850 billion US dollar global healthcare expenditure was spent on people with diabetes (Cho et al., 2018). There is an increased risk towards the development of serious life-threatening health conditions when living with diabetes. As a result, there is an increase in monthly medical care costs, an increased chance of earlier mortality, and an overall reduced quality of life (Baena-Díez et al., 2016).

When diabetics are left untreated, they become vulnerable to acute fatal complications such as ketoacidosis and coma when their blood glucose levels increase dramatically. High glucose levels can lead to the damage of vascular vessels resulting in macrovascular disorders such as cardiovascular complications, retinopathy or neuropathy. Diabetic complications also include sexual dysfunction, depression, and lower-limb amputations (Forbes & Cooper, 2013). Furthermore, diabetes mellitus is a known risk factor for dementia, and diabetic ketoacidosis may further increase the risk of Alzheimer's disease in Type-2 diabetics (Y. L. Chen et al., 2019).

For the body to efficiently uptake circulating blood glucose, muscle and fat cells require insulin. Insulin is a hormone released by the β -cells of the pancreas and by uptake into the muscle and adipocytes (as glycogen stores and fatty acids respectively), glucose levels are appropriately maintained (Errico, 2018).

Although insulin will always be a requirement, there are various other ways to regulate the body's blood glucose levels, such as pharmaceutically produced anti-diabetic drugs. These anti-diabetic drugs can be categorised into different classes depending on their functions and mechanisms of regulating glucose levels such as α -glucosidase inhibitors, thiazolidinediones etc. α -Glucosidase inhibitors inhibit key digestive enzymes which breakdown starch into glucose (Ghani, 2020). Acarbose, miglitol, and voglibose are α -glucosidase inhibitors. Thiazolidinediones, are a class of peroxisome proliferator-activated receptor gamma (PPAR- γ) agonists that increase insulin sensitivity. By acting on the peroxisome proliferator-activated

receptor, thiazolidinediones reduce the burden on β -cells (Zeka et al., 2019). Other classes of current anti-diabetic drugs include biguanides, bile acid sequestrants, dipeptidyl peptidase-4 (DPP-4) inhibitors, meglitinides, sodium-glucose cotransporter-2 (SGLT2) inhibitors, and sulfonylureas.

Natural products have become an increasingly popular source of anti-diabetic medication and scientific investigation due to the current anti-diabetic drugs on the market often showing adverse side effects (Chaudhury et al., 2017). The development of metformin was originally developed from natural compounds found in *Galega officinalis* (Bailey & Day, 1989). Although herbal sources of drugs may have the same therapeutic effect as classic anti-diabetic drugs, some side effects may be inherent to the latter because of the mechanism by which these drugs act. α -Glucosidase inhibitors, for example, may cause gas or diarrhoea due to the digestion of starch by bacteria in the colon after the starch is passed undigested through the small intestine by the inhibited key digestive enzymes (Zeka et al., 2019). Many plant species have been traditionally used to treat diabetes such as *Cycas pectinata* Griff, traditionally used by the Maibi-Maibi in India (Laishram et al., 2015), *Rosa rugosa* Thunb extracts, used in Uygur medicine (Liu et al., 2017) and the South American species *Myrcia palustris* DC (Wubshet et al., 2015). Traditional plant species have been phytochemically analysed and their anti-diabetic properties are attributed to specific class of compounds such as flavonoids, terpenes, alkaloids, quinines, phenols, phenylpropanoids and steroids (Yin et al., 2014).

Since diabetics are affected by hyperglycaemia during the metabolic process of sugar breakdown in the digestive system, inhibition of key digestive enzymes such as α -amylase and α -glucosidase can retard the rate of glucose uptake into the blood, thus reducing the risk of hyperglycaemia. These digestive enzymes are briefly discussed below.

1.6.1 α -Amylase

α -Amylase is one of the digestive system's key enzymes that involves the breakdown of starch into a mixture of maltose, maltotriose, as well as α -(1–6) and α -(1–4) oligoglucans (Naveen & Baskaran, 2018). The initial breakdown of starch begins with salivary α -amylase in the oral cavity but the majority of the starch digestion occurs in the duodenum (between the stomach and small intestine) where pancreatic amylase is found (Wahbeh & Christie, 2011). Although only a small amount of free glucose is generated during amylase activity, the α -glucosidase enzyme is required to further break down the remaining oligosaccharides into absorbable glucose.

1.6.2 α -Glucosidase

α -Glucosidase is located in the brush border of the small intestine and is the enzyme that acts on the sugar substances resulting from α -amylase breakdown of starch. α -Glucosidase further degrades the mixtures to glucose which can then enter the blood circulation (Naveen & Baskaran, 2018; Malunga et al., 2016). By inhibiting the α -glucosidase digestive enzyme, the rate at which glucose is absorbed into the blood is decreased (figure 1.1).

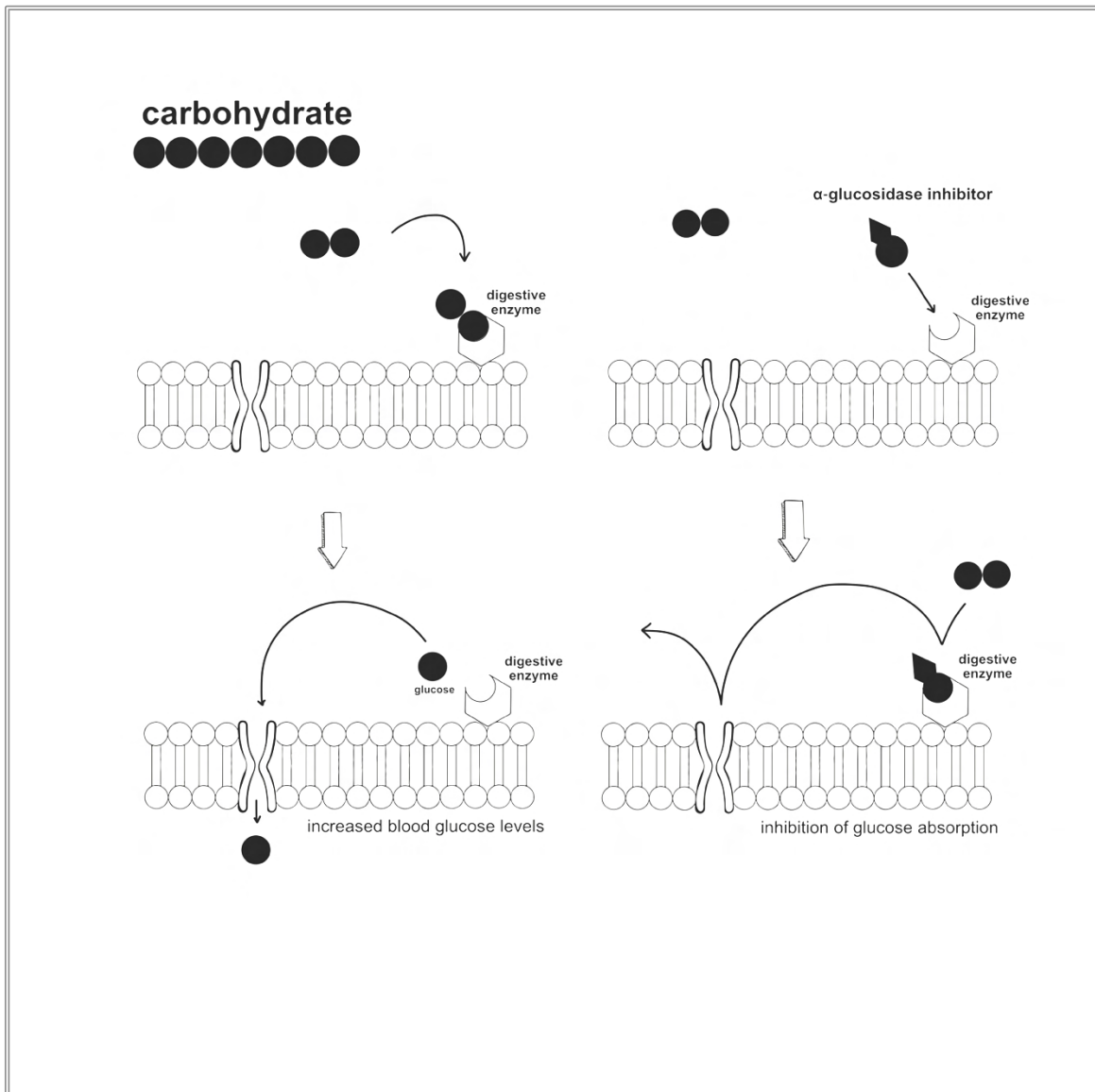


Figure 1.1: The role of α -amylase and α -glucosidase in starch digestion and metabolism

1.6.3 The Use of Natural Products as Sugar Regulators for Diabetics

When α -amylase and α -glucosidase enzymes are inhibited, the result is a decrease in postprandial blood glucose levels due to the retardation of starch digestion (Eichler et al., 1984). This plays a fundamental role in controlling the rate of glucose uptake in the body (Figure 1.1) and is thus considered to be an important target for the treatment of Type-2 diabetes. Effective phytochemicals from plant-derived sources, such as flavonoids, have been reported to inhibit such enzymes (Ahmed et al., 2014; Jung et al., 2006). *Helichrysum* belongs to one of the plant families with the most potent hypoglycaemic effects, the Asteraceae family (Patel et al., 2012).

1.7 Thesis Statement

This investigation explores the chemistry of a previously unstudied South African plant species, *H. pandurifolium* Schrank. As local *Helichrysum* species often show potential therapeutic benefits, *H. pandurifolium* Schrank may provide a natural source of anti-diabetic medication.

1.8 Rationale of the Study

As previously discussed, *Helichrysum* plays an important role in South African tradition – naturally, medicinally, and culturally. Research has proven that the genus possesses a wide variety of medicinal properties such as antioxidant, anti-diabetic, anti-bacterial, and anti-fungal properties to name a few. South Africa's biodiversity hotspot is home to around 250 different species of *Helichrysum* (Lourens et al., 2008a). Although *Helichrysum* spp. has been thoroughly researched both biologically and chemically worldwide, there are many species in South Africa that have not been chemically investigated and *H. pandurifolium* is one of these. This study is therefore the first scientific report to investigate some of the phytochemicals found in *H. pandurifolium*, as well as their antioxidant and anti-diabetic properties.

Research has shown that 463 million people currently live with diabetes (2019), of which 79% live with low-middle class incomes. Globally, one in eleven adults currently live with diabetes and it has been reported that 10% of the global health expenditure is spent on diabetes (International Diabetes Federation, 2019). Conversely, according to a Lancet study undergone in 2017, there is a predicted global shift in deaths – from infectious diseases to noncommunicable diseases like diabetes (Gouda et al., 2019). In the South African context, according to the South African Integrated Development Plan Report published in 2019, the number of adults with diabetes has drastically increased to 4.5 million people which is more than double the figure estimated in 2017 (Anon, 2017; International Diabetes Federation, 2019; Saeedi et al., 2019). In this regard, South Africa has the highest volume of diabetic adults on the African continent and the largest number of deaths due to the disease. The International

Diabetes Federation's 2019 Diabetes Atlas shows 12.7% of adults in South Africa had diabetes in 2019, a 137% increase on the 5.4% figure from 2017 (International Diabetes Federation, 2019; Anon, 2017).

Although the greatest causes of diabetes are attributed to poor diet, lack of physical exercise and obesity (National Institute of Diabetes and Digestive and Kidney Diseases, 2016), it does not change the reality that, for most people living with diabetes, neither the diabetic medication is readily affordable nor is it accessible to those who need it most (National Aids Treatment Advocacy Project, 2019). In this gap, many people turn to and depend upon traditional medicines to treat and alleviate chronic disease, clearly outlining an urgent need for short term trustworthy medical solutions, such as the scientific confirmation that these traditional medicines in fact work. Additionally, with the recent outbreak of SARS-COVID19 (coronavirus) pandemic sending the entire globe ushered into lockdown as to avoid complete crisis due to hospital overload, it was stated by that a total of 34% of coronavirus deaths are attributed to people with diabetes in South Africa (Winde, 2020). Interestingly, plants within the same family as *Helichrysum* (Asteraceae), such as *Echinacea purpurea* have been shown to possess multiple beneficial actions in the treatment of viral respiratory infections and antiviral activity (Hudson & Vimalanathan, 2011). Plant species within this family may be an aid in the fight against the COVID19 virus. The president of Madagascar, Andry Rajoelina, for example, promoted the *artemisia* plant (Asteraceae) to possess protective effects against the coronavirus and launched the *artemisia* plant product "COVID-Organics" on the 20th April 2020 (Finnan, 2020). The *artemisia* plant is known to have remarkable anti-HIV activity and has been recognised by the World Health Organisation (WHO) as a form of antimalarial treatment (Lubbe et al., 2012; WHO, 2012). Given these inter-relations as well as diabetes burden on an already overburdened healthcare system, there is great rationality and necessity to further investigate *H. pandurifolium* and other endemic herbs of the Asteraceae family for potential anti-diabetic treatment and to further study their antiviral and other potential therapeutic effects.

1.9 Aims & Objectives of Study

The aim of this study is to chemically investigate the previously unstudied species of *Helichrysum pandurifolium* Shrank for potential medicinal applications via the identification of its main phytochemical constituents. These phytochemicals along with its total extracts, are biologically evaluated to confirm the plant's potential as natural anti-diabetic and antioxidant medication.

The primary objectives of this research study are:

- Collection of *H. pandurifolium* from its natural habitat, documentation and identification.

- Extraction of plant constituents and the isolation of plant secondary metabolites via application of different chromatographic methods.
- Elucidation of phytochemical structures using various spectroscopic techniques such as $^1\text{H NMR}$, $^{13}\text{C NMR}$, UV/Vis spectroscopy, GC/MS.
- Determination of total antioxidant activities of the various isolated secondary metabolites using methods of multiple free radical scavenging mechanisms.
- Determination of the inhibitory activities of the isolated compounds against α -amylase and α -glucosidase enzymes.
- Study of the structure-activity relationship.
- Discuss the potential for *H. pandurifolium* as a therapeutic alternative to costly anti-diabetic medication locally.
- Conclude on the discoveries of the research study and provide further recommendations.

1.10 Research Questions

- What are the major phytochemical components of *H. pandurifolium*?
- Does the total extract of *H. pandurifolium* possess any antioxidant/anti-diabetic properties?
- Which of the isolated phytochemicals are responsible for the antioxidant/anti-diabetic properties observed?
- How do the total phenolic content and antioxidant/anti-diabetic activities of *H. pandurifolium* compare to other *Helichrysum* species?
- Do the isolated phytochemicals present any structure-activity correlation?
- Does *H. pandurifolium* extract or any of its phytochemical isolates have anti-diabetic potential?

1.11 Scope and Delimitations of Study

The study is limited to a single *Helichrysum* spp., *H. pandurifolium*. The plant material was collected from a single plant in a single location at the Cape of Good Hope, South Africa. Plant material was collected during the flowering season of *Helichrysum* (between September and December). Only the non-volatile components of *H. pandurifolium* are investigated in this study. The whole plant is investigated due to the limited quantity of plant material that was available for collection, this includes the flowering heads, leaves, and plant stem (excluding the root). The biological assays used for analysis were limited by those available during the study, namely TPC, FRAP, TEAC, α -glucosidase, and α -amylase assays.

1.12 Thesis Chapters Outlines

Chapter 1 gives a brief introduction, complimenting the topic of this thesis and introducing the various concepts which are elaborated upon in the upcoming chapters. This is followed by **Chapter 2**, which reviews the chemistry of *Helichrysum* and provides an in-depth literature review on the antioxidant and anti-diabetic properties of *Helichrysum* and an important class of phytochemicals called flavonoids. This is used to subsidise the discussion and conclusion in the final chapter of this thesis. **Chapter 3** presents the materials and methods used to obtain experimental results, while **chapter 4** describes the isolation procedure, chemical characterisation and structure elucidation of the phytochemical components of *H. pandurifolium* in great detail. These chapters aim to provide future researchers with all the knowledge required to repeat the experiment and present the methods of extraction which can be used to obtain phytochemicals for analysis from other plant species in the future. **Chapter 5** discusses the biological characterisation of the total extract and purely isolated phytochemicals in this study, with a focus on antioxidant and anti-diabetic activity. **Chapter 6** concludes the study, providing an in-depth discussion regarding current investigation and further recommendations.

CHAPTER 2: LITERATURE REVIEW

“Look deep into nature, and then you will understand everything better.”

– Albert Einstein

2.1 Chapter Overview

In this chapter, an overview of the genus *Helichrysum* is described. This is followed by a literature review of the traditional uses of *Helichrysum* in South Africa, and the documentation of all the available information about *Helichrysum pandurifolium* Shrank. A summary of the phytochemistry of *Helichrysum* is reported, and a deeper look into flavonoids is presented. Finally, the antioxidant and anti-diabetic properties of *Helichrysum* phytochemicals and flavonoids are reviewed for further discussion in the upcoming chapters. At the end of this chapter are tables summarising information of important phytochemicals that are used for continuous reference throughout the chapter.

2.2 The Asteraceae Family (Sunflower Family)

The Asteraceae family is the largest family of flowering plants, containing over 1 620 genera and 23 600 species occurring throughout the world (Tamokou et al., 2017). The family owes its uniqueness to a combination of its flowers being borne in capitula, five stamens with laterally fused anthers, and the fruit being an achene. Often woody at the base, species in the Asteraceae family are annual or perennial herbs (lasting for several years). The leaves can be petiolate or sessile depending on the species and are usually found to alternate (simple and entire), sometimes oppositely, pinnately (resembling a feather) or palmately (lobes radiating from one point) with the absence of a stipule. Flowers are small and usually numerous, found in dense terminal heads (capitula). The Asteraceae family of medicinal plant species was recorded to be the most commonly used traditional Zulu medicine in South Africa (Mhlongo & Van Wyk, 2019).

2.3 The Genus of *Helichrysum*

Helichrysum genus contains 500-600 different species (Merxmiiller et al., 1977; Anderberg, 1994; Bohm & Stuessy, 2001) is by far the largest genus of the Inuleae/Gnaphalieae tribe. The widely occurring genus can be found in Europe, Asia, Africa, Madagascar, Australia, and New Zealand (Hilliard, 1983; Goldblatt & Manning, 2002). The capitula of many species are often referred to as the “everlastings” and the dried flowering heads finding their use as long-lasting decorations (Bohm & Stuessy, 2001). As mat-forming shrubs, *Helichrysum* are either perennial

or annual woody plants. With erect or spreading stems, the leaves are found forming as an alternate, simple and entire. The flower capitula is usually terminal and solitary or sometimes observed to form in a corymb. Involucral bracts can form in several rows and are described as scarious, white, yellow, orange, or red. The flowers are typically tubular and 5-lobed with the inner being bisexual and the outer female with corolla (yellow or cream). Anthers have tails, and apical appendage is ovate and flat. Style is oblong-linear, truncate branches. The achenes are more or less cylindrical and the receptacle is slightly convex without scales (Sell & Murrell, 2006). *Helichrysum* strains with yellow or bronze-coloured bracts owe their pigmentation to the accumulation of chalcone and aurones due to the lack of chalcone isomerase activity (Forkmann, 1989).

2.4 Traditional uses of South African *Helichrysum*

The first recorded medicinal use of *Helichrysum* in South Africa dates back to as far as 1727 where the Dutch botanist Herman Boerhaave reported that a South African species of *Helichrysum* was used to treat nervousness and hysteria (Lourens et al., 2008b). Such early enlightenment could have been gathered from the local Khoi and San people but is more realistically due to European botanists utilizing their knowledge of medicinal properties regarding European species of the genera (Scott & Hewett, 2008). Traditionally, *Helichrysum* is used for a multitude of purposes. Various species are used in the treatment of respiratory conditions and chest problems by eating the plant material raw or drinking a brewed decoction. The grounded leaves are used directly to dress infected wounds, burns, and in the treatment of circumcision. Leaves and stems are burned as incense to invoke the goodwill of the ancestors and induce trance-like states. Tea infusions are used to treat coughs and colds, and vapours from the boiling leaves are inhaled to help with headaches. Table 2.1 provides a summary of the traditional uses of *Helichrysum* in South Africa (Lourens et al., 2008b).

Table 2.1: Reported traditional uses of *Helichrysum* in South Africa

Reported traditional use	Species	Form	Part of plant used	References
Treatment of diarrhea and vomiting in children	<i>H. adenocarpum</i> DC.	Decoction	Root	(Watt & Breyer-Brandwijk, 1962)
Chest problems and respiratory tract infections	<i>H. cochleariforme</i> DC. <i>H. mundtii</i> Harv.	Decoction	Whole plant	(Watt & Breyer-Brandwijk, 1962; Arnold et al., 2002)
	<i>H. nudifolium</i> (L.) Less.	Decoction	Root	(Watt & Breyer-Brandwijk, 1962)
Wound dressing	<i>H. appendiculatum</i> (L.f.) Less. <i>H. foetidum</i> (L.) Moench <i>H. nudifolium</i> (L.) Less. <i>H. odoratissimum</i> (L.) <i>H. longifolium</i> DC. <i>H. petiolare</i> Hilliard & B.L.Burt.	Whole leaves/Ground leaves	Leaves	(Aiyegoro & Okoh, 2009; Aiyegoro et al., 2010; Lourens et al., 2008b; Arnold et al., 2002)
Used to invoke the goodwill of ancestors and induce trance-like states	<i>H. aureonitens</i> Sch. Bip. <i>H. decorum</i> DC. <i>H. epapposum</i> Bolus. <i>H. flanaganii</i> Bolus. <i>H. foetidum</i> (L.) Moench. <i>H. gymnocomum</i> DC. <i>H. herbaceum</i> (Andrews) Sweet. <i>H. natalitium</i> DC. <i>H. nudifolium</i> (L.) Less.	Burnt as incense	Leaves and stems	(Ziaratnia et al., 2009; Zanetsie Kakam et al., 2011; Watt & Breyer-Brandwijk, 1962; Arnold et al., 2002; Walker, 1996; Cunningham, 1988; Pooley, 2003)
Intestinal troubles	<i>H. argyrophyllum</i> DC.	Infusion	Root	(Arnold et al., 2002)
Used topically for skin infections	<i>H. aureonitens</i> Sch. Bip. <i>H. foetidum</i> (L.) Moench	Extracts	Whole plant	(Afolayan & Meyer, 1997; Zanetsie Kakam et al., 2011)
Headaches	<i>H. cymosum</i> (L.) D.Don subsp. <i>calvum</i> Hilliard. <i>H. petiolare</i> Hilliard & B.L.Burt.	Boiled and vapours inhaled	Leaves	(Arnold et al., 2002)
	<i>H. odoratissimum</i> (L.)	Smoke inhaled	Leaves	(Arnold et al., 2002)
	<i>H. subglomeratum</i> Less.	Smoke inhaled	Aerial parts	(Arnold et al., 2002)

Headaches and chest colds	<i>H. caespitium</i> DC. <i>H. dregeanum</i> Sond. and Harv. <i>H. nudifolium</i> (L.) Less.	Smoke inhaled	Whole plant	(Watt & Breyer-Brandwijk, 1962; Arnold et al., 2002)
Coughs	<i>H. cochleariforme</i> DC <i>H. crispum</i> (L.) D. Don	Tea infusion	Whole plant	(Arnold et al., 2002; Watt & Breyer-Brandwijk, 1962)
Coughs and colds	<i>H. cymosum</i> (L.) D. Don subsp. <i>calvum</i> Hilliard. <i>H. melanacme</i> DC. <i>H. nudifolium</i> (L.) Less. <i>H. petiolare</i> Hilliard & B.L. Burt.	Decoction/tea	Leaves	(Watt & Breyer-Brandwijk, 1962; Arnold et al., 2002)
	<i>H. odoratissimum</i> (L.)	Not specified	Root	(Arnold et al., 2002)
Treat flu (influenza)	<i>H. foetidum</i> (L.) Moench.	Extract	Leaves	(Zanetsie Kakam et al., 2011; Arnold et al., 2002)
Relief of muscle tension and cramps	<i>H. odoratissimum</i> (L.)	Tea	Whole plant	(Arnold et al., 2002)
Heartburn	<i>H. odoratissimum</i> (L.)	Sap	Leaves	(Arnold et al., 2002)
Malaria treatment in children	<i>H. panduratum</i> O. Hoffm.	Sap	Whole plant	(Neuwinger, 1996)
Kidney stones and kidney disease	<i>H. pandurifolium</i> Schrank. <i>H. patulum</i> (L.) D. Don.	Not specified	Not specified	(Neuwinger, 1996)
Used to treat rheumatism	<i>H. splendidum</i> (Thunb.).	Not specified	Roots	(Mashigo et al., 2015)

2.5 *Helichrysum pandurifolium* Schrank

H. pandurifolium (synonym: *H. auriculatum*) was collected along the shorelines of Cape Point (Cape of Good Hope), South Africa. It was found to grow in small bundles of scattered families in sandy flat and slope environments (figures 2.1a and 2.1b). The plant can be described as a straggling, grey-woolly shrub with ovate, pseudopetiolate, crisped, and auriculate-clasping leaves. The flower heads (figures 2.1c and 2.1d), which are believed to contain the greatest concentration of flavonoids are described as discoid, with few to many in terminal corymbs on peduncle-like branches, campanulate, creamy coloured, ± 5-8 mm by 6-10 mm in volume, 12-40 florets and ovary glabrous. *H. pandurifolium*, like most South African *Helichrysum* species has its flowering season between October and January (Manning & Goldblatt, 2012).

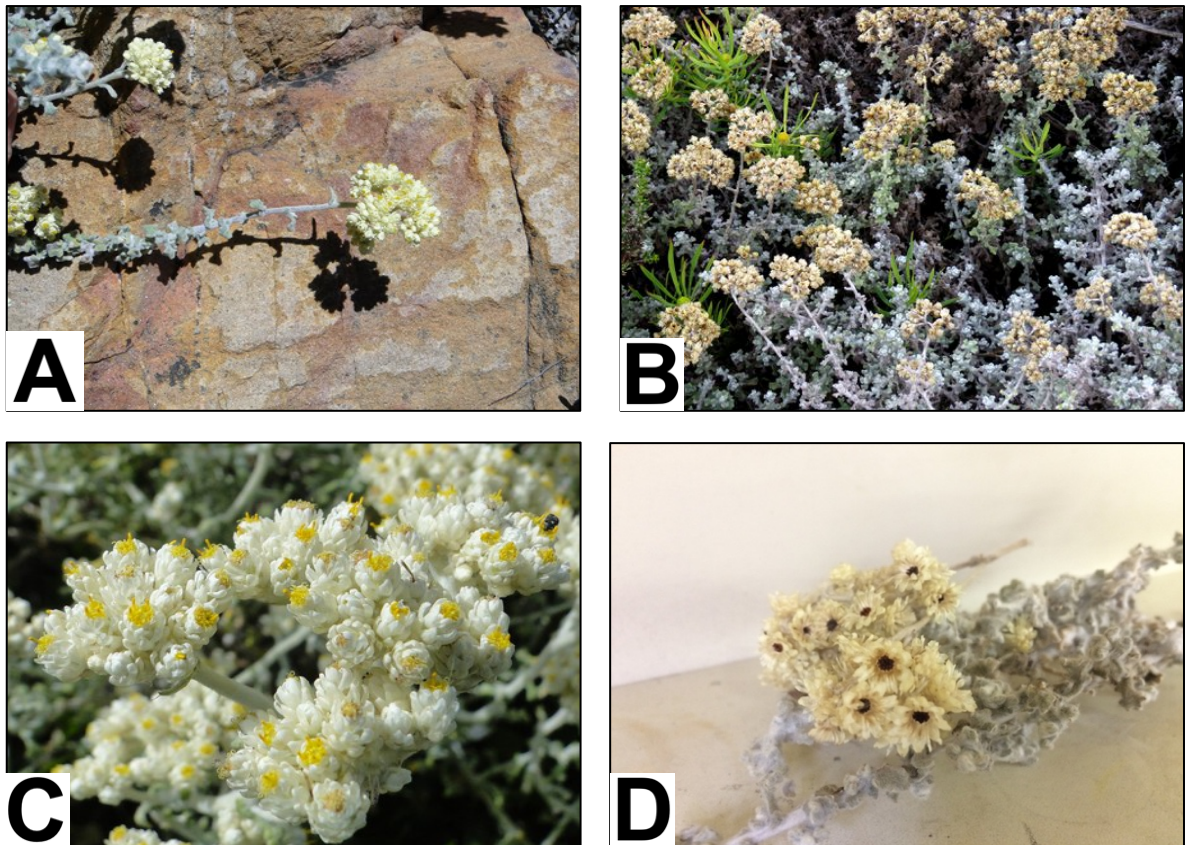


Figure 2.1: (a) *H. pandurifolium* found in rocky/sandy flat and slope environments, (b) grey/wooly appearance of *H. pandurifolium*, (c) *H. pandurifolium* flowering heads and (d) *H. pandurifolium* everlasting

Historically, *H. pandurifolium* has been used as a tea, a highly polar extract of its phytochemicals, for consumption. Traditionally, *H. pandurifolium* and *H. patulum* were used to treat respiratory conditions, back pain, heart troubles, and kidney stones (Lourens et al., 2008b). Biological activity of *H. pandurifolium* total extract using chloroform:methanol (1:1) has been previously tested for antibacterial activity and cytotoxicity (Lourens A, Van Vuuren S, Viljoen A, Davids H, 2011). Antibacterial activity was observed against two (2) main Gram-positive micro-organisms, namely *S. aureus* and *B. cereus* which displayed sensitivities of 2 mg/mL and 4 mg/mL respectively. Cytotoxicity of the total extract was tested at a concentration of 0,1 mg/mL using cell growth of two cancer cell lines, namely SF-268 (glioblastoma cells) and MCF-7 (adenocarcinoma breast cancer cell line), which showed percentage cell growths of $71,8 \pm 0,8$ % and $34,2 \pm 0,1$ % respectively. A measure of *H. pandurifolium* toxicity was assessed by observing Graham cell growth in which the total extract (0,01 mg/mL) showed $57,1 \pm 1,2$ % cell growth. It should be noted that species with potential toxicity usually has less than 10 % Graham cell growth at a 0.1 mg/mL test concentration.

A literature search for the phytochemistry of *H. pandurifolium* did not result in any scientific report.

2.6 Chemistry of *Helichrysum*

2.6.1 The General Chemistry of *Helichrysum*

The *Helichrysum* genus has been found to produce a diverse variety of useful secondary metabolites, many of which are polyphenolics with scientifically proven medicinal value. Of the many classes of compounds found in *Helichrysum*, the most commonly occurring secondary metabolites (tables 2.3 - 2.9) are polyphenols, flavonoids, terpenoids, phloroglucinols, α -pyrone derivatives, coumarins and acetophenones derivatives (Lourens et al., 2008b). Of the various polyphenols, the most commonly occurring are the flavonoids (table 2.6 – 2.8), wherein the genus provides us with rich flavonoid chemistry (figure 2.2) including chalcones, dihydrochalcones, flavanones, flavones, flavonols, dihydroflavonols, and anthocyanins (Bohm & Stuessy, 2001). *Helichrysum* owes its aromatic fragrance to the natural production of various terpenoids which are widely isolated via distillation of the fresh plant material and sold internationally as essential oils (Asekun et al., 2007). Extracts of *Helichrysum* species have been widely reported revealing antimicrobial activities against numerous micro bacteria (Süzgeç-Selçuk & Birteksöz, 2011; Coşar & Çubukçu, 1990; Meyer & Afolayan, 1995; Lourens et al., 2004; Lourens A, Van Vuuren S, Viljoen A, Davids H, 2011; Albayrak et al., 2010). Additionally, antifungal activity of extracts has also been widely reported (Albayrak et al., 2010; Stupar et al., 2014; Kutluka et al., 2018; Mashigo et al., 2015). Anti-inflammatory activities have been exhibited via anti-inflammatory enzyme inhibition, scavenging of free radicals, and corticoid-like effects (Sala et al., 2002; Minaiyan et al., 2004; Legoalea et al., 2013). Anti-malarial activities have been reported to be greater in crude extracts than in essential oils of various *Helichrysum* (Afoulous et al., 2011; van Vuuren et al., 2006). The flavonoids and phloroglucinols of *Helichrysum italicum* have exhibited anti-HSV and anti-HIV properties (Antunes Viegas et al., 2014), whereas the aqueous extracts of various South African species have also shown anti-HIV results (Heyman et al., 2013). Examples of commonly occurring secondary metabolites found in *Helichrysum* are listed in the preceding tables (tables 2.3-2.9). Antioxidant and anti-diabetic properties of *Helichrysum* have been well documented and are discussed in further detail (sections 2.6.3 – 2.6.6) due to its relevance in this study.

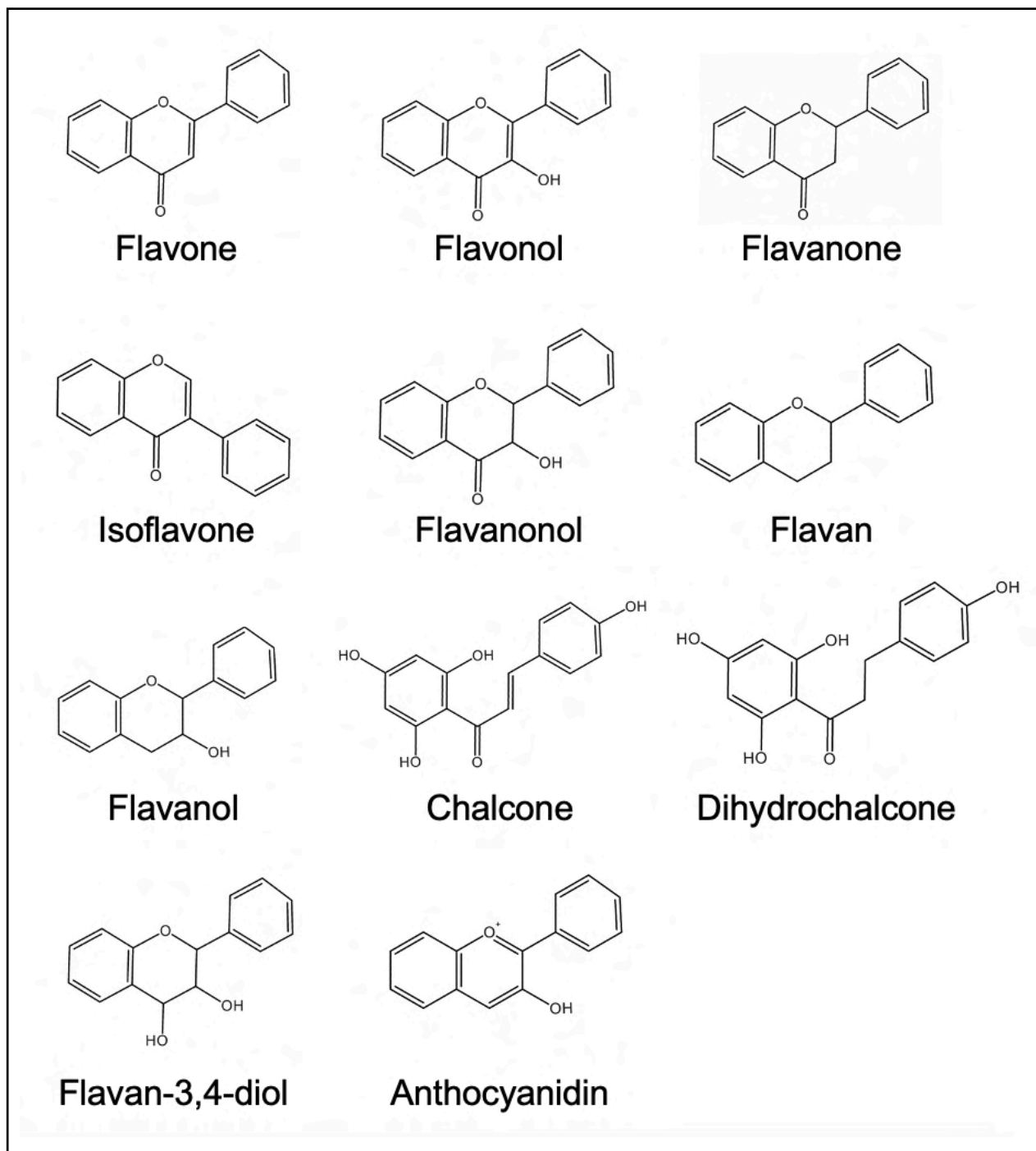


Figure 2.2: Common flavonoid backbone structures

2.6.2 Flavonoids

Flavonoids are a class of phenolic substances found in nature as plant secondary metabolites. The omnipresence of flavonoids within the plant kingdom, with the exception of most algae (Mabry & Ulubelen, 1980), is evidence of the importance of such secondary metabolites within plant biological systems (Manthey & Buslig, 1998). In plants, flavonoids are formed from malonate and the aromatic amino acids phenylalanine and tyrosine and act as antioxidants, antimicrobials, photoreceptors, visual attraction, and feeding repellants (Pietta, 2000). Over 9000 flavonoids have been discovered to date (Wang et al., 2011), and their daily dietary supplement intake varies between 20 mg and 500 mg mainly from the consumption of fruits, teas, and red wine (Giuliani et al., 2014). Flavonoids are becoming an increasingly popular subject of study in medical research as flavonoid-rich plant extracts have been reported to have a broad spectrum of biological activities, especially in *Helichrysum* (Süzgeç et al., 2005; Süzgeç-Selçuk & Birteksöz, 2011; Albayrak et al., 2010). They are the main phenolic components of the genus *Helichrysum*, and many have been shown to possess remarkable antioxidant activity (Czinner et al., 2000). The antioxidant and anti-diabetic activities of flavonoids are discussed in greater detail in the following sections (2.6.4 and 2.6.6).

Untreatable infections caused by prevailing antibiotic resistant bacteria has led scientists towards conducting ever-increasing studies on flavonoids acting as potential substitutes for antibiotics. Flavonoids, being abundantly available to us from natural sources, have been widely studied for their antibacterial activity with over one hundred and fifty articles published on this topic alone since 2005 (Farhadi et al., 2019). Today, it is general knowledge that hydroxyl functional groups at specific sites on the flavonoid backbone increase antibacterial activity, whereas methylated hydroxyl groups generally decrease the activity (Xie et al., 2015). Flavonoids of *H. italicum* have been found to possess effective antibacterial activity against *Staphylococcus aureus* (Antunes Viegas et al., 2014), and extracts of *H. compactum* have also shown antibacterial activity, primarily attributed to its large flavonoid content (Süzgeç et al., 2005). As mentioned previously, flavonoids isolated from *Helichrysum* have exhibited anti-HIV and anti-HSV properties (Antunes Viegas et al., 2014). Flavonoids of *Helichrysum* have shown anti-erythematous, anti-inflammatory, and photoprotective activities (Antunes Viegas et al., 2014). *Helichrysum simillimum* DC (South Africa) showed mutagenic activity in the salmonella/microsome assay, where it was shown that the isolated flavonol kaempferol was responsible for its crude extract activity (Elgorashi et al., 2008). The anti-cancer and flavonoid intake relationship is weak at present, and epidemiological studies have proposed that there is evidence that flavonoid intake can protect against certain types of cancer (Pietta, 2000). One study has even shown an inverse correlation between the consumption of flavonoids and lung cancer (Knekt et al., 1997). Flavonoids are grouped into different classes depending on

their backbone structures (figure 2.2). Examples of such classes are flavones, flavonols, flavanones, and chalcones (tables 2.6 - 2.9).

2.6.3 The Antioxidant Activity of *Helichrysum*

The total phenolic content of plant extracts is commonly estimated using the Folin-Ciocalteu reagent method, giving us insight into the potential antioxidant capabilities that specific plant species possess. Here, the results are usually reported as milligram gallic acid equivalents per gram (mg GAE/g) of the dry weight test samples. Another common measure of antioxidant activity is known as the Ferric-ion reducing antioxidant power (FRAP) assay, where the results are usually reported as mg ascorbic acid equivalents per gram (mg AAE/g) of the dry weight test samples. This assay (along with Trolox equivalent absorbance capacity, or TEAC assay) allows for the determination of the antioxidant capacity of plant extracts and pure compounds. Table 2.2 presents the various antioxidant measurements obtained from methanolic extracts of 16 *Helichrysum* species using the Folin-Ciocalteu reagent method and the FRAP assay (Albayrak et al., 2010). When it comes to *Helichrysum* extracts, essential oils often shown poor antioxidant activities, probably due to the lack of larger non-volatile phytochemicals such as flavonoids (Afoulous et al., 2011).

Table 2.2: Antioxidant activities of 16 methanolic *Helichrysum* extracts (Albayrak et al., 2010)

<i>Helichrysum</i> species	Total phenolic content (mg GAE/g)	FRAP Antioxidant activity (mg AAE/g)
<i>H. arenarium</i> subsp. <i>aucheri</i>	115.76 ± 1.2	147.68 ± 0.3
<i>H. armenium</i> subsp. <i>armenium</i>	89.02 ± 0.8	157.29 ± 0.2
<i>H. artvinense</i>	83.98 ± 1.0	171.02 ± 0.5
<i>H. chionophilum</i>	106.97 ± 0.6	140.43 ± 0.5
<i>H. compactum</i>	79.59 ± 0.6	165.00 ± 0.3
<i>H. goulandrionum</i>	114.41 ± 1.0	124.86 ± 0.2
<i>H. graveolens</i>	92.77 ± 0.6	160.34 ± 0.9
<i>H. heywoodianum</i>	93.85 ± 0.4	191.97 ± 0.4
<i>H. kitianum</i>	75.16 ± 0.6	172.17 ± 0.5
<i>H. noeanum</i>	160.63 ± 1.2	194.64 ± 0.4
<i>H. orientale</i>	73.70 ± 0.3	110.03 ± 0.3
<i>H. pallasii</i>	94.13 ± 0.1	118.99 ± 0.5
<i>H. peshmenianum</i>	66.74 ± 1.3	125.47 ± 0.3
<i>H. plicatum</i> subsp. <i>plicatum</i>	87.36 ± 0.6	163.47 ± 0.5
<i>H. plicatum</i> subsp. <i>polyphyllum</i>	154.64 ± 0.6	152.64 ± 0.3
<i>H. stoechas</i> subsp. <i>barellieri</i>	94.16 ± 0.5	188.26 ± 0.5

Flavonoids being the main component in *Helichrysum* species are generally responsible for the observed antioxidant effects of the plant extracts. Therefore, more emphasis needs to be put onto the antioxidant properties of flavonoids themselves.

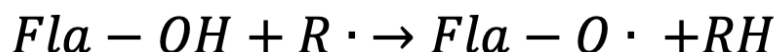
2.6.4 Antioxidant Properties of Flavonoids

Flavonoids possess significant antioxidant and chelating properties. Mechanisms of the observed flavonoid antioxidant properties are due to the suppression of ROS formation through the inhibition of enzymes and chelation of trace elements, free radical scavenging, and upregulation of antioxidant defences (Halliwell & Gutteridge, 1998). Flavonoids have been shown to inhibit xanthine oxidase and protein kinase C involved in superoxide anion production, and enzymes responsible for ROS generation such as cyclooxygenase, lipoxygenase, microsomal monooxygenase, glutathione S-transferase, mitochondrial succinoxidase and nicotinamide adenine dinucleotide phosphate oxidase (NADH oxidase) (Ursini et al., 1994; Brown et al., 1998; Correlation et al., 1994). The chelation of iron and copper reduces hydrogen peroxide and the generation of aggressive hydroxyl radicals, as seen in equation 2.1 (Pietta, 2000).



Equation 2.1: Hydroxyl radical generation by iron and copper

Flavonoids have lower redox potentials (usually between 0.23 and 0.75 V) than ROS (usually in the range of 1.0 and 2.13 V) and can therefore reduce highly oxidizing free radicals (equation 2.2) such as superoxide, peroxy, alkoxy, and hydroxyl radicals by hydrogen donation. Additionally, the peroxy radical (Fla-O•) can react with a second radical resulting in a stable quinone structure (Buettner, 1993; Hodnick et al., 1988; Jovanovic et al., 1996). Apart from scavenging, flavonoids can also react with free radicals to stabilise them (Shahidi et al., 1992).



Equation 2.2: Free radical neutralization by flavonoids (Fla-OH), where R. represents superoxide anion, peroxy, alkoxy and hydroxyl radicals

The structure of a flavonoid (figure 2.3) is linked to its ability to inhibit free radicals and chelate metals. The type of substitutions on the flavonoid backbone, their relative positions, and the total substitution count all affect the flavonoid's overall antioxidant activity. There is a clear evidence that supports substantial antioxidant potency and chelating ability depending on the number of hydroxyl groups on the structure (the more hydroxyl groups, the greater the activity) (Heim et al., 2002; Pietta, 2000; Lin et al., 2014; Sarian et al., 2017). On the other

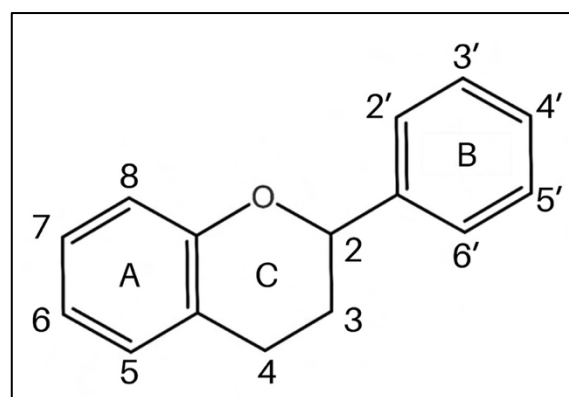


Figure 2.3: The flavonoid backbone (flavan) and its numbering system

hand, methoxy substituted hydroxyl functional groups cause a decrease in activity due to steric effects (Heim et al., 2002). Evidence reveals that the presence of 3' and 4' hydroxyl groups (catechol group) on ring-B increase antioxidant activity as they have better electron donating properties and are a radical scavenging target. In addition, the 2,3-double bond conjugated with a 4-oxo group allows for electron delocalization and is almost a requirement (Pietta, 2000).

The binding sites to which flavonoids chelate trace metals are at the catechol moiety in the B-ring, between the 3-position hydroxyl functional group and 4-oxo group of the C-ring, and the 5-position hydroxyl and 4-oxo between rings A and C respectively (figure 2.4). The catechol functional group has been found to be the major contributor to metal chelation, as observed by a more pronounced bathochromic shift when the quercetin spectrum is compared to that of the kaempferol spectrum during copper chelation (Van Acker et al., 1996). This metal chelation mechanism is used experimentally to determine

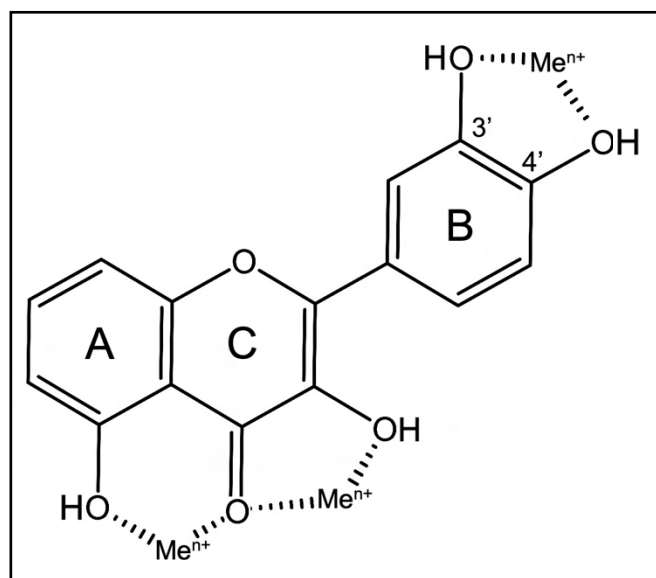


Figure 2.4: Metal chelation of flavonoids (Pietta, 2000)

the positions of functional groups by observing specific shifts in the UV spectrum of each isolated flavonoid when forming complexes with various reagents such as AlCl_3 , which is discussed further in chapter 3 (section 3.3.3.3).

2.6.5 Anti-diabetic Properties of *Helichrysum*

In Turkey (Anatolia), *Helichrysum* is used as a folk remedy in the treatment of diabetes (Subramoniam, 2016). *In vivo* tested aqueous leaf extracts of Turkish *Helichrysum odoratissimum* have been shown to lower glucose blood levels in alloxan-induced diabetic mice (Njagi et al., 2015). In addition, the *in vivo* study revealed no extract toxicity on the major

organs of the animals in the study, thus concluding that *Helichrysum odoratissimum* has safe bioactivity in the management of diabetes mellitus. In a similar study, the capitulum of Turkish *Helichrysum plicatum* and *Helichrysum graveolens* were extracted using ethanol and water. Both resulted in significant antihyperglycaemic and antioxidant activity when tested in streptozotocin (STZ)-induced rats (Aslan, Orhan, Nilufer Orhan, et al., 2007a; Aslan, Orhan, Nilufer Orhan, et al., 2007b). Additionally, *in vitro* studies confirmed Turkish folklore after an ethanolic extract of *Helichrysum graveolens* resulted in a 55.7 ± 2.2 % α -amylase inhibition (Subramoniam, 2016). *Helichrysum italicum* extracts (methanol/water, 3:1) inhibited α -glucosidase ($IC_{50} = 0.19$ mg/mL) and α -amylase ($IC_{50} = 0.83$ mg/mL), with bioactivities being attributed to flavonoids (De La Garza et al., 2013). This again indicates that the flavonoids are one of the major components of *Helichrysum* spp. and therefore more emphasis needs to be put on the anti-diabetic properties of flavonoids themselves.

2.6.6 Anti-diabetic Properties of Flavonoids

Flavonoids are quickly becoming renowned for their widespread anti-diabetic properties. Being readily available from a healthy human diet, flavonoids help to protect the body from developing diabetes and aid in the prevention of diabetic complications (Ross & Kasum, 2002; Duthie et al., 2003). In high-fat diet (HFD) and STZ-induced rats/mice, flavonoids have been shown to help the glucose regulation and lipid metabolism and can ameliorate endothelial dysfunction by down-regulating oxidative stress and inflammation, two of the leading causes of diabetic complications (Ren et al., 2016). Flavonoids have been reported to attenuate inflammation by significantly lowering the levels of pro-inflammatory cytokines (Samie et al., 2018). Flavonoids reduce the blood glucose levels and insulin resistance, improve glucose tolerance, insulin sensitivity, and lipid profiles (Oza & Kulkarni, 2018). Flavonoids also help to control the hyperglycaemia by slowing the production of glucose in the liver (Xu et al., 2018). Flavonoids have exhibited antihyperglycemic and hypolipidemic properties via significant reductions in blood glucose, cholesterol, triglycerides, low-density lipoproteins (LDL) and very low-density lipoproteins (VLDL) levels (Rekha et al., 2019). Flavonoids have shown protective effects against HFD-induced hepatic inflammation and lipid accumulation (Minxuan et al., 2019), and the renoprotective effects of flavonoids could even slow down the damage of diabetic nephropathy (Y. J. Chen et al., 2019).

α -Glucosidase and α -amylase inhibition assays are standard *in vitro* biological experiments which are commonly used to screen plant extracts for anti-diabetic properties. These biological tests can aid in targeting the pure anti-diabetic phytochemicals during the chromatographic separation process. Structure-activity relationships for flavonoids and key digestive enzymes have been well documented and are briefly reviewed here for further discussion in later chapters. It should be noted that in some cases flavonoids have exhibited greater α -

glucosidase inhibition than that of acarbose, a common antihyperglycemic drug on the market (Sechi et al., 2016).

Studies of structure-activity relationships for α -glucosidase inhibition revealed four (4) main requirements for maximum activity (figure 2.5). Based on the flavan backbone structure (figure 2.3), the catechol group on ring-B, hydroxy functional groups at 5-, 7- or 8-position of ring-A, 3-hydroxy functional group and C2=C3 double bond in ring-C are all crucial for flavonoid α -glucosidase activity (Proença et al., 2017).

Similarly, α -amylase inhibition requires the 3'- and 4'- position catechol group on ring-B, the C2=C3 double bond in ring-C, and the 5- hydroxyl group on ring-B. Interestingly, when the 3-hydroxyl group in ring-C is replaced by Cl- atom, inhibition is increased. The 8-hydroxyl group in ring-A is not as necessary for α -amylase inhibition as for α -glucosidase activity, but the 7-hydroxy is significant to α -amylase inhibition (Proença et al., 2019). Figure 2.6 presents flavonoid substitution patterns for increased α -amylase activity.

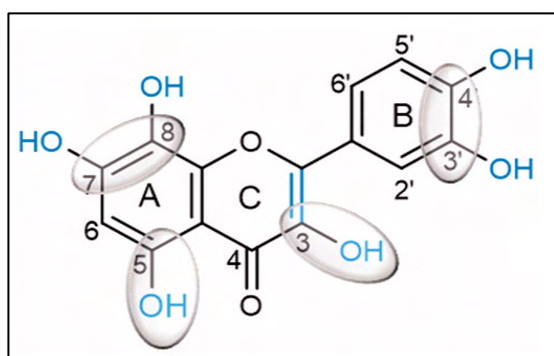


Figure 2.5: Flavonoid substitution patterns for increased α -glucosidase activity (Proença et al., 2017)

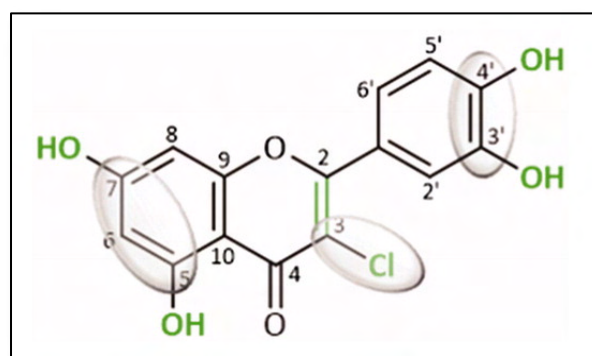


Figure 2.6: Flavonoid substitution patterns for increased α -amylase activity (Proença et al., 2019)

2.7 Conclusion

It has been shown that *Helichrysum* plays an important role in South African tradition, not only medically, but spiritually too. *Helichrysum* extracts have been scientifically proven to exhibit anti-malarial, anti-bacterial, anti-HIV, antioxidant, and anti-diabetic properties to name but a few (tables 2.3 - 2.9). *Helichrysum* contains a multitude of useful phytochemicals which show therapeutic potential, flavonoids often being the main components of these plant extracts. Such flavonoids provide us with interesting natural alternatives to pharmaceutical drugs, often having similar or greater relative therapeutic properties, without the warranted side effects (Chaudhury et al., 2017). *H. pandurifolium* is a relatively rare species of *Helichrysum* which is phytochemically unexplored and investigating the antioxidant and antidiabetic potential of this species is the main focus of the present study.

In the following chapter, the details of plant collection are described. This provides information as to the geographical location of *H. pandurifolium* which may be important in later studies. Methods and procedures as to how the plant material was extracted are described as well as all the details for spectroscopic and biological analysis such that the experiment can be repeated in the future to attain the same accurate results if necessary.

Various phytochemicals found in *Helichrysum* species and their activities:

Table 2.3: Terpenoids found in *Helichrysum*

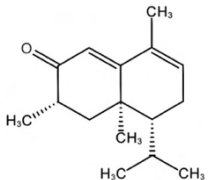
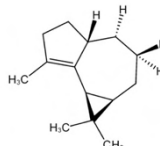
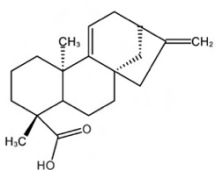
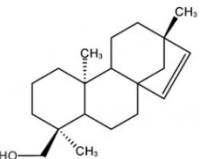
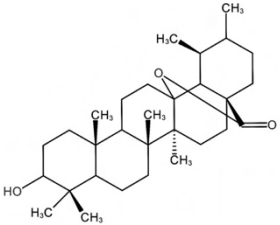
<u>Compound</u>	<u>Compound structure</u>	<u>Plant source</u>	<u>Activity</u>
1		<i>H. petiolare</i>	Antiseptic activity. (Jakupovic et al., 1989)
2		<i>H. nudifolium</i>	Antiseptic activity. (Bohlmann et al., 1978)
3		<i>H. athrixia</i>	Trypanosomicidal and antibacterial activity. (Bohlmann et al., 1978)
4		<i>H. tenax</i>	Antimicrobial. (Drewes et al., 2006)
5		<i>H. italicum</i>	Exhibits spasmolytic activity. (Mezzitti et al., 1970)

Table 2.4: Phloroglucinols and derivatives found in *Helichrysum*

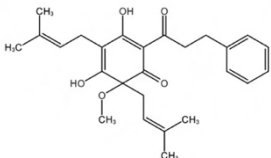
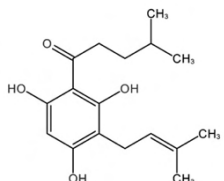
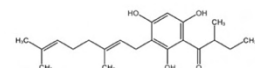
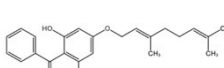
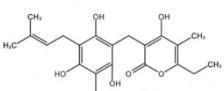
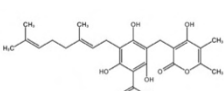
<u>Compound</u>	<u>Compound structure</u>	<u>Plant source</u>	<u>Activity</u>
6		<i>H. cymosum</i> (L.) D. Don subsp. <i>cymosum</i>	Antimicrobial. (van Vuuren et al., 2006)
7		<i>H. caespitium</i>	Antimicrobial. (Dekker et al., 1983)
8		<i>H. natalitium</i> <i>H. ballum</i> <i>H. stoechas</i>	Anti-inflammatory. (Bohlmann & Mahanta, 1979)
9		<i>H. spathulatum</i>	Cytotoxic. (Randriaminahy et al., 1992)
10		<i>H. arenarium</i> , <i>H. italicum</i> var. <i>microphyllum</i>	Anti-HIV-1, antibacterial, anti-inflammatory, and antioxidant activity. (Taglialatela-Scafati et al., 2013)
11		<i>H. decumbens</i>	Antifungal activity and fairly weak activity against Gram- positive bacteria. (Tomás-Lorente et al., 1989)

Table 2.5: Coumarins found in *Helichrysum*

<u>Compound</u>	<u>Compound structure</u>	<u>Plant source</u>	<u>Activity</u>
12		<i>H. arenarium</i> <i>H. stoechas</i>	Antibacterial activity. (Vrkoc et al., 1975)

Table 2.6: Flavones found in *Helichrysum*

<u>Compound</u>	<u>Compound structure</u>	<u>Plant source</u>	<u>Activity</u>
13		<i>H. nitens</i>	Shows antiviral activity against HSV-1, human cytomegalovirus, and poliovirus. Inhibitor of PGE2 production. (Buckingham & Munasinghe, 2015)
14		<i>H. viscosum</i>	Antimutagenic activity. (Geissman et al., 1967)
15		<i>H. nitens</i>	Pesticide and antiviral activity against HSV-1. Inhibitor of PGE2 production. (Tomas-Barberan et al., 1988)

Table 2.7: Flavonols found in *Helichrysum*

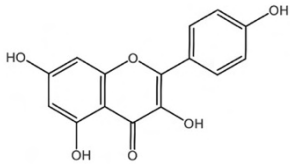
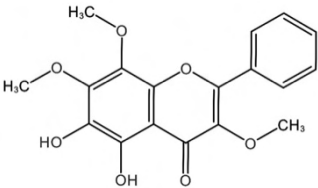
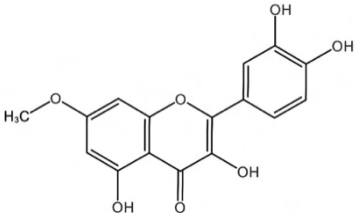
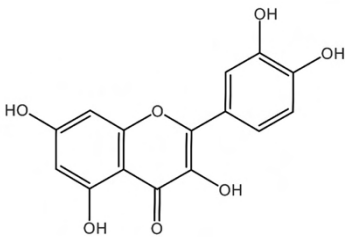
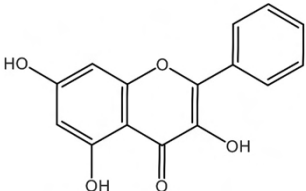
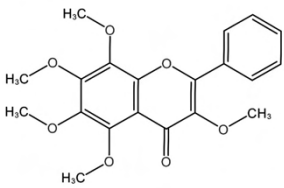
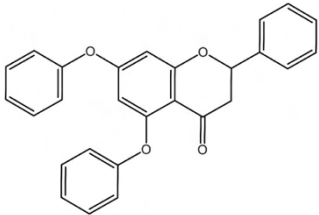
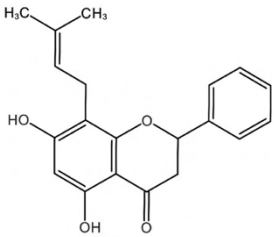
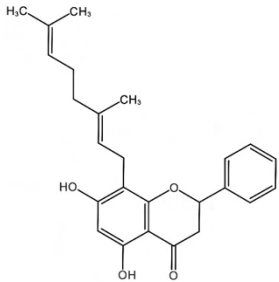
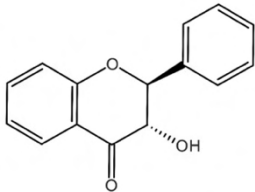
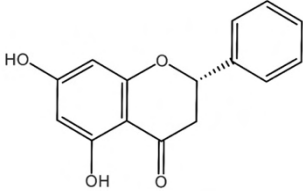
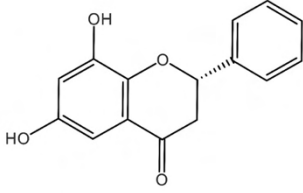
<u>Compound</u>	<u>Compound structure</u>	<u>Plant source</u>	<u>Activity</u>
16		<i>H. simillimum</i> DC	Mutagenic activity. (Elgorashi et al., 2008)
17		<i>H. kraussii</i>	Antioxidant activity; 44.4% DPPH free radical scavenging at 1 mg/mL. Anti-inflammatory activity; COX-1 and COX-2, 54.4 % and 84.7 % inhibition at 250 µg/mL. (Legoalea et al., 2013)
18		<i>H. odoratissimum</i>	Antioxidant activity; 32.3 % DPPH free radical scavenging at 1 mg/mL. Anti-inflammatory activity; COX-2, 16.5 % inhibition at 250 µg/mL. (Legoalea et al., 2013)
19		<i>H. melanacme</i> <i>H. bracteatum</i>	Mutagenic activity, anticarcinogenic, antitumour, Inhibitor of various enzymes, algaecide, antioxidant, anti-HIV activity; enhances apoptosis in colon cancer cells. (Lall et al., 2006; Liu et al., 2007) (MacGregor & Jurd, 1978)
20		<i>H. aureonitens</i>	Antibacterial activity against <i>Staphylococcus aureus</i> . MIC: 500 µg/ml. (Cushnie et al., 2007)
21		<i>H. nitens</i>	Antifungal activity. (Tomas-Barberan et al., 1988)

Table 2.8: Flavanones found in *Helichrysum*

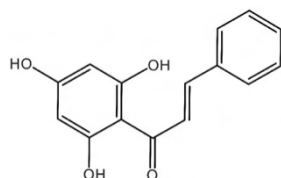
<u>Compound</u>	<u>Compound structure</u>	<u>Plant source</u>	<u>Activity</u>
22		<i>H. gymnocomum</i>	Antibacterial against <i>Staphylococcus aureus</i> with MIC value $\leq 125 \mu\text{g/mL}$. (Drewes & van Vuuren, 2008)
23		<i>H. forskahlii</i>	Exhibits antibacterial activity against <i>Staphylococcus aureus</i> and <i>Bacillus subtilis</i> . (Buckingham & Munasinghe, 2015; Al-Rehaily et al., 2008)
24		<i>H. hypocephalum</i>	Exhibits strong inhibitory effects on aminopeptidase N activity. (Buckingham & Munasinghe, 2015)
25		<i>H. stirlingii</i>	Antioxidant activity. (Buckingham & Munasinghe, 2015)
26		<i>H. Iryanthera</i> <i>H. acutatum</i> <i>H. tenuifolium</i> <i>H. cymosum</i>	Strong antimicrobial and antibacterial activity, and ketosteroid reductase inhibitor. (Bohlmann & Mahanta, 1979)
27		<i>H. Larix</i>	Ketosteroid reductase inhibitor, immunostimulant. Inhibits murine B16 melanoma and mushroom tyrosinase. (Bohlmann & Mahanta, 1979)

28		<i>H. polycladum</i>	Inhibits aromatase, cytotoxic to human breast cancer, SF-268, and NCI-H460 cells. (Bohlmann & Zdero, 1980)
29		<i>H. arthrixiifolium</i>	Phytoestrogen, cytotoxic, antifungal, cancer chemopreventive, antiosteoporosis, an aromatase inhibitor. (Bohlmann & Misra, 1984)

Table 2.9: Chalcones found in *Helichrysum*

<u>Compound</u>	<u>Compound structure</u>	<u>Plant source</u>	<u>Activity</u>
30		<i>H. gymnocomum</i>	Antibacterial activity against <i>Staphylococcus aureus</i> with MIC: 63 µg/mL. (Drewes & van Vuuren, 2008)
31		<i>H. rugulosum</i>	Exhibits weak antineoplastic activity against sarcoma. (Buckingham & Munasinghe, 2015)
32		<i>H. splendidum</i>	Shows antioxidant activity. Bactericidal. Inhibitor of topoisomerase II. (Buckingham & Munasinghe, 2015)
33		<i>H. odoratissimum</i> <i>H. heterolasium</i>	Exhibits antileishmanial and antiproliferative effect against human HT-1080 fibrosarcoma cells. (Buckingham & Munasinghe, 2015)

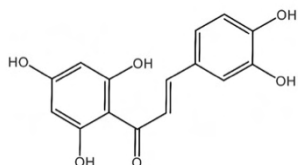
34



H. athrixiifolium

Exhibits antiviral and antituberculosis. (Buckingham & Munasinghe, 2015)

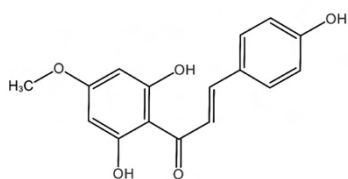
35



H. bracteatum

Shows free-radical scavenging activity and antioxidative activity. Protein tyrosine phosphatase, antioxidant, antidepressant, and potent 5-lipoxygenase inhibitor. (Liu et al., 2007)

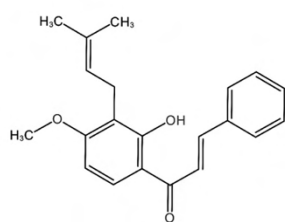
36



H. odoratissimum
H. heterolasium

Antileishmanial and antiproliferative. (Van Puyvelde et al., 1989)

37



H. rugulosum

Exhibits weak antineoplastic activity against sarcoma. (Bohlmann & Misra, 1984)

CHAPTER 3: MATERIALS AND METHODS

“The proper method for inquiring after the properties of things is to deduce them from experiments.”

– Isaac Newton

3.1 Chapter Overview

In this chapter, the plant collection process is described. A list of all chemicals used in the isolation process, identification of compounds, and bioassay procedures are reported. Chromatographic and spectroscopic methods and equipment details are described. Antioxidant and anti-diabetic biological assay procedures are described in detail.

3.2 Collection and Identification of Plant Material

H. pandurifolium was collected from the Cape Point Nature Reserve in Cape Town, South Africa between November 2017 and January 2018. The species was confirmed *via* professional botanical taxonomist.

3.3 General Experimental Procedures for Phytochemical Identification

3.3.1 Reagents and Solvents

Ethanol, acetone, ethyl acetate, dichloromethane, n-hexane, vanillin, and deuterated chloroform were supplied by Merck (Darmstadt, Germany). Methanol was supplied by Crest Chemicals (Cape Town, South Africa). Sulphuric acid, hydrochloric acid (HCl) and acetic acid were obtained from Kimix (Cape Town, South Africa). Deionised water used was obtained via the reverse osmosis process at CPUT. The following reagents were used for UV analysis of isolated compounds: analytical grade sodium hydroxide (Sigma-Aldrich, South Africa), analytical grade sodium acetate anhydrous (Kimix, South Africa), aluminium chloride (BDH Chemicals, Poole, England) and boric acid (Sigma-Aldrich, South Africa).

3.3.2 Chromatography

Two main chromatography techniques were utilised in the isolation of pure *H. pandurifolium* phytochemical components namely thin layer chromatography (TLC), primarily used to identify target components and visualise phytochemical purity and column chromatography, used in the large-scale separation and isolation of compounds from the total extract.

3.3.2.1 Thin Layer Chromatography (TLC)

For TLC analysis, pre-coated plates of 60 F₂₅₄ silica gel (Merck, Germany) were used. The various fractions of the extract were spotted using capillary tubes onto the TLC plates and then developed using solvent systems of varying polarity as mobile phase. The phytochemical components are then identified by observing the developed plates under UV at wavelengths of 254 and 366 nm using a UV lamp (CAMAG, Switzerland), followed by visual interpretation after vanillin/sulphuric acid spray reagent was applied and heated up to a temperature of 120°C. Table 3.1 provides the different solvent systems used for TLC development of *H. pandurifolium* fractions. Each solvent system is assigned a different code to which each solvent system is referred to from this point forward.

Table 3.1: TLC plate solvent systems

Code	Solvent System	Ratio
A	Hexane : ethyl acetate	90 : 10
B	Hexane : ethyl acetate	85 : 15
C	Hexane : ethyl acetate	80 : 20
D	Hexane : ethyl acetate	50 : 50
E	DCM : methanol	99 : 1
F	DCM : methanol	98 : 2
G	DCM : methanol	96 : 4
H	DCM : methanol	95 : 5
I	DCM : methanol	90 : 10

3.3.2.2 Column Chromatography

The primary method of purification is carried out on silica gel 60 H (Merck, South Africa) followed by further separation using Sephadex LH-20 (Sigma-Aldrich, South Africa) as stationary phases. Mobile phases differed depending on the polarity of the fraction being separated and the type of stationary phase that was selected for separation. Both gradient and isocratic elutions were performed during the purification process.

3.3.3 Spectroscopy

3.3.3.1 Nuclear Magnetic Resonance (NMR) Spectroscopy

NMR spectra were recorded on a Bruker Avance 400 MHz NMR spectrometer (Germany) using deuterated organic solvents. Chemical shifts of proton (¹H) and carbon 13 (¹³C) spectra are reported as δ values in ppm relative to tetramethylsilane (TMS) as an internal reference. 2-Dimensional NMR was used for compounds displaying interesting structures and biological activities.

3.3.3.2 Gas Chromatography/Mass Spectroscopy (GC/MS)

Mass spectral data was obtained using an Agilent 7820 GC-MS. Samples were dissolved in methanol and injected with an injection volume of 1 μL . Initial column temperature was set to 60 $^{\circ}\text{C}$ with a hold time of 2 minutes. The column temperature was increased at a gradient rate of 3 $^{\circ}\text{C}/\text{min}$ until 280 $^{\circ}\text{C}$ with a total run time of 75 minutes. The front inlet heater was set to 280 $^{\circ}\text{C}$ with a pressure of 13.385 psi. The column flow was set to 1.5 mL/min, with an average velocity of 44.854 cm/sec.

3.3.3.3 Ultraviolet (UV) Spectroscopy

UV spectroscopy has proven to be a useful tool in the identification of flavonoids. The shifts in the wavelength of maximum absorption (λ_{max}) under various conditions have been well documented for flavonoid spectra and studied to such an extent that it is possible to deduce the positions of hydroxy and methoxy functional groups on the flavonoid backbone (Mabry et al., 1970). The various reagents used in the determination of flavonoid structures were of analytical grade. The UV analysis was performed using Molecular Devices Spectra Max i3X between the wavelength range of 230-500 nm measured at 10 nm intervals. The software used was SoftMax Pro 7.0 and clear 96-well microplates (Greiner, height 14,8 mm) were used to perform the analysis.

UV Reagent Preparation

Preparation of UV spectroscopy reagents: HPLC grade methanol (> 99%) was used as the primary solvent in the determination of the pure flavonoid spectrum, where approximately 0,1 mg of the pure compounds (C1 – C4) was dissolved into 10 mL of methanol such that the major absorption peaks between 250 and 400 nm gave an optical density reading between 0,6 and 0,8. 100 μL of the sample stock solution was injected into the wells for analysis after which the reacting solutions (5 μL) were added to alter the UV spectrum. The sodium methoxide solution (NaOMe reagent) was made by dissolving 4,337 g of sodium hydroxide (Sigma-Aldrich) to 100 mL of methanol. This was stirred on a magnetic stirrer and filtered through Whatman filter paper (Grade 1, 110 mm \varnothing) before being stored. The aluminium chloride solution (AlCl_3 reagent) was made up by the addition of 0,99 g AlCl_3 to 20 mL methanol, stirred and filtered as with the NaOMe reagent. The hydrochloric acid (HCl) solution was prepared by careful addition of 50 mL concentrated HCl to 100 mL methanol, resulting in a total volume of 150 mL and stored in a glass stoppered bottle. Anhydrous powdered reagent grade sodium acetate (NaOAc) was used. The boric acid (H_3BO_3) reagent was prepared by saturating 50 mL of methanol with 5,3 g H_3BO_3 such that the boric acid crystals did not fully dissolve in solution.

UV Analysis Procedure

100 μL of the pure flavonoid stock solutions (C1-C4) were injected into a 300 μL capacity clear 96-well microplate (Greiner, height 14,8 mm) and spectra measured between the wavelengths 230-500 nm at 10 nm intervals (Molecular Devices Spectra Max i3X). To the same well, 5 μL of the NaOMe reagent was added and spectra measured immediately after. After 10 min the spectrum was measured again to check for flavonoid decomposition. The solution was then discarded. To a fresh 100 μL of flavonoid stock solutions, 5 μL of the AlCl_3 reagent was added and spectra measured immediately. The AlCl_3/HCl spectrum was attained after the addition of 5 μL HCl solution to the same wells. Solutions were discarded after the measurement. The NaOAc spectrum was measured immediately after the addition of 5 μL of the NaOAc reagent to 100 μL of flavonoid stock solutions and a second run was performed after 10 min to check for flavonoid decomposition. To these wells 5 μL of the H_3BO_3 reagent was added and spectra measured to obtain the NaOAc/ H_3BO_3 spectrum. The solutions were discarded after use.

3.4 General Experimental Procedures for the Antioxidant and Biological Assays

3.4.1 Reagents and Solvents

Folin-Ciocalteu reagent (Sigma-Aldrich, South Africa), phosphomolybdate, phosphotungstate, sodium carbonate, gallic acid, TPTZ (2,4,6-Tri(2-pyridyl)-s-triazine), FeCl_3 , acetic acid, sodium acetate, L-ascorbic acid, ABTS (2,2'-azino-bis(3-ethylbenzothiazoline-6-sulfonic acid), Trolox (6-hydrox-2,5,7,8-tetramethylchroman-2-carboxylic acid), α -glucosidase enzyme, α -amylase enzyme, maleic acid, sodium chloride, calcium chloride, sodium azide solution, sodium hydroxide and DNS (3,5-dinitrosalicylic acid) were all purchased from Sigma-Aldrich, South Africa. Potassium peroxydisulfate, methanol (HPLC grade > 99%) were purchased from Merck, South Africa

3.4.2 Antioxidant Assays

3.4.2.1 Total Polyphenolic Content Determination (Folin-Ciocalteu assay)

The Folin-Ciocalteu reagent used was purchased from Sigma-Aldrich, South Africa. A 1:10 dilution of the Folin-Ciocalteu reagent was made up into a vial. A sodium carbonate reagent was then made up in H_2O at a concentration of 7.5 %. Gallic acid was used as the standard and 6 standard stock solutions were made up in H_2O within the concentration range of 0-500 mg/L. Into a 96-well clear visible range microplate, 25 μL of each standard stock solution and sample were transferred, followed by 125 μL of the Folin-Ciocalteu reagent and 100 μL of the Na_2CO_3 solution into each well. Each concentration of the stock solutions and samples was measured in triplicate. The plate was allowed to stand for 2 hours before being read at a wavelength of 765 nm in the plate reader (Molecular Devices Spectra Max i3X). The results

are reported as milligram gallic acid equivalents per gram (mg GAE/g) of the dry weight test samples.

3.4.2.2 Ferric-ion Reducing Antioxidant Power (FRAP) Assay

The FRAP mechanism is based on electron transfer rather than hydrogen atom transfer and is based on the ability of phenols to reduce Fe^{3+} to Fe^{2+} ions by transferring an electron. The reaction is carried out at a pH of 3.6 to maintain iron solubility and to decrease the ionization potential that drives hydrogen atom transfer. As a result the redox potential increases resulting in electron transfer being the dominant mechanism (Cerretani & Bendini, 2010). Fe^{2+} in the presence of TPTZ (tripiryridyl triazine) forms a coloured complex ($\lambda_{\text{max}} = 593 \text{ nm}$) which can then be measured using a spectrophotometer to determine the extent of iron reduction by the sample.

The FRAP reagent is prepared using a combination of pre-prepared stock solutions namely the FeCl_3 solution, the TPTZ solution, and the acetate buffer solution. The FeCl_3 solution was prepared by dissolving 0,053 g FeCl_3 into 10 mL H_2O . The TPTZ solution was prepared by dissolving 0,0186 g TPTZ into 6 mL of a 0,1 M HCl solution. The acetate buffer solution was prepared using acetic acid and the conjugate base sodium acetate such that the buffer solution maintained a pH of 3.6. The FRAP reagent was prepared by combining 3 mL of the FeCl_3 solution, 3 mL of the TPTZ solution, 30 mL of the buffer solution, and 6 mL H_2O into a 50 mL test tube. Into a 96-well clear visible range microplate, 10 μL of the isolated compound stock solutions (**C1** and **C4** = 1 mg/mL; **C2** = 0,0625 mg/mL; **C3** = 0,25 mg/mL), as well as the total extract (1 mg/mL) were added into separate microplate wells in triplicate and then mixed with 300 μL of the FRAP reagent. The standard calibration curve was obtained using L-ascorbic acid (Sigma Aldrich, South Africa) as a standard. The concentration range was made up between 0 mg/L (blank) and 500 mg/L L-ascorbic acid for analytical measurement, where each concentration of L-ascorbic acid was measured in triplicate. Epigallocatechingallate (EGCG) was used as a reference standard. The microplate was incubated at room temperature for 30 min, after which the plate was read in a Molecular Devices Spectra Max i3X at a wavelength of 593 nm. The results were reported as μmol ascorbic acid equivalents per gram (μmol AAE/g) of the dry weight test samples.

3.4.2.3 Trolox Equivalent Absorbance Capacity (TEAC) Assay

The TEAC assay measures the ability of antioxidants to scavenge free radicals. In this assay, the stable free radical $\text{ABTS}^{\cdot+}$ (2,2'-azino-bis(3-ethylbenzothiazoline-6-sulfonic acid)), is a blue-green chromophore ($\lambda_{\text{max}} = 734 \text{ nm}$) which in the presence of antioxidants decreases its absorption intensity. This occurs by the antioxidants' neutralisation of free radicals either by direct reduction (electron transfer) or by hydrogen atom donation. The balance between these

two mechanisms is usually determined by the antioxidant structure and the pH of the reaction medium (Zhong & Shahidi, 2015).

The working solution was prepared by combining two pre-prepared stock solutions namely; 7 mM ABTS and 140 mM potassium-peroxodisulfate ($K_2S_2O_8$) (Merck, South Africa). To 5 mL of the ABTS solution, 88 μ L of $K_2S_2O_8$ solution was added, mixed thoroughly and then allowed to react in the absence of light for 24 hours. Trolox (6-hydroxy-2,5,7,8-tetramethylchroman-2-carboxylic acid), a water-soluble analogue of vitamin E, was used as the standard to obtain the standard calibration curve (see appendix 1-3) with the concentration range between 0 mg/L and 500 mg/L. Into a 96-well clear microplate, 25 μ L of the isolated compound and total extract stock solutions (1 mg/mL) were added in triplicate wells with 275 μ L of the working solution and allowed to react in the absence of light at room temperature for 30 min. Epigallocatechingallate (EGCG) was used as a reference standard. The absorbance was measured at 25°C at a wavelength of 734 nm in the plate reader. Final results are reported as μ mol Trolox equivalents per gram (μ mol TE/g) of the dry weight test samples.

3.4.3 Anti-diabetic Studies

3.4.3.1 α -Glucosidase Inhibition

Into a 96-well clear microplate, 50 μ L of the α -glucosidase phosphate buffer solution (pH 6.5) was added to all wells. 10 μ L of the α -glucosidase enzyme solution was added to the odd-numbered wells and 10 μ L of the phosphate buffer solution added to the even-numbered wells. To the designated control wells 20 μ L of methanol (HPLC grade > 99%) was added and 20 μ L of the sample stock solutions (concentration range of 1 mg/mL to 0,125 mg/mL) were added in triplicate. The plate was then incubated at 37°C for 15 min. 20 μ L of the substrate solution was added to the wells containing enzyme and 20 μ L of the phosphate buffer solution was added to the remaining wells to keep the total volume constant. The plate was incubated for a further 20 min at 37,5°C after which 50 μ L of the stop solution (Na_2CO_3) was added to all wells. The absorbance was measured at 25°C at a wavelength of 405 nm in the plate reader (Molecular Devices Spectra Max i3X). Acarbose was used as a positive control.

Final results are reported as the half-maximal inhibitory (IC₅₀) concentration in μL/mL. Here, the difference between the absorbance of the enzyme-containing well and blank is calculated. The percentage inhibition was then calculated (equation 3.1, where: A = difference absorbance sample; B = difference blank average) along with the average absorbance of the blank differences. The average percentage inhibition for each sample was calculated at varying concentrations and plotted against sample concentration to obtain a best fit straight line from which the IC₅₀ is calculated by substituting the percentage inhibition variable with 50 (y = 50) in the best straight-line formula (equation 3.2, where: y = average % inhibition; x = concentration (ug/mL); m = gradient; c = intercept). The standard deviation of the IC₅₀ was calculated using equation 3.3, where σ = standard deviation, x_i = observed measurement (absorbance - blank), μ = population mean and N = population size.

$$\% \text{ inhibition} = \frac{B - A}{B} \times 100$$

Equation 3.1: Percent inhibition equation

$$y = mx + c$$

Equation 3.1: General straight-line formula

$$\sigma = \sqrt{\frac{\sum(x_i - \mu)^2}{N}}$$

Equation 3.3: Standard deviation formula

3.4.3.2 α-Amylase Inhibition

Into a 96-well clear microplate 50 μL of the α-amylase buffer solution (maleic acid, sodium chloride, calcium chloride, and sodium azide solution adjusted to pH 6.5 using sodium hydroxide) was added to all wells. 10 μL of the α-amylase enzyme solution was added to the odd-numbered wells and 10 μL of the buffer solution added to the even-numbered wells. To the designated control wells, 20 μL of methanol (HPLC grade > 99%) was added and 20 μL of the sample stock solutions (concentration range between 4 mg/mL to 0,03125 mg/mL) were added in triplicate. The plate was then incubated at 37,5°C for 15 min after which 20 μL of the starch solution was added to all the wells. The plate was then incubated for a further 20 min at 37,5°C. 50 μL of the DNS reagent (3,5-dinitrosalicylic acid) was added to stop the reaction and react with the reducing sugars. The plate was then incubated in a covered casing and placed

into a water bath at 98,5 °C for 20 min. The absorbance was then measured at a wavelength of 540 nm in the plate reader (Molecular Devices Spectra Max i3X). Acarbose was used as a positive control. Final results are reported as the half-maximal inhibitory (IC₅₀) concentration in µL/mL and calculated in the same fashion as described for α-glucosidase (4.1.3.1).

3.5 Statistical Analysis

All data was imported, graphs plotted (see appendix 1-12), and statistical analysis performed using Microsoft Excel 2019. All *in vitro* measurements were made in triplicate for all of the antioxidant and biological experiments. All IC₅₀ biological data are presented as mean IC₅₀ with standard deviations.

CHAPTER 4: CHEMICAL CHARACTERISATION OF HELICHRYSUM PANDURIFOLIUM AND STRUCTURE ELUCIDATION OF CONSTITUENTS

“Physicists are made of atoms. A physicist is an attempt by an atom to understand itself.”

– Michio Kaku

4.1 Chapter Overview

In this chapter, the method by which the raw plant material was extracted is described. The details as to how the total extract was separated using column chromatography is reported, and the isolation procedures for four pure phytochemicals are documented. The analytical techniques used to determine the structures of four isolated flavonoids are reported with all the relevant spectroscopic data, and explanations as to how the compound structures were elucidated are described in detail.

4.2 Extraction and Fractionation of Total Extract

The aerial parts (leaves and flowers) with a mass of 374.5 g were allowed to dry at room temperature. The plant material was blended and extracted twice-fold using methanol in a water bath at 40 °C for 24 hours. The methanol extracts were then filtered and washed using methanol in a Buchner funnel and evaporated to dryness using a rotary evaporator at 50 °C. The total extract obtained was 42.20 g (11.27% yield).

A sample of the total extract of *H. pandurifolium* was kept for reference in a separate vial (>1 g). The remaining extract was applied to silica gel column (height 70 cm, radius 5.5 cm, 6.6 L volume) with a dead volume of 1.8 L. The sample was eluted using a gradient elution of hexane, ethyl acetate, and methanol as indicated in table 4.1. Fifty fractions of 500 mL were collected and combined according to observations of TLC plate analysis. The result was twelve main fractions (figure 4.1) which are summarized in table 4.2. Main fractions were labelled using roman numerals (I-XII).

Table 4.1: Solvent System used for the Fractionation of the *H. pandurifolium* methanol extract

Solvent system	Ratio of solvents	Volume of solvent	Fractions collected
Hexane	100%	2 L	1 – 4
Hexane : ethyl acetate	90 : 10	2 L	5 – 8
Hexane : ethyl acetate	70 : 30	2 L	9 – 12
Hexane : ethyl acetate	50 : 50	2 L	13 – 16
Hexane : ethyl acetate	30 : 70	2 L	17 – 20
Hexane : ethyl acetate	10 : 90	2 L	21 – 24
Ethyl acetate	100%	2 L	25 – 28
Ethyl acetate : methanol	90 : 10	2 L	29 – 32
Ethyl acetate : methanol	70 : 30	2 L	33 – 36
Ethyl acetate : methanol	50 : 50	2 L	37 – 40
Ethyl acetate : methanol	30 : 70	2 L	41 – 44
Ethyl acetate : methanol	10 : 90	2 L	45 – 48
Methanol	100%	1 L	49 – 50

Table 4.2: Main fractions from *H. pandurifolium* total extract

Main fraction	Combined fractions	Weight
I	1 – 4	0.7852 g
II	5 – 7	0.5007 g
III	8 – 11	3.9816 g
IV	12	5.8751 g
V	13 – 15	5.2837 g
VI	16 – 20	8.1683 g
VII	21 – 24	2.0010 g
VIII	25 – 31	1.3453 g
IX	32 – 35	1.2613 g
X	36 – 39	3.3126 g
XI	40 – 43	5.5756 g
XII	44 – 50	4.1753 g

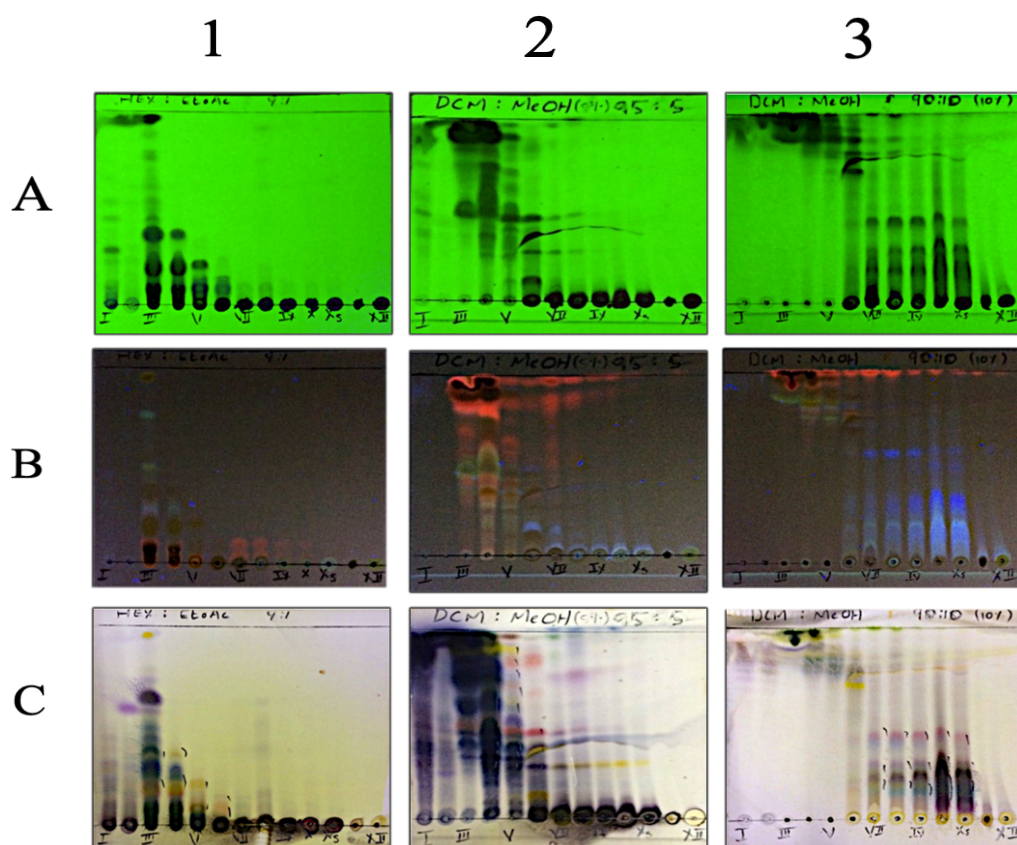


Figure 4.1: TLC profile of main fractions under UV (254/366 nm; Fig. 4.1A and Fig. 4.1B respectively), and after spraying with H_2SO_4 /vanillin followed by heating (Fig. 4.1C). TLC plates 1, 2 and 3 were developed using solvent systems A, H and I (section 3.3.2.1) respectively. Silica gel TLC plate was used.

4.3 Isolation of Pure Compounds

In this section, the detailed steps taken to obtain pure compounds from main fractions are described. Sub-sections are presented in order of increasing main fraction polarity.

4.3.1 Isolation of Compound C1 - Column Chromatography of Main Fraction III

The main fraction III (3.9816 g) was subjected to a medium sized silica gel column (90 X 2.5 cm, 1.76L volume) and filtered using a gradient elution of hexane and ethyl acetate as indicated below in table 4.3. Thirty-four fractions were collected and then combined according to their TLC profile (figure 4.2) using solvent system E. The result was twelve sub-fractions which are summarised in table 4.4.

Table 4.3: Solvent System used for the Fractionation of the main fraction III

Solvent system	Ratio of solvents	Volume of solvent	Fractions collected
Hexane	100%	1 L	1 – 4
Hexane : ethyl acetate	98 : 2	1 L	5 – 8
Hexane : ethyl acetate	96 : 4	1 L	9 – 12
Hexane : ethyl acetate	94 : 6	1 L	13 – 16
Hexane : ethyl acetate	92 : 8	1 L	17 – 20
Hexane : ethyl acetate	90 : 10	1 L	21 – 24
Hexane : ethyl acetate	85 : 15	0.2 L	25
Hexane : ethyl acetate	80 : 20	0.2 L	26
Hexane : ethyl acetate	50 : 50	0.2 L	27
Ethyl acetate	100%	0.6 L	28 – 30
Methanol	100%	0.8 L	31 – 34

Table 4.4: Sub-fractions obtained from main fraction III

Sub-fraction	Combined fractions
1	1 – 3
2	4 – 8
3	9 – 10
4	11 – 14
5	15 – 16
6	17 – 19
7	20 – 23
8	24 – 25
9	26 – 28
10	29 – 31
11	32 – 34
12	44 – 50

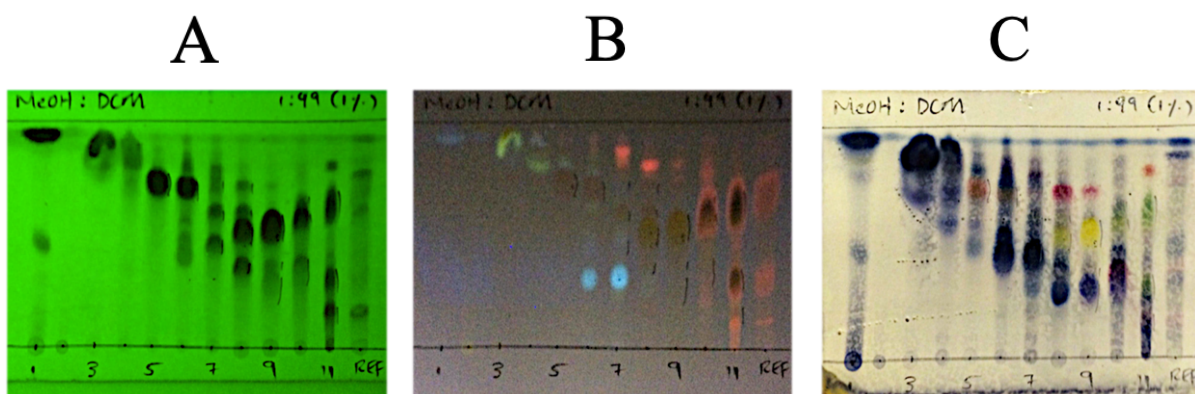


Figure 4.2: TLC profile of the sub-fractions of main fraction III under UV (254 and 366 nm; Plates A and B respectively), and after spraying with H_2SO_4 /vanillin followed by heating (Plate C). Silica gel TLC plates were developed using solvent system E (section 3.3.2.1)



Figure 4.3: Pure crystals of compound **C1**

C1 (± 60 mg) was obtained via the crystallization of sub-fractions III-5 and 6 (where III-5 represents the 5th sub fraction of main fraction III). Sub-fractions III-5 and 6 were dissolved in methanol and allowed to evaporate slowly at atmospheric pressure. After the evaporation of methanol had completed, yellow crystals were found to be suspended in an orange mother liquor. The mother liquor was dissolved in cold hexane and crystals of **C1** were collected. The **C1** crystals were insoluble in ethyl acetate and only sparingly

soluble in acetone (figure 4.3). **C1** crystals were also obtained by the same procedure from the sub-fraction IV-9, and all crystals were combined together for further analysis.

4.3.2 Isolation of Compound C2 - Column Chromatography of Main Fraction IV

The main fraction IV (5.8751 g) was subjected to a medium-sized silica gel column (90 X 2.5 cm, 1.76 L volume) and eluted using a gradient solvent of hexane and ethyl acetate as indicated below in table 4.5. One hundred and eighty-nine fractions were collected

Table 4.5: Fractionation of the main fraction IV

Solvent system	Ratio of solvents	Volume of solvent
Hexane	100%	1 L
Hexane : ethyl acetate	98 : 2	0.5 L
Hexane : ethyl acetate	95 : 5	1.1 L
Hexane : ethyl acetate	93 : 7	0.5 L
Hexane : ethyl acetate	92 : 8	0.5 L
Hexane : ethyl acetate	91 : 9	0.5 L
Hexane : ethyl acetate	90 : 10	1 L
Hexane : ethyl acetate	89 : 11	0.5 L
Hexane : ethyl acetate	88 : 12	0.9 L
Hexane : ethyl acetate	85 : 15	0.5 L
Hexane : ethyl acetate	80 : 20	1 L
Hexane : ethyl acetate	75 : 25	0.5 L
Hexane : ethyl acetate	50 : 50	0.5 L
Ethyl acetate	100%	0.5 L

and then combined according to their profile on the TLC plate using solvent systems B and C (figure 4.4). Twenty-four were obtained as summarised in table 4.6.

Table 4.6: Sub-fractions obtained from main fraction IV

Sub-fraction	Combined fractions	Sub-fraction	Combined fractions
1	1 – 32	13	93 – 96
2	33 – 38	14	97 – 120
3	39 – 50	15	121 – 124
4	51 – 55	16	125 – 129
5	56 – 57	17	130 – 139
6	58 – 62	18	140 – 144
7	63	19	145 – 152
8	64 – 67	20	153 – 156
9	68 – 76	21	157 – 161
10	77 – 84	22	162 – 164
11	85 – 87	23	165 – 168
12	88 – 92	24	169 – 189

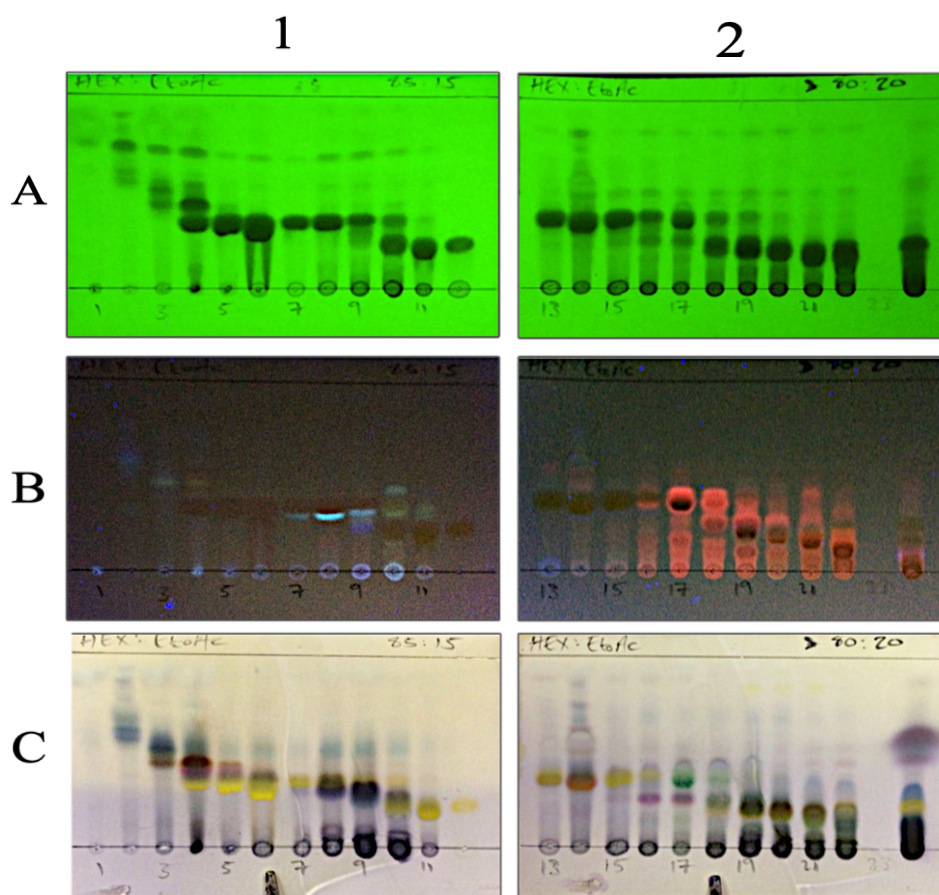


Figure 4.4: TLC profile of the sub-fractions of main fraction IV under UV (254 and 366 nm; Plates A and B respectively), and after spraying with H_2SO_4 /vanillin followed by heating (Plate C). Silica gel TLC plates 1 and 2 were developed using solvent system B and C (section 3.3.2.1) respectively



Figure 4.5: Pure crystals of compound **C2**

C2 (± 100 mg) was obtained via crystallisation of sub-fractions 12, 13 and 14. In each case, individual sub-fractions were dissolved in methanol and allowed to evaporate slowly. In the case of sub-fraction 13, large orange crystals were found to be suspended in yellow oily mother liquor. These were carefully removed and washed using cold MeOH. Figure 4.5 presents an image of the orange crystals (**C2**) obtained.

It is not uncommon to find that main fractions often contain the same compounds after combination. It is thus possible to isolate the same compound from neighbouring MAIN fractions when larger quantities of the pure compound are required. With that being said, it should be noted that **C2** was also obtained from main fraction III via the fractionation of subfraction III-9 which involved two subsequent column chromatography methods. The first being the fractionation of III-9 on a medium sized silica gel column (90 X 2.5 cm, 1.76L volume) with gradient elution mobile phase of hexane:ethyl acetate (100% hexane, 200 mL; 98:2, 200 mL; 96:4, 200 mL; 90:10, 1L; 100% ethyl acetate, 1L). The collection volume was approximately 50 mL, resulting in 36 sub-fractions. These were combined according to their TLC profile (figure 4.6). The sub-fraction III-9-7 obtained afforded crystal growth after slow evaporation in MeOH.

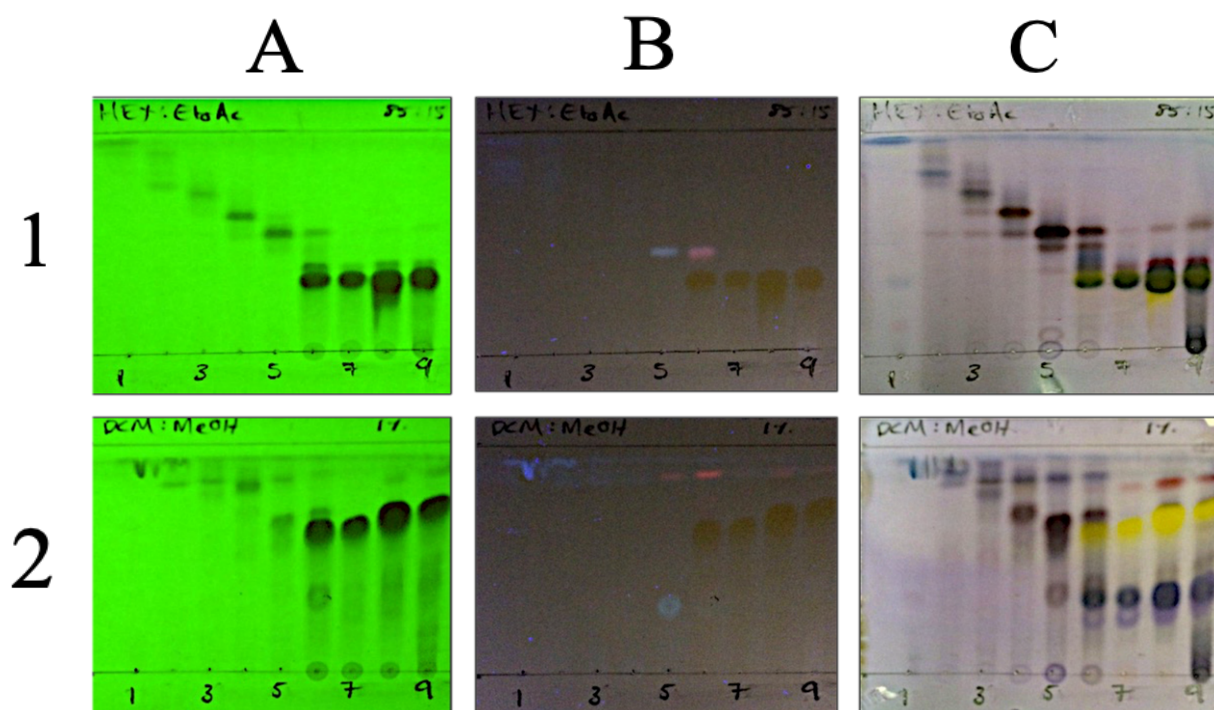


Figure 4.6: TLC profile of the sub-fraction III-9 after silica gel column chromatography under UV (254 and 366 nm; Plates A and B respectively), and after spraying with H_2SO_4 /vanillin followed by heating (Plate C). TLC plates 1 and 2 developed using solvent system B and E (section 3.3.2.1)

The second purification step involved a series of small sephadex columns (70 X 1.25 cm, 0.34L volume) involving the sub-fractions III-9-7/8 (20 mg loaded per column) using mobile phase methanol:water (95:5). This resulted in obtaining more of the pure compound **C2**. The subsequent column fractions were combined according to the TLC plate analysis (figure 4.7) to get the pure compound **C2** (\pm 18 mg).

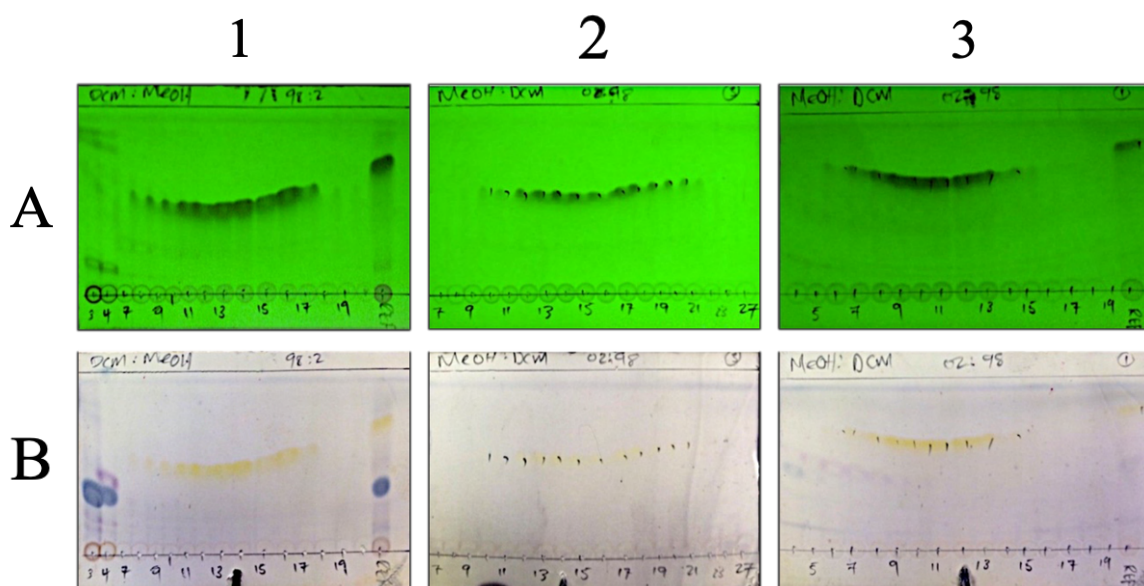


Figure 4.7: TLC profile of the sub-fraction III-9-7/8 after silica gel column chromatography under UV (254 nm; Plates A), and after spraying with H_2SO_4 /vanillin followed by heating (Plate B). TLC plates 1, 2 and 3 were developed using solvent system F (section 3.3.2.1)

4.3.3 Isolation of Compounds C3 and C4 - Column Chromatography of Main Fraction VI

The main fraction VI (8.1683 g) was subjected to a medium-sized silica gel column (height 90 cm, radius 2.5 cm, 1.76L volume) using a gradient elution of hexane and ethyl acetate as indicated in table 4.9. One hundred and thirty-nine fractions were collected into round bottom flasks of approximately 100 ml per collection. The fractions collected during the separation were concentrated using vacuum evaporation at 50 °C and transferred into test tubes for TLC analysis. The resulting fractions were numbered 1 to 139. These were then combined according to the observation attained from TLC plate analysis using solvent system D (figure 4.11). The result was twenty-one subfractions which are summarized in table 4.10.

Table 4.7: Fractionation of the main fraction VI

Solvent system	Ratio of solvents	Volume of solvent	Fractions collected
Hexane	100%	1 L	1 – 10
Hexane : ethyl acetate	90 : 10	1 L	11 – 20
Hexane : ethyl acetate	80 : 20	1 L	21 – 30
Hexane : ethyl acetate	70 : 30	1 L	31 – 40
Hexane : ethyl acetate	60 : 40	2 L	41 – 60
Hexane : ethyl acetate	50 : 50	7 L	61 – 130
Methanol	100%	1 L	130 – 139

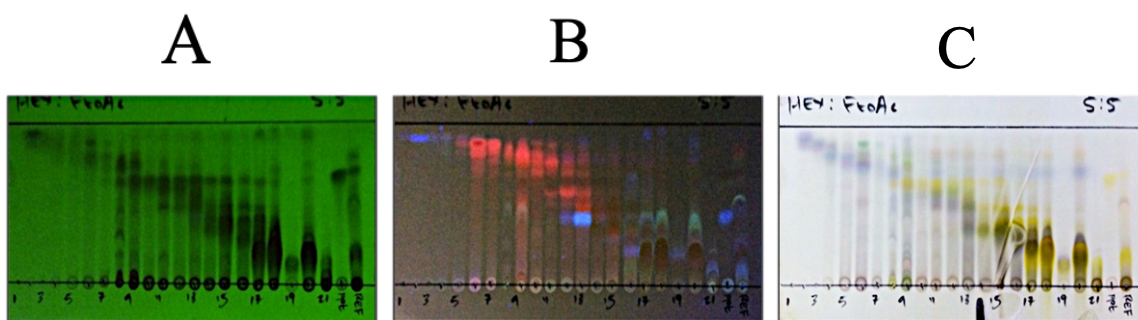


Figure 4.8: TLC profile of the sub-fractions of main fraction VI under UV (254 nm and 366 nm; Plates A and B respectively), and after spraying with H_2SO_4 /vanillin followed by heating (Plate C). TLC plate was developed using solvent system D (section 3.3.2.1)

Table 4.8: Sub-fractions from main fraction VI

Sub-fraction	Combined fractions	Sub-fraction	Combined fractions
1	1 – 3	12	55 – 58
2	4 – 10	13	59 – 70
3	11 – 13	14	71 – 76
4	14 – 17	15	77 – 86
5	18 – 19	16	87 – 95
6	20 – 25	17	96 – 100
7	26 – 27	18	101 – 109
8	28 – 38	19	110 – 130
9	39 – 44	20	132
10	45 – 47	21	133 – 138
11	48 – 54		

C3 (\pm 132 mg) was obtained after sub-fractions 18, 19 and 20 were combined and chromatographed using a medium sized sephadex column (height 90 cm, radius 3.5 cm, 0.86L volume), mobile phase being methanol:water (95:5). Collection volumes were approximately 2 mL and collected into small glass test tubes. Figure 4.9 shows the isolation of pure **C3** after TLC plate analysis confirmed purity. **C3** was obtained after combinations of sub-fractions 24-32 (figure 4.9).

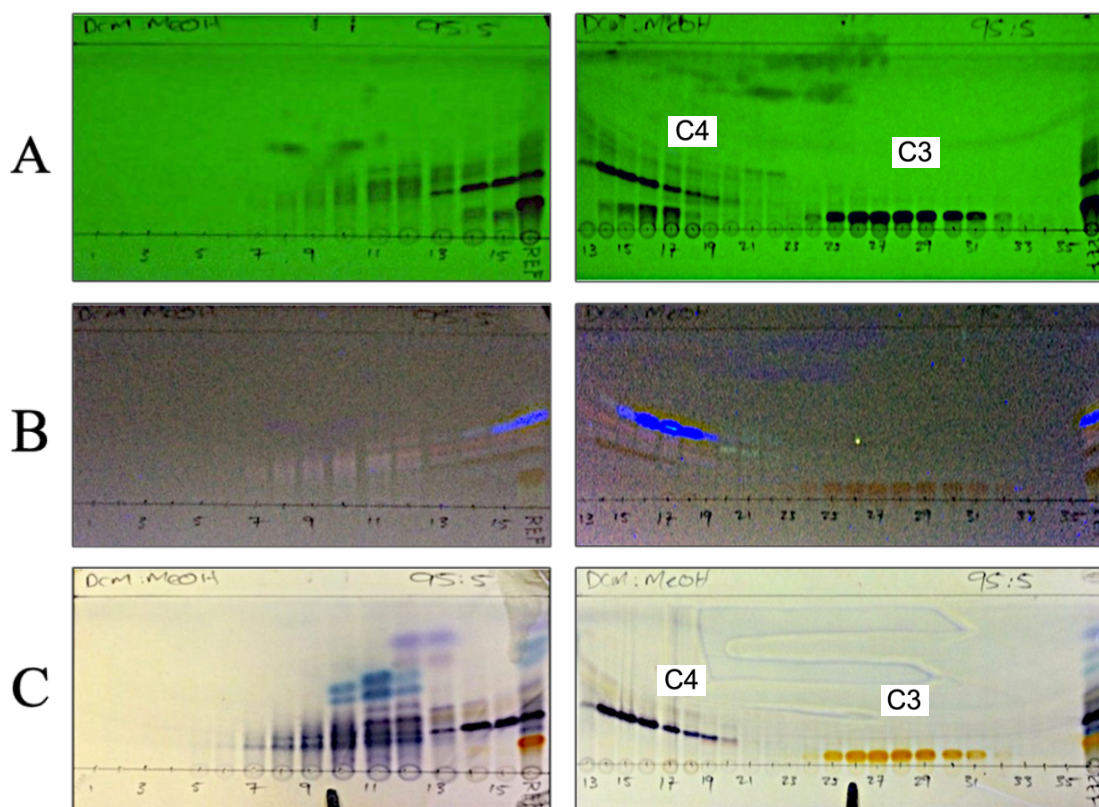


Figure 4.9: TLC profile of the sub-fractions of VI-18 under UV (254 nm and 366 nm; Plates A and B respectively), and after spraying with H₂SO₄/vanillin followed by heating (Plate C). TLC plates were developed using solvent system H (section 3.3.2.1)

Sub-fractions 13-22 containing compound **C4** were combined and subjected to prep TLC separation. Approximately 10 mg of the mixture was applied using a small glass pipette to multiple separate 10 X 20 cm TLC plates. Plates were developed using 4% MeOH:DCM as the solvent (figure 4.10). Each plate was first developed halfway, and then allowed to dry before being developed completely to afford greater separation of peaks. Each band was carefully scratched off the surface of the TLC plate and washed with methanol to recover the compounds. Band 3 (figure 4.10) from the prep TLC plate separation was then subjected to a small sephadex column (height 70 X 1.25cm, 0.34L volume) using 5% water in methanol as the mobile phase. The resulting TLC plate revealed a two component mixture (figure 4.11), and subfractions 8-13 were combined to obtain **C4**. Over time it was observed that the two component mixture was a result of the degradation of compound **C4** breaking down, and ultimately one last prep TLC plate had to be performed to purify **C4** (\pm 20 mg) before NMR analysis and biological activity studies.

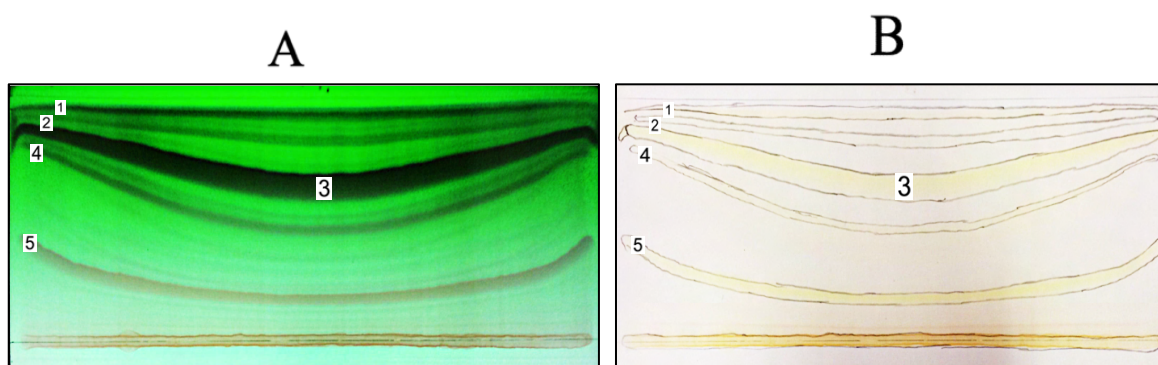


Figure 4.10: Prep TLC plates of subfractions 13-22 after separation with 4% MeOH:DCM, where band 3 contains compound C4

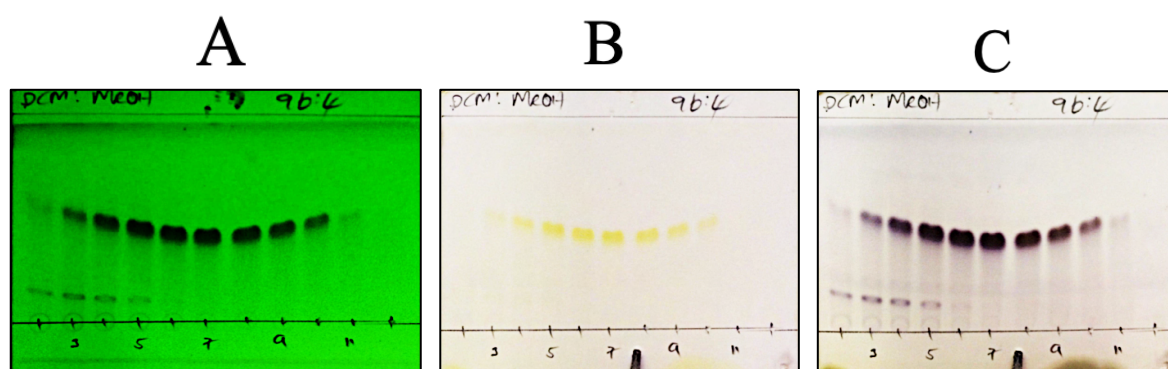


Figure 4.11: TLC profile of the band 3 after sephadex separation under UV (Plate A; 254 nm), under normal light (Plate B) and after spraying with H_2SO_4 /vanillin followed by heating (Plate C). TLC plates were developed using solvent system G (section 3.3.2.1).

4.4 Chemical Evaluations: Results and Discussion

The structure elucidation of four isolated phytochemicals is summarised and described in detail. Through the use of UV spectroscopy, NMR and GC/MS analysis, a total of four flavonoids were identified.

4.4.1 Summary of the Isolated Compounds

The methanolic extract of *H. pandurifolium* was subjected to a series of silica gel columns, followed by Sephadex LH-20 columns (scheme 4.1), resulting in four pure compounds (flavonoids).

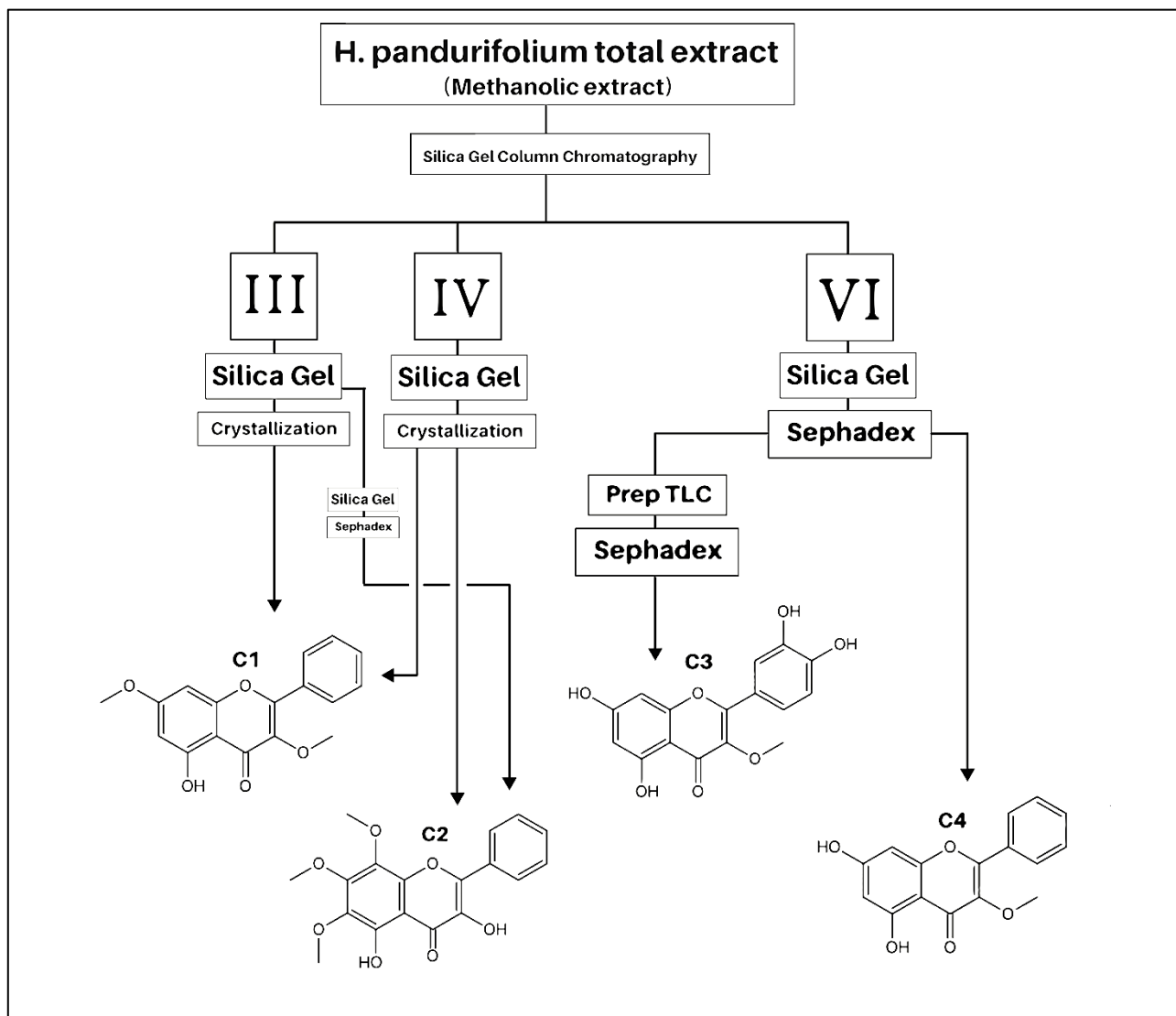


Figure 4.12: Flow diagram summarising the isolation procedure of phytochemicals from *H. pandurifolium*

4.4.2 Summary of Spectral Data of Isolated Flavonoids

The isolated compounds **C1-C4** were assigned structures based on NMR, UV, and MS spectroscopic analysis as discussed in detail in the following sections. The structural elucidation revealed that the compounds **C1**, **C3** and **C4** were found to be methylated derivatives of flavonols. Below are two tables (tables 4.9 and 4.10) summarising the UV and NMR spectroscopic data which are used to aid in the structure elucidation of isolated flavonoids.

4.4.2.1 UV Spectrums of Isolated Flavonoids

The preparation of reagents and UV analysis procedures were described in Chapter 3 (3.3.3.3). The UV spectrums are presented in sections 4.4.2.3 – 4.4.2.7 whereas table 4.9 reports the UV spectral data obtained for each isolated flavonoid. The spectral data is presented as absorbance against wavelength and is compared in the analysis of each isolated flavonoid. The preparation of reagents and UV analysis procedure was described in Chapter 3 (3.3.3.3). Physical spectrums are presented in sections 4.4.2.3 – 4.4.2.7 where spectrums are presented as absorbance against wavelength and are compared in the analysis of each isolated flavonoid. Reference to each band label is presented in figure 4.13.

Table 4.9: UV spectral analysis of pure compounds (λ_{max} for each band)

	C1			C2			C3			C4		
	Band lb	Band la	Band II	Band lb	Band la	Band II	Band lb	Band la	Band II	Band lb	Band la	Band II
MeOH	310	330	270	320	375	280	360	-	260	320sh	-	270
NAOME	-	380	280	340	420	260	335	400	270	370	-	280
ALCL₃	330	395	280	365	430	280	365	420	270	330	400	280
ALCL₃/HCL	330	395	280	350	430	280	355	390	270	330	400	280
NAOAC	310	340	270	320	420	270	-	380	270	360	-	270
NAOAC/H₃BO₃	310	330	270	320	380	280	-	375	260	320	-	270

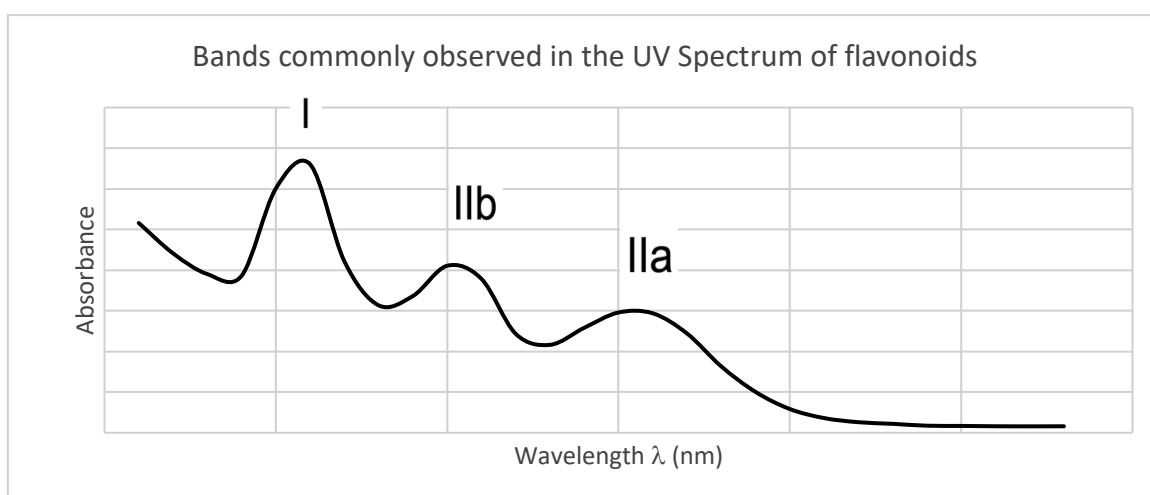


Figure 4.13: Bands observed in the UV spectrum of flavonoids

4.4.2.2. NMR Spectral Data of Isolated Compounds

All the NMR spectra data (table 4.10) was obtained from UWC using a 400 MHz liquid state spectrometer. Compounds **C1** and **C2** were analysed in CDCl₃, **C3** in DMSO and **C4** in (CD₃)₂CO.

Table 4.10: NMR spectral data for of pure compounds **C1-C4**

NO.	C1		C2		C3		C4	
	¹ H	¹³ C	¹ H	¹³ C	¹ H	¹³ C	¹ H	¹³ C
2	-	155.9	-	145.8	-	157.0	-	156.5
3	-	139.7	-	136.6	-	139.1	-	140.4
4	-	178.9	-	176.2	-	179.4	-	179.8
5	-	162.1	-	148.0	-	162.8	-	163.3
6	6.46 d	98.0	-	136.0	6.19 d	99.6	6.26 d	100.0
7	-	165.6	-	153.5	-	165.8	-	166.3
8	6.37 d	92.2	-	133.4	6.41 d	94.6	6,49 d	95.0
9	-	156.5	-	145.4	-	157.9	-	158.3
10	-	106.2	-	105.5	-	105.5		105.9
1`	-	130.5	-	130.9	-	122.6	-	-
2`	8.08 dd	128.4	8.27 s	127.8	7.54 d	116.3	8.06 m	129.4
3`	7.52 m	128.6	7.47 m	128.9	-	146.2	7.56 m	129.7
4`	7.52 m	131.0	7.57 m	130.6	-	149.6	7.56 m	131.9
5`	7.52 m	128.6	7.47 m	128.9	6.90 d	116.2	7.56 m	129.7
6`	8.08 dd	128.4	8.27 s	127.8	7.44 dd	122.0	8.06 m	129.4
OME-3	3.88 s	60.4	-	-	3.77 s	60.3	3.88 s	60.8
OME-6	-	-	3.99 s	61.4	-	-	-	-
OME-7	3.87 s	55.8	3.96 s	62.3	-	-	-	-
OME-8	-	-	4.13 s	61.9	-	-	-	-
5-OH	12.59 s	-	11.45 s	-	12.70 s	-	-	-
3-OH	-	-	6.79 br s	-	-	-	-	-

4.5.1 Structure Elucidation of Compound C1

UV spectral data

The UV spectrum (in methanol) showed absorption with λ_{\max} of 270 nm (Band II) and a shoulder band of 310-330 nm (Bands I-Ia) indicating that the flavone has an unsubstituted B-ring, a free hydroxyl on C-5, and a 3-methylated flavonol (figure 4.14A). The addition of AlCl_3 and HCl (figure 4.14B) to the methanolic UV spectrum resulted in a stable bathochromic shift, suggesting the formation of a stable aluminum complex between the hydroxy group at C-5 and the keto oxygen at position C-4, which does not decompose in the presence of acid. The addition of NaOMe to the methanolic UV spectrum (figure 4.14A) showed a bathochromic shift (50 nm Band Ia and 10 nm Band II) also indicating that a free hydroxy functional group is present within the structure at position C-5. No bathochromic shift was observed for Band II after addition of NaOAc (figure 4.14C), suggesting that position 7 methylated rather than being a free 7-hydroxyl functional group.

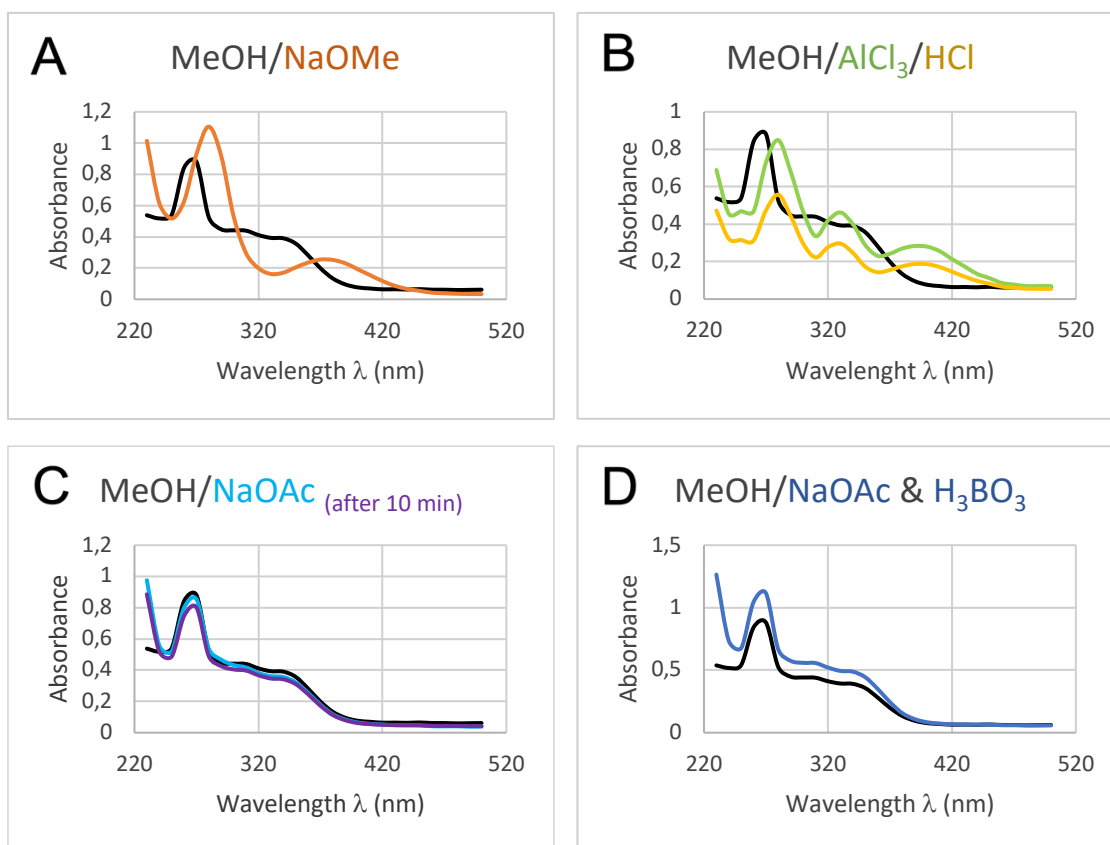


Figure 4.14: UV spectra of compound C1 after addition of various reagents. Black lines represent the methanol spectra. Graph A: Spectrum obtained after addition of NaOMe (orange). Graph B: Spectrum obtained after addition of AlCl_3 (green), followed by the addition of HCl (yellow). Graph C: Spectrum obtained after addition of NaOAc. Measured at two intervals, first immediately (light blue) and second after 10 min (purple) to observe degradation of the flavonoid structure. Graph D: Spectrum obtained after addition of NaOAc and H_3BO_3 (blue)

Mass spec data:

Mass spectroscopy (GC/MS) analysis of **C1** established a mass to charge ratio ($m/z = 297$) corresponding to that of a dimethoxyflavone, in accordance with that observed in the following NMR spectra.

NMR data

^1H NMR (400 MHz, CDCl_3) δ : 12.59 (s, 1H, 5-OH), 8.08 (dd, $J = 7.2, 3.0$ Hz, 2H, H-2', H-6'), 7.52 (t, $J = 2.8$ Hz, 3H, H-3', H-4', H-5'), 6.46 (d, $J = 2.2$ Hz, 1H, 6-H), 6.37 (d, $J = 2.2$ Hz, 1H, 8-H), 3.88 (s, 3H, 3-OCH₃), 3.87 (s, 3H, 7-OCH₃). ^{13}C NMR and DEPT-135 (100 MHz, CDCl_3) δ : 178.9 (C=O, C-4), 165.6 (C-7), 162.1 (C-5), 156.5 (C-9), 155.9 (C-2), 139.7 (C-3), 131.0 (C-4'), 130.5 (C-1'), 128.6 (C-3', C-5'), 128.4 (C-2', C-6'), 106.2 (C-10), 98.0 (C-6), 92.2 (C-8), 60.4 (CH₃, 3-OMe), 55.9 (CH₃, 7-OMe).

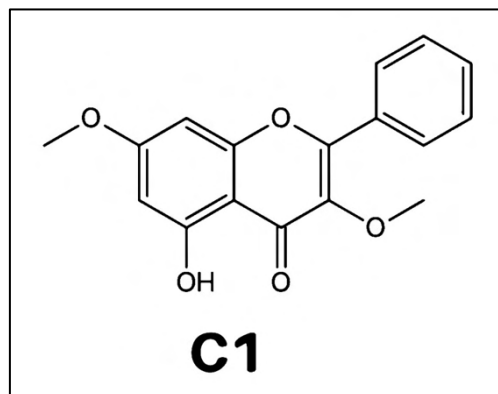


Figure 4.15: Structure of 5-hydroxy-3,7-dimethoxyflavone

The proton NMR (figure 4.16, table 4.12) revealed the presence of two singlets at δ_{H} 3.87 and 3.88 ppm representing two methoxyl groups at positions C-3 and C-7. The spectrum revealed

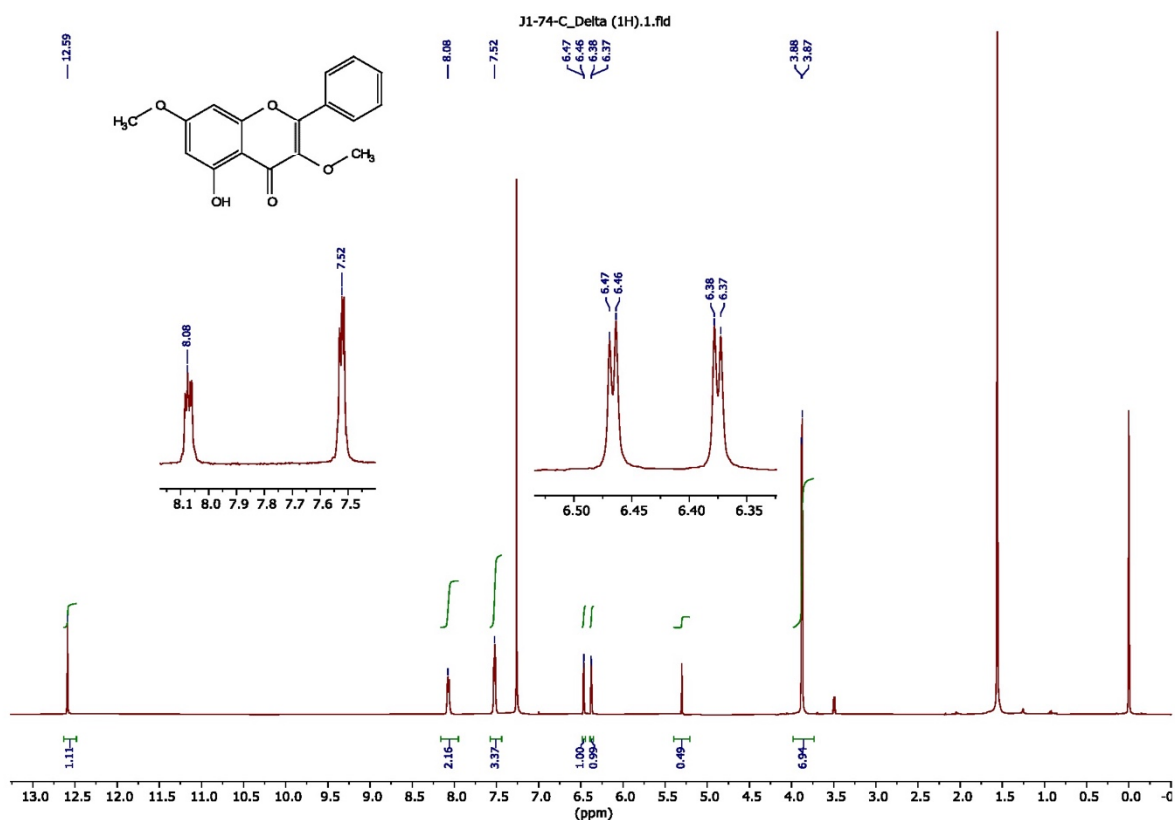


Figure 4.16: ^1H NMR spectrum of compound **C1**

the -ring-B to be unsubstituted and a singlet peak representing a hydroxy group at the C-5 position (δ_{H} 12.59 ppm). Two protons at C-6 and C-8 on ring-A exhibited two doublets at δ_{H} 6.46 and 6.37 ppm respectively. Meta coupling of these two protons was confirmed with characteristic coupling constant $J = 2.2$ Hz as calculated for each doublet.

The ^{13}C spectrum (figure 4.17) revealed a characteristic signal for a keto functional group at 178.9 ppm which was absent in DEPT analysis (figure 4.18), and two methoxyl groups at C-3 and C-7 show peaks at 60.4 and 55.8 ppm respectively in the ^{13}C NMR spectrum.

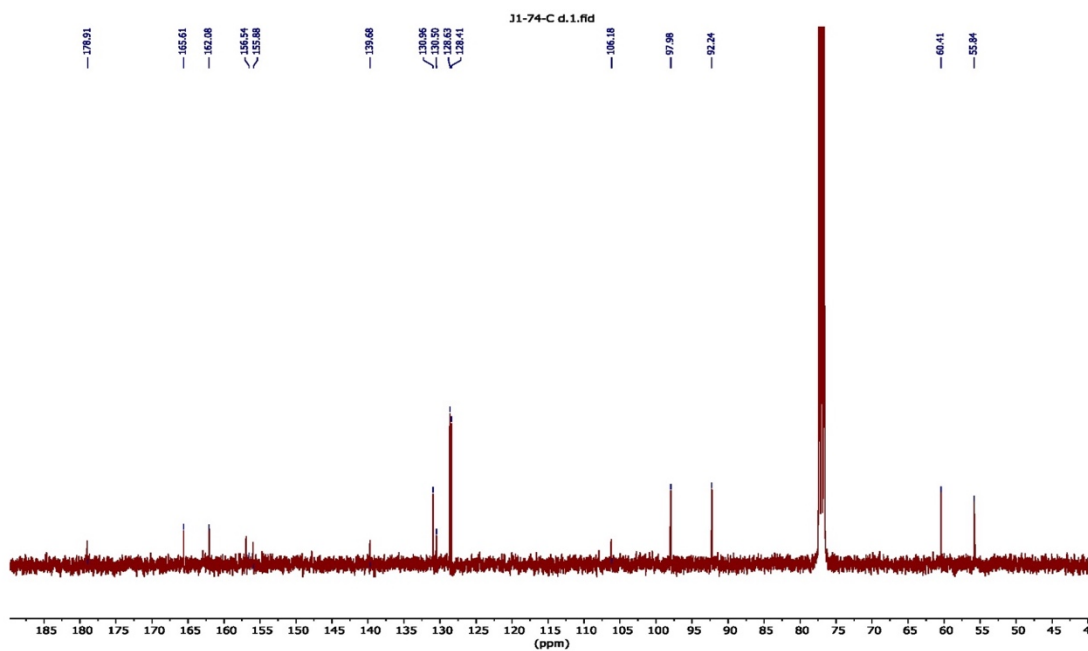


Figure 4.17: ^{13}C spectrum of compound C1

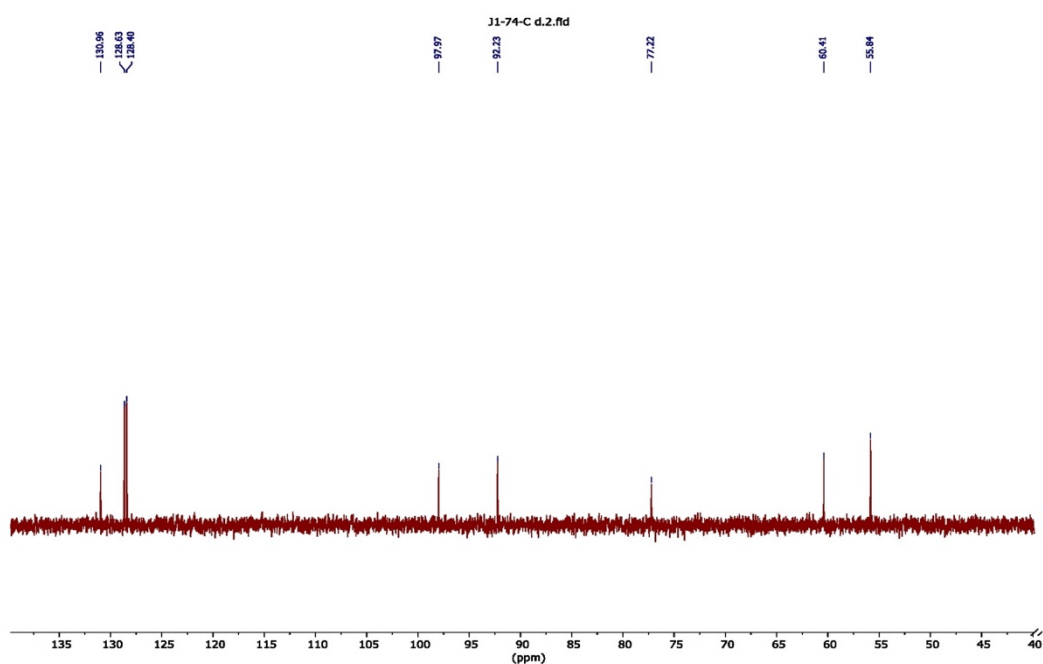


Figure 4.18: DEPT spectrum for compound C1

This analysis corroborated the structure to be 5-hydroxy-3,7-dimethoxyflavone (figure 4.15) and was compared with ^1H NMR and ^{13}C NMR from literature and has been previously isolated from *Kaempferia parviflor* (Sutthanut et al., 2007).

4.5.2 Structure Elucidation of Compound C2

UV spectral data

The 50-60 nm bathochromic shift observed in Band I after addition of NaOMe is usually diagnostic of 3-hydroxyl functional group when no 4'-hydroxyl group is present on ring B (figure 4.19A). Interestingly, Band Ia showed an increase in intensity after addition of NaOMe and an unexplained hypsochromatic shift to Band II. The large ± 30 nm bathochromic shift observed in Band Ib and ± 60 nm shift to Band Ia are diagnostic of aluminium complexes formed between the 3-hydroxyl and 5-hydroxyl groups with the 4-keto functional group (figure 4.19B). These are stable due to the unchanging wavelength observed when HCl is added to the complex. The UV spectra after the addition of sodium acetate (figure 4.19C, table 4.11) indicated that the compound has a substituted 7-hydroxy due to the fact that flavonols containing a free 7-hydroxyl group usually exhibit a bathochromic shift of 5-20 nm in Band II. The UV spectra after the addition of sodium acetate (figure 4.19C, table 4.11) indicated that the compound has a substituted 7-hydroxy due to the fact that flavonols containing a free 7-hydroxyl group usually exhibit a bathochromic shift of 5-20 nm in Band II.

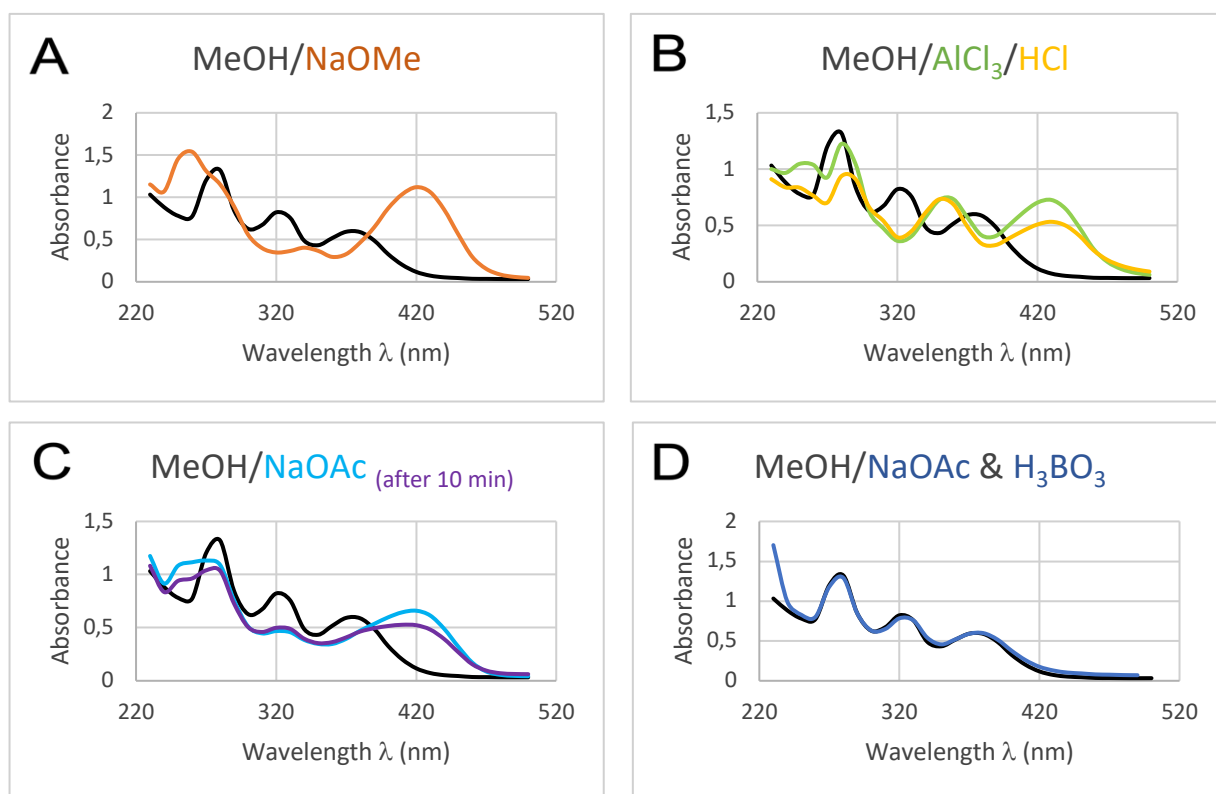


Figure 4.19: UV spectrums of compound **C2** after addition of various reagents. Black lines represent the methanol spectra. Graph A: Spectrum obtained after addition of NaOMe (orange). Graph B: Spectrum obtained after addition of AlCl₃ (green), followed by the addition of HCl (yellow). Graph C: Spectrum obtained after addition of NaOAc. Measured at two intervals, first immediately (light blue) and second after 10 min (purple) to observe degradation of the flavonoid structure. Graph D: Spectrum obtained after addition of NaOAc and H₃BO₃ (blue)

Mass spec data

Mass spectroscopy (GC/MS) revealed **C2** to have a mass to charge ratio ($m/z = 344$) corresponding to a dihydroxytrimethoxyflavone, in accordance with that observed in the following NMR spectra.

NMR data

^1H NMR (400 MHz, CDCl_3): δ 11.45 (s, 1H, 5-OH), 8.27 (d, $J = 8.0$ Hz, 2H, H-2', H-6'), 7.57-7.47 (m, 3H, H-3', H-4', H-5'), 6.81-6.73 (br, 1H, 3-OH), 4.13 (s, 3H, 8-OMe), 3.99 (s, 3H, 6-OMe), 3.96 (s, 3H, 7-OMe). ^{13}C NMR/DEPT-135 (100 MHz, CDCl_3): δ 176.2 (C=O, C-4), 153.5 (C-7), 148.0 (C-5), 145.8 (C-2), 145.4 (C-9), 136.6 (C-3), 136.0 (C-6), 133.4 (C-8), 130.9 (C-1'), 130.6 (C-4'), 128.9 (C-3', C-5'), 127.8 (C-2', C-6'), 105.5 (C-10), 62.3 (CH_3 , 7-OMe), 61.9 (CH_3 , 8-OMe), 61.4 (CH_3 , 6-OMe).

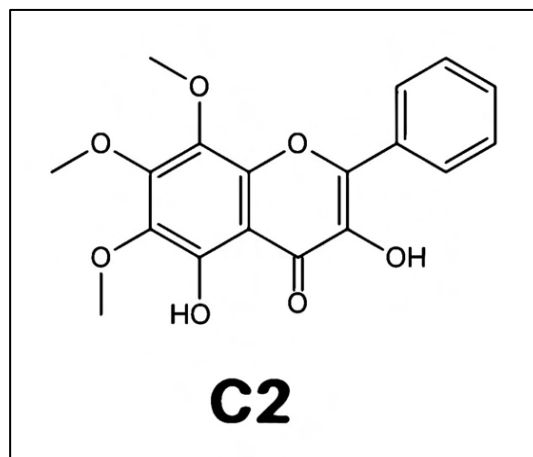


Figure 4.20: Structure of 3,5-dihydroxy-6,7,8-trimethoxyflavone

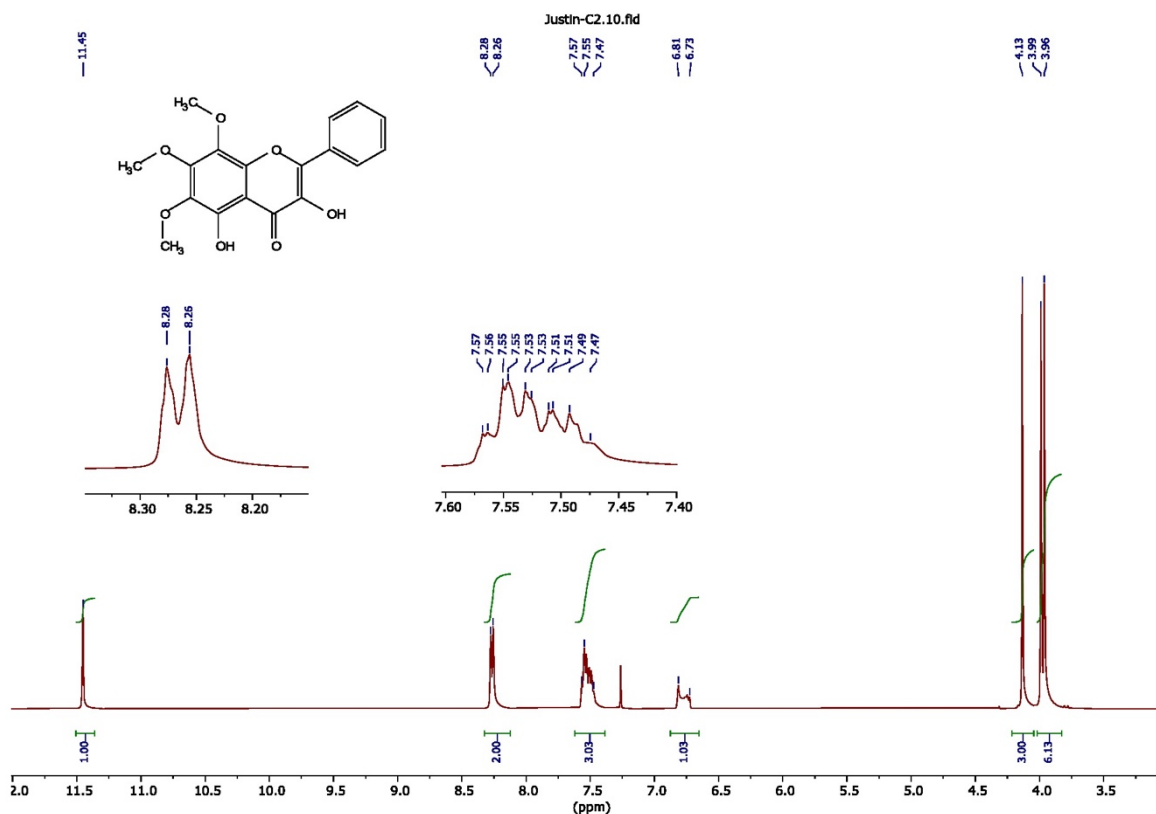


Figure 4.21: ^1H NMR spectrum of compound **C2**

The proton NMR of **C2** (figure 4.21) showed three singlets 4.13, 3.99 and 3.96 ppm representing three methoxyl groups at C-8, C-6 and C-7 respectively. The equivalent protons at position 2' and 6' of ring B exhibited a doublet at 8.27 ppm with $J = 8.0$ Hz, suggesting an *ortho* coupling. The ^{13}C spectrum (figure 4.22) showed a characteristic signal for a keto group at 176.2 ppm which was absent in DEPT analysis (figure 4.23).

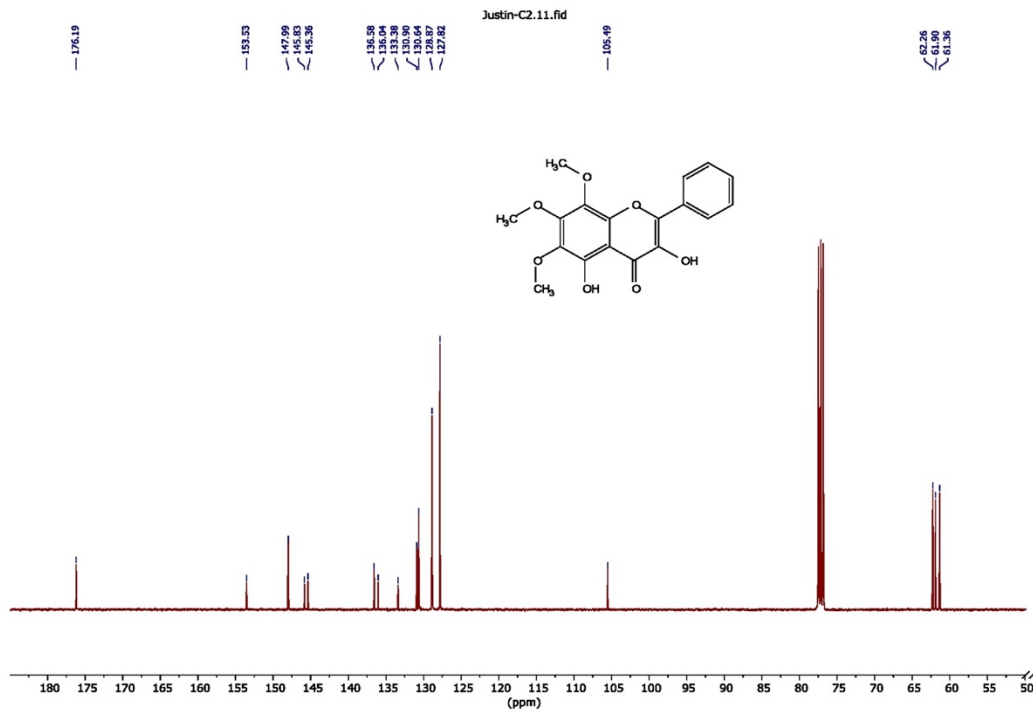


Figure 4.22: ^{13}C NMR spectrum for compound **C2**

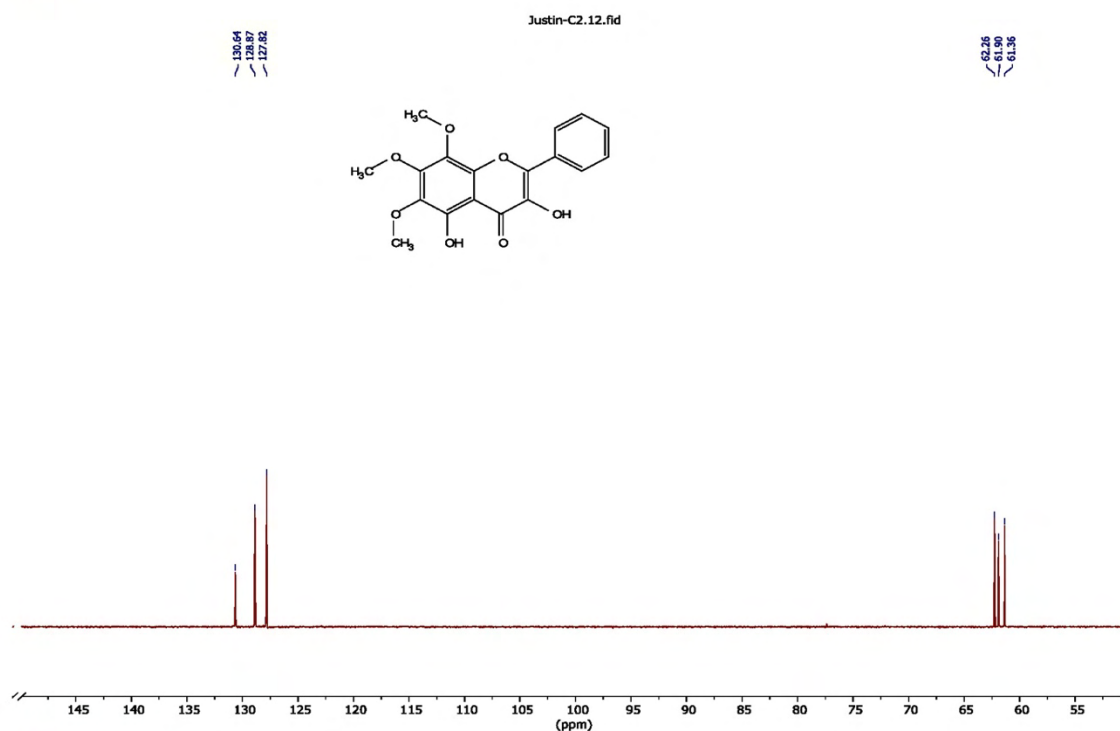


Figure 4.23: DEPT spectra for compound **C2**

The COSY spectrum of **C2** (figures 4.24 and 4.25) showed absence of any coupling with the exception of aromatic protons of ring B, where the doublet at δ 8.27 shows cross peaks at 7.55 ppm. The findings in the DEPT spectrum were confirmed by Heteronuclear Single Quantum Coherence (HSQC) spectrum (figures 4.26 and 4.27) which showed a correlation between the protons at 3.96, 3.99 and 4.13 ppm to the carbons at 61.4, 62.3 and 61.9 ppm. The proton at 7.51 ppm (H-4') showed a correlation with carbon at 130.6 whereas the protons at 7.56 ppm (H-3', H-5') and 8.28 ppm (H-2', H-6') exhibited correlations with carbons at 128.9 and 127.8 respectively. The assignments of 5-OH and 3-OH peaks were confirmed by Heteronuclear Multiple Bond Correlation (HMBC) spectrum (figure 4.28). The 5-OH assignment at 11.45 ppm is confirmed by its HMBC interaction with C-10 (105.5 ppm), C-6 (136.0 ppm), C-5 (148.0) and a four bond weak interactions with C-7 (153.5 ppm) and C-4 (176.2 ppm). On the other hand, the 3-OH assignment was confirmed by its HMBC interaction with C-3 (136.6 ppm), C-2 (145.8 ppm), C-4 (176.2 ppm) and a weaker four bond interaction with C-10 (105.5 ppm).

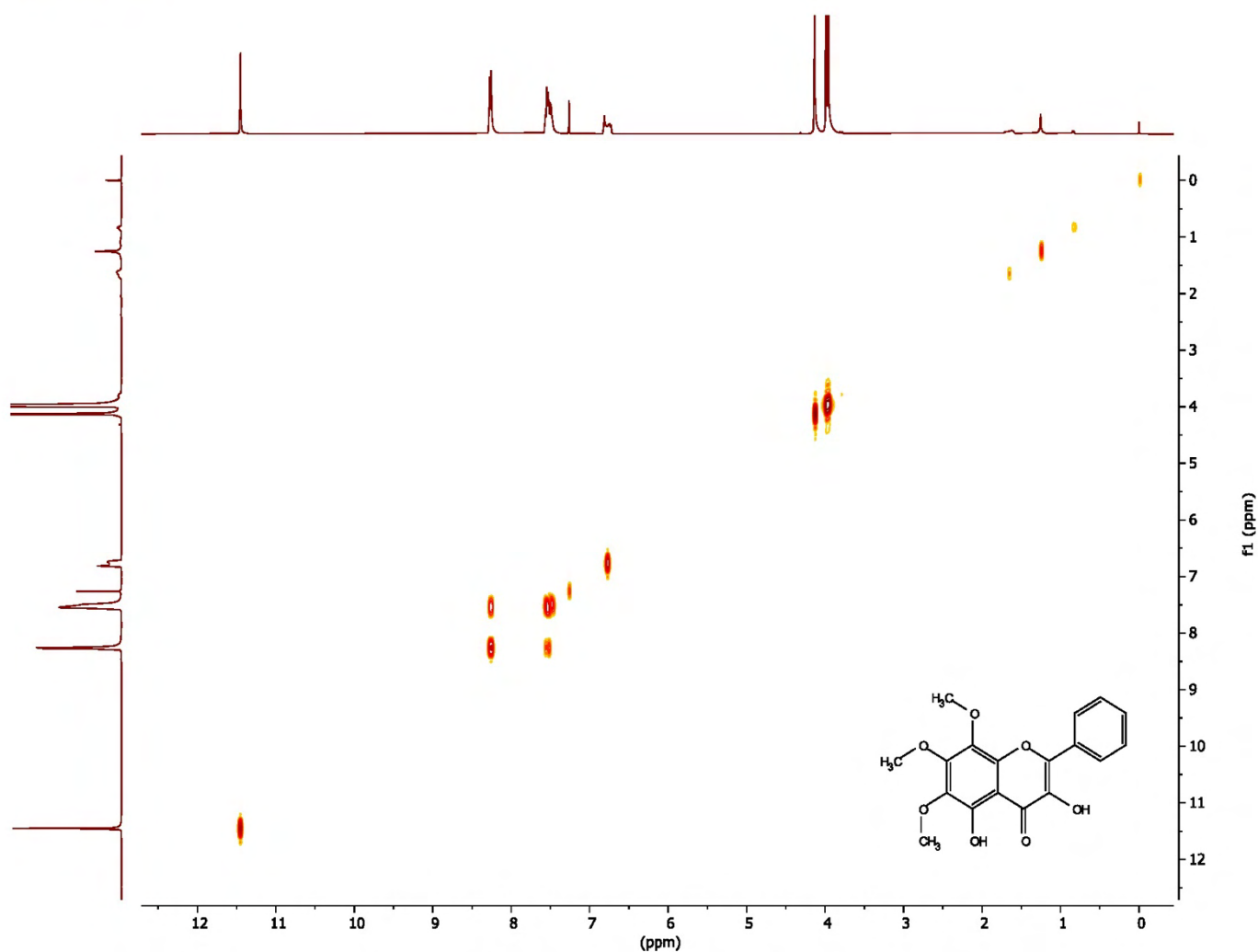


Figure 4.24: COSY spectra for compound **C2**

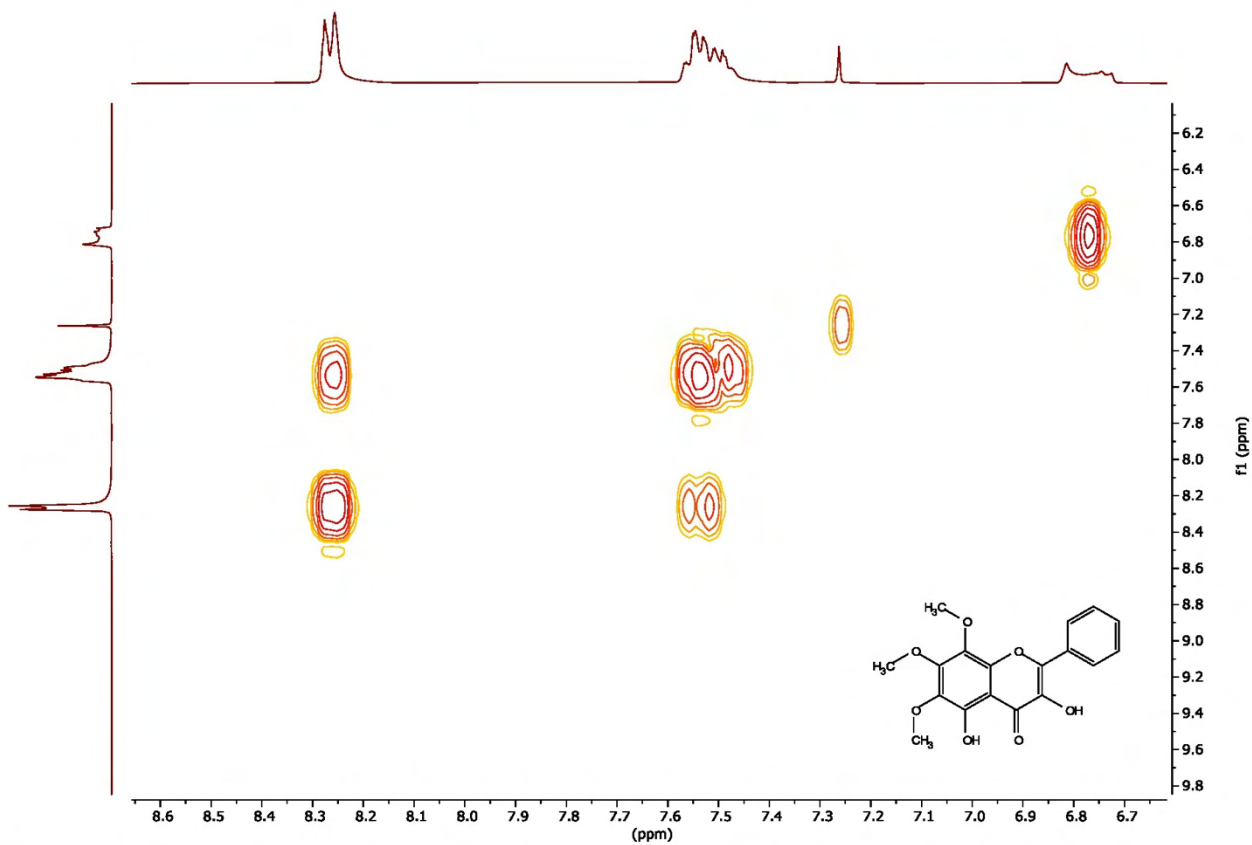


Figure 4.25: COSY spectra for compound C2 (zoomed)

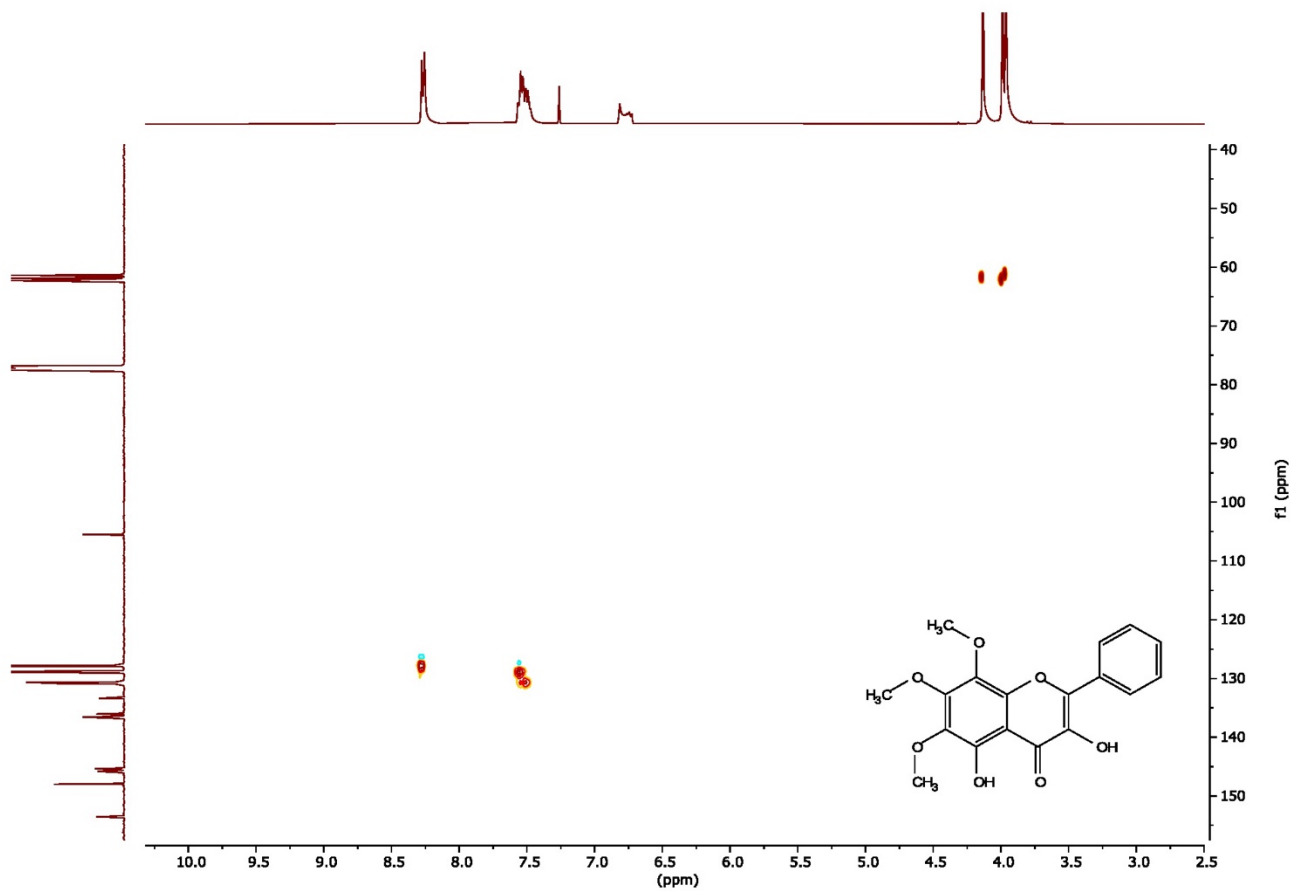


Figure 4.26: HSQC spectrum for compound C2

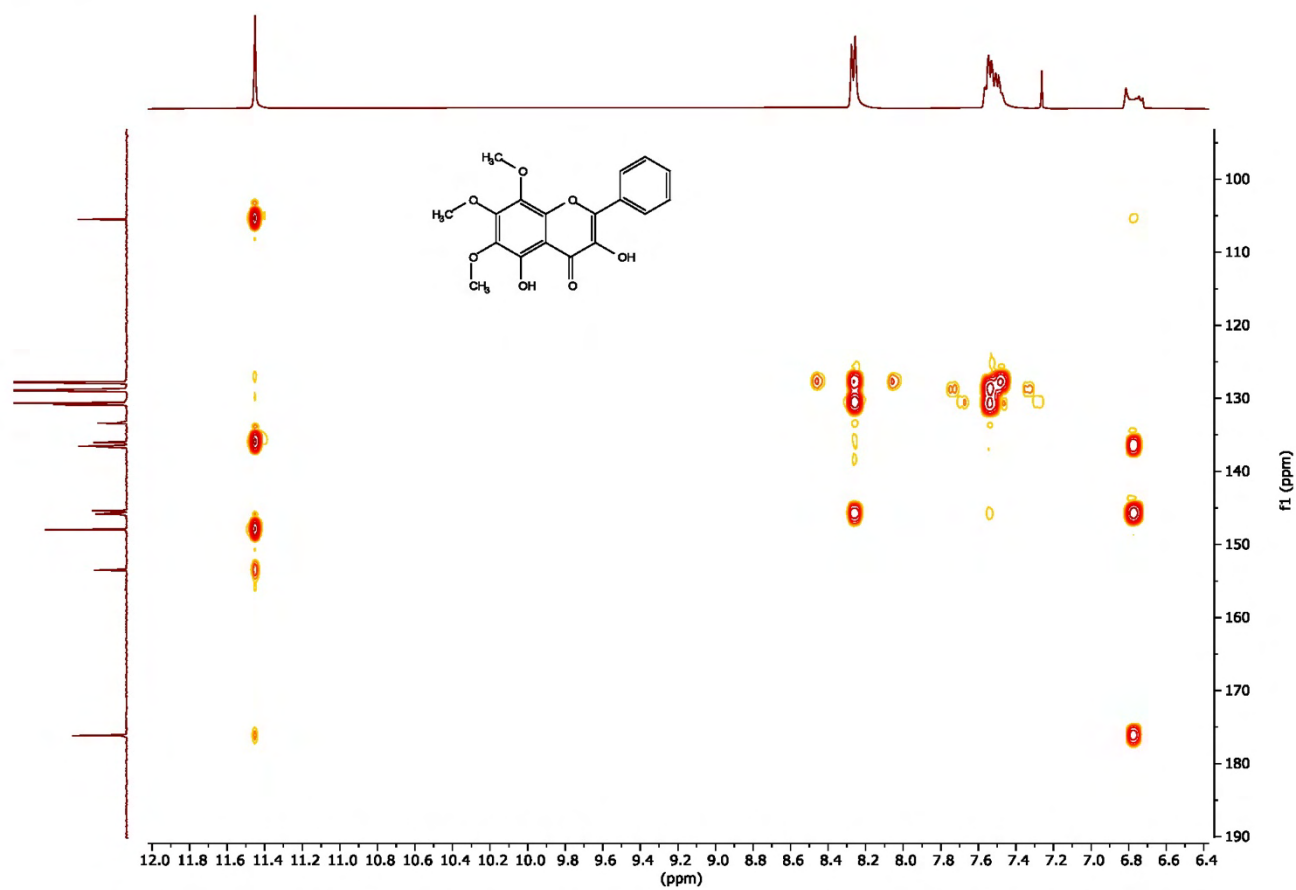


Figure 4.27: HSQC spectrum for compound **C2** (zoomed)

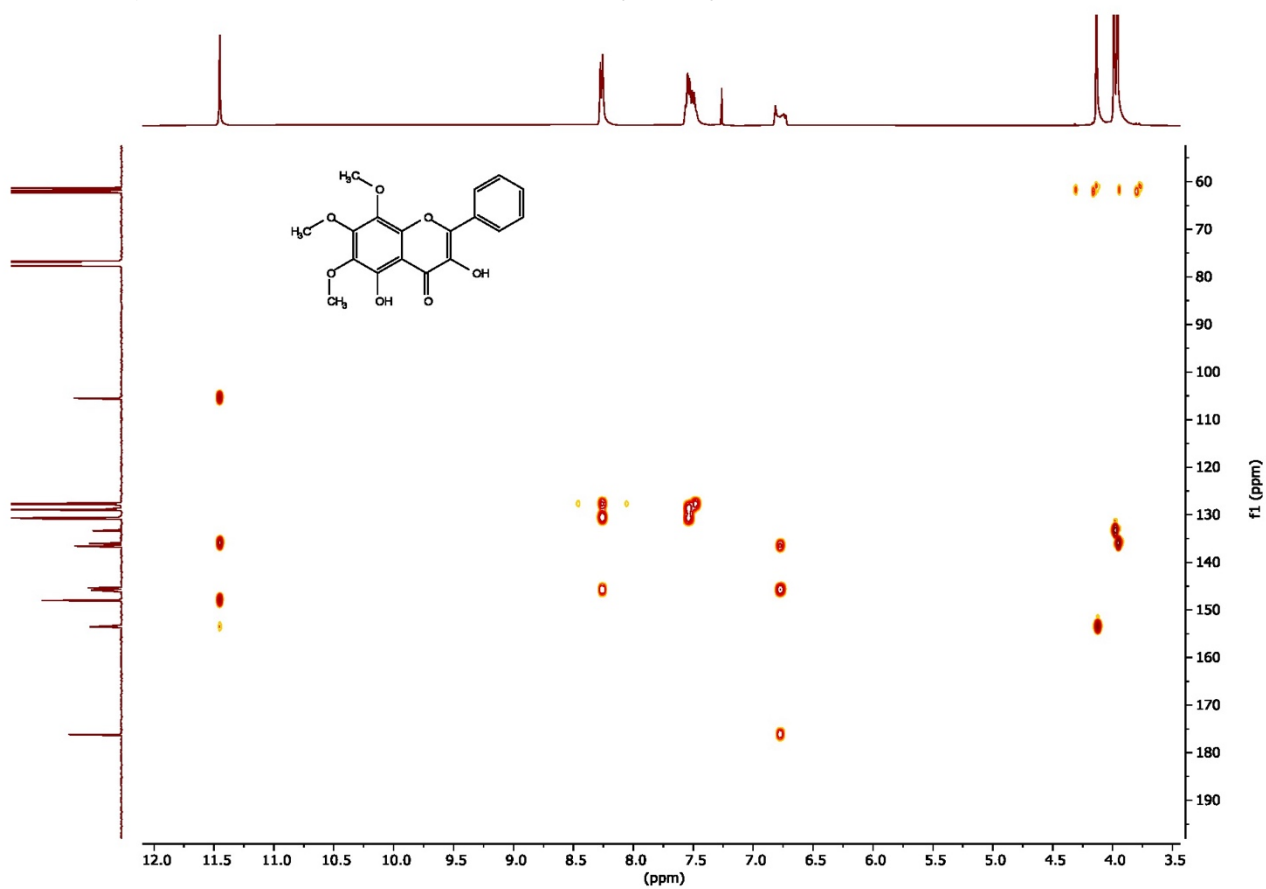


Figure 4.28: HMBC spectrum for compound **C2**

Thus, compound **C2** was identified as 3,5-dihydroxy-6,7,8-trimethoxyflavone (figure 4.20). The experimental UV and MS data obtained for **C2** matched the data presented by Tomás-Lorente et al., confirming the proposed structure. The compound was been previously reported from *Helichrysum decumbens* and *Helichrysum graveolens* (Tomás-Lorente et al., 1989).

4.5.3 Structure Elucidation of Compound C3

UV spectral Data

The methanolic UV spectra (figure 4.29A, table 4.11) indicates that the structure has a free hydroxy at the C-5 position. The AlCl_3 spectrum (figure 4.29B) shows a ± 30 nm bathochromic shift to the band I, evidence of a 3' and 4' dihydroxy B-ring complex formation with AlCl_3 . Additionally, the ± 10 nm hypsochromic shift in Band Ia after addition of HCl is due to the decomposition of ortho-hydroxy B-ring aluminum chloride complex after addition of an acid. Furthermore, the stable aluminium complex between position 5-hydroxyl group and the 4-keto group is observed by Band Ib remaining unchanged after addition of acid. The ± 15 nm bathochromic shift observed in the $\text{NaOAc}/\text{H}_3\text{BO}_3$ spectrum (figure 4.29D), forming a complex with the orthodihydroxyl groups. The 10 nm bathochromic shift observed for the band II when NaOAc was added (figure 4.29C) is representative of the ionisation of a hydroxy group at C-7.

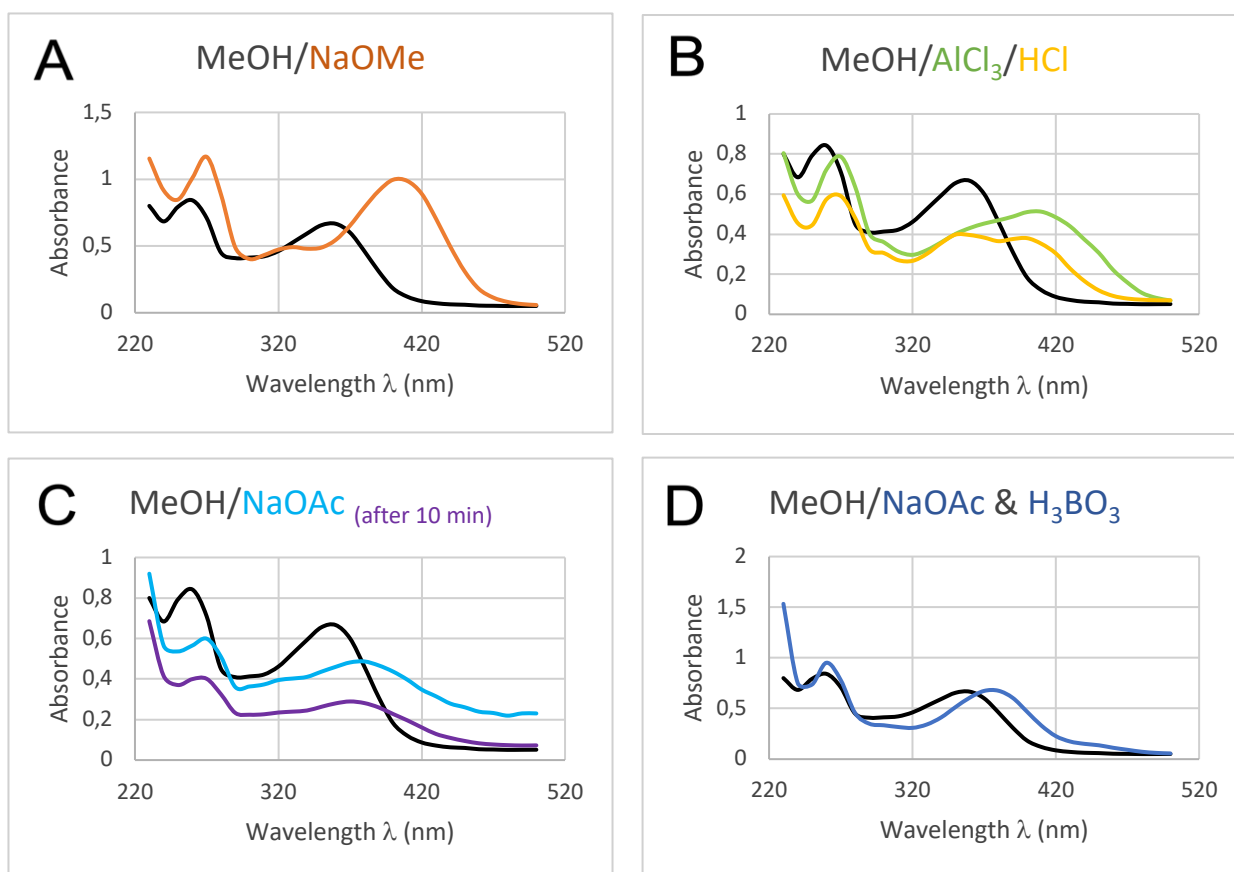


Figure 4.29: UV spectrums of compound **C3** after addition of various reagents. Black lines represent the methanol spectra. Graph A: Spectrum obtained after addition of NaOMe (orange). Graph B: Spectrum obtained after addition of AlCl_3 (green), followed by the addition of HCl (yellow). Graph C: Spectrum obtained after addition of NaOAc. Measured at two intervals, first immediately (light blue) and second after 10 min (purple) to observe degradation of the flavonoid structure. Graph D: Spectrum obtained after addition of NaOAc and H_3BO_3 (blue)

NMR data

^1H NMR (400 MHz, DMSO): δ 12.70 (s, 1H, 5-OH), 7.54 (d, $J = 2.4$ Hz, 1H, H-2'), 7.44 (dd, $J = 8.4$, 2 Hz, 1H, H-6'), 6.90 (d, $J = 8.4$ Hz, 1H, H-5'), 6.41 (d, $J = 2$ Hz, 1H, H-8), 6.19 (d, $J = 2$ Hz, 1H, H-6), 3.77 (s, 3H, 3-OMe). ^{13}C NMR (100 MHz, DMSO) and DEPT-135: δ 179.4 (C=O, C-4), 165.8 (C-7), 162.8 (C-5), 157.9 (C-9), 157.0 (C-2), 149.6 (C-4'), 146.2 (C-3'), 139.1 (C-3), 122.6 (C-1'), 121.9 (C-6'), 116.3 (C-2'), 116.2 (C-5'), 105.5 (C-10), 99.6 (C-6), 94.6 (C-8), 60.3 (CH₃, 3-OMe).

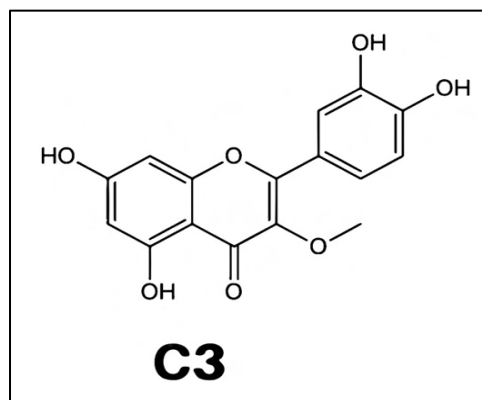


Figure 4.30: Structure of 3',4',5,7-tetrahydroxy-3-methoxyflavone

The proton NMR (figures 4.31 and 4.32) showed a singlet at 3.77 ppm for the three methoxy protons attached to C-3. The protons attached to the 2' displayed a doublet at 7.54 ppm with $J = 2.4$ Hz, suggesting a long range *meta* coupling. H-6' exhibited a doublet of doublets ($J = 8.4$, 2 Hz) because of the effect of both short range and long range couplings. The proton at C-5' exhibited a doublet at 6.90 ppm with strong *ortho* coupling ($J = 8.4$ Hz). The unsubstituted protons of ring A at positions 8 and 6 showed doublets at 6.41 and 6.19 ppm with $J = 2$ Hz, indicating a *meta* coupling among them.

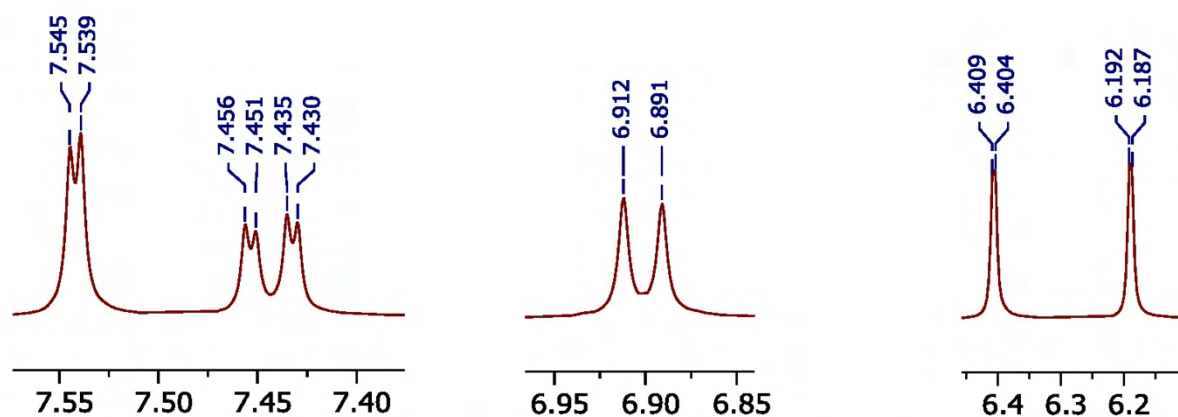


Figure 4.31: ^1H NMR peaks for compound C3

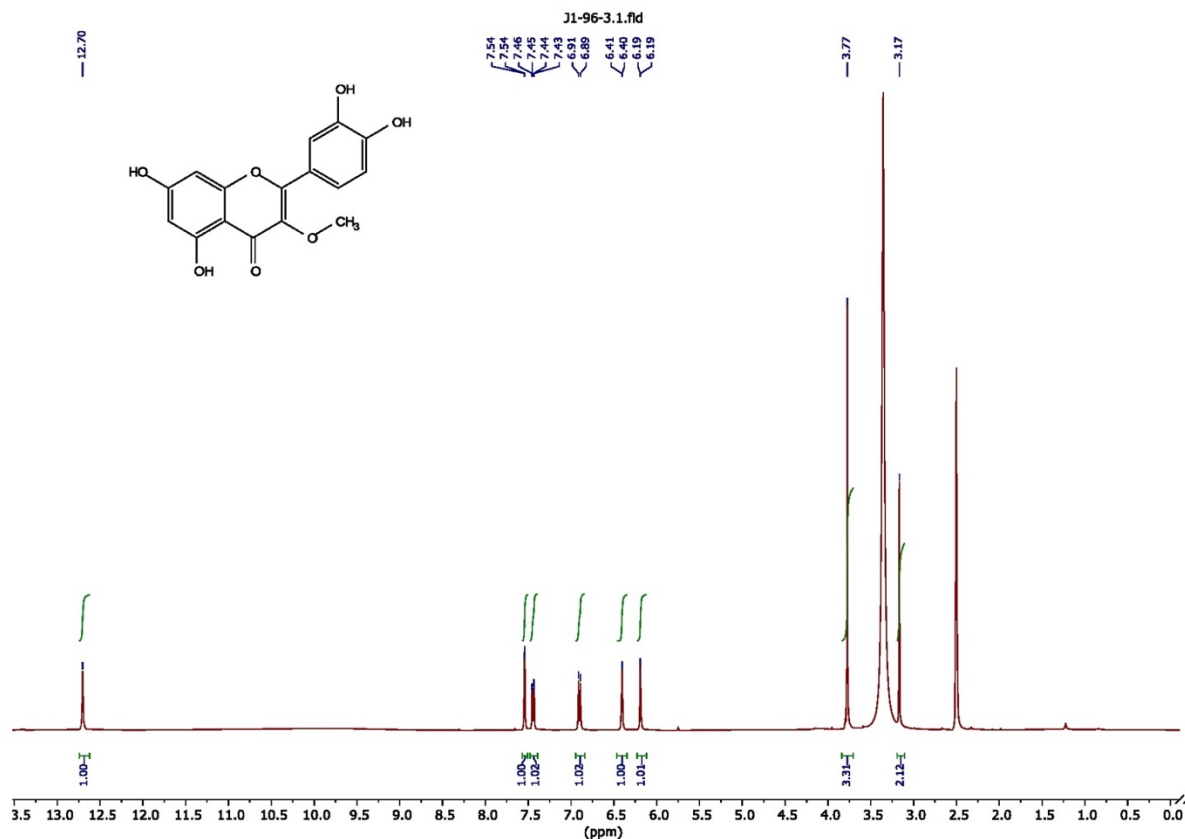


Figure 4.32: ^1H NMR spectrum of compound **C3**

The ^{13}C spectrum (figure 4.33) showed a signal for a keto group at 179.4 ppm which was absent in DEPT spectrum (figure 4.34). The 3-OMe and other unsubstituted carbons (C-6, C-8, C-2', C-5' and C-6') on the ring A and B displayed positive signals in DEPT spectrum. Signals of all other substituted carbons on the three rings were absent in DEPT spectrum. These observations were further supported by the HSQC (figure 4.35) spectrum where the protons at the positions 2', 6', 5', 6 and 8 showed correlation with carbons at 116.3, 122.0, 116.2, 99.6 and 94.6 ppm. In HMBC (figure 4.36), the methoxyl protons showed three bond interactions with C-3 at 139.1 ppm. The proton at the position 6 of ring A displayed strong three bond interactions with C-8 (94.6 ppm), C-10 (105.5 ppm) and weak three bond interactions with C-5 (162.8 ppm) and C-7 (165.8 ppm). Likewise, in ring B the proton 6' showed three bond interaction with C-2' (116.3 ppm), C-4' (149.6 ppm) and C-2 (157.0 ppm).

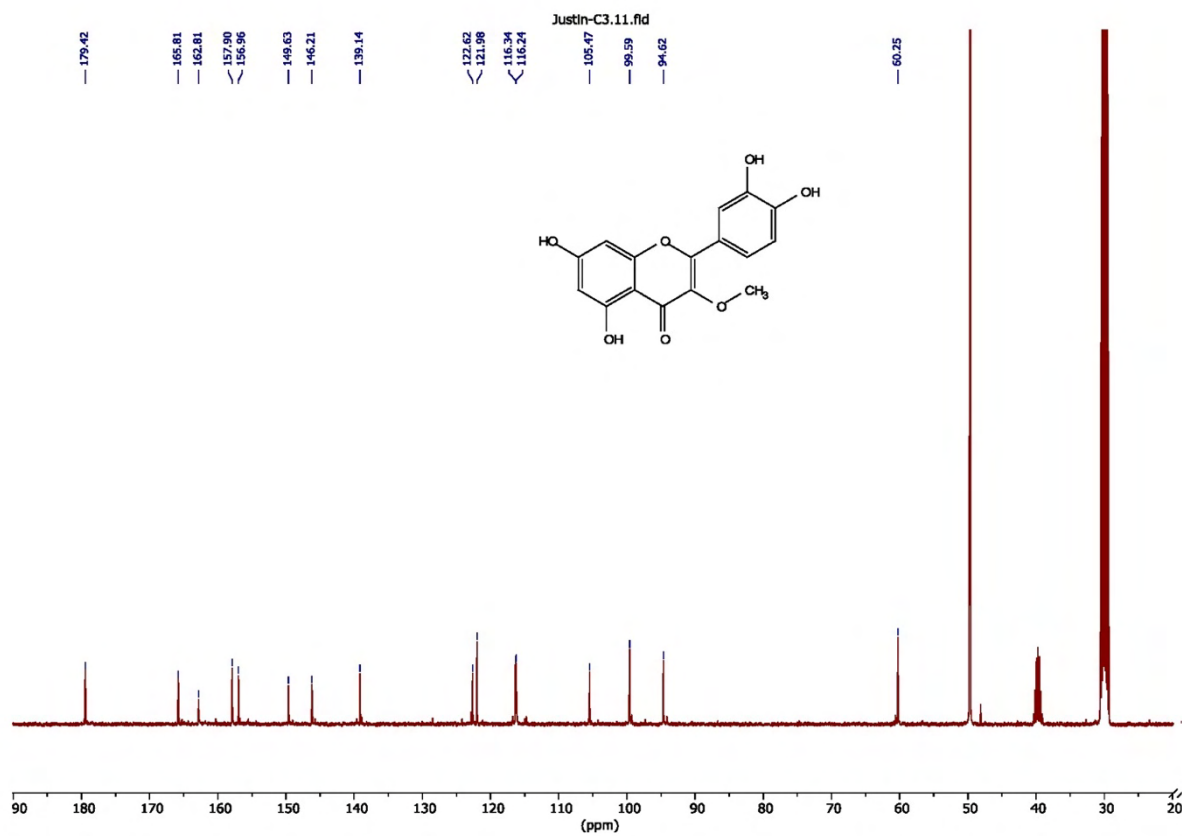


Figure 4.33: ^{13}C NMR spectrum of compound C3

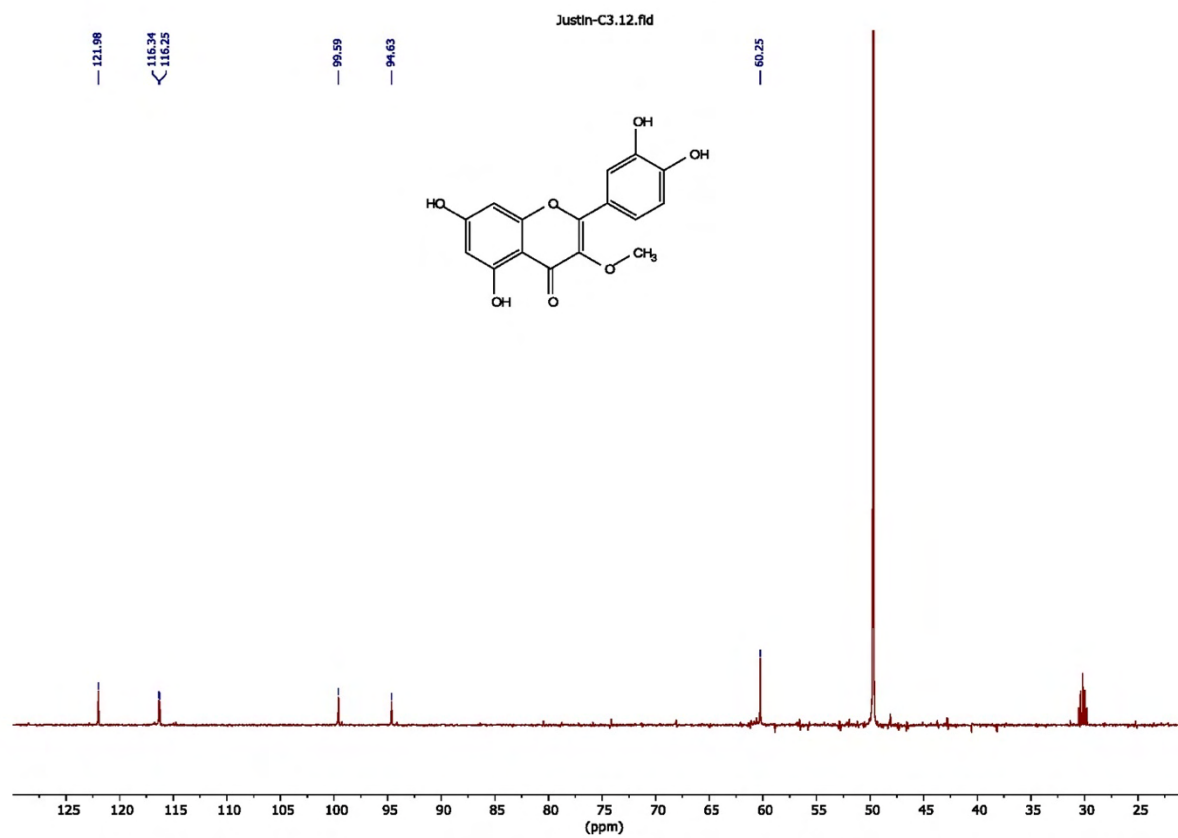
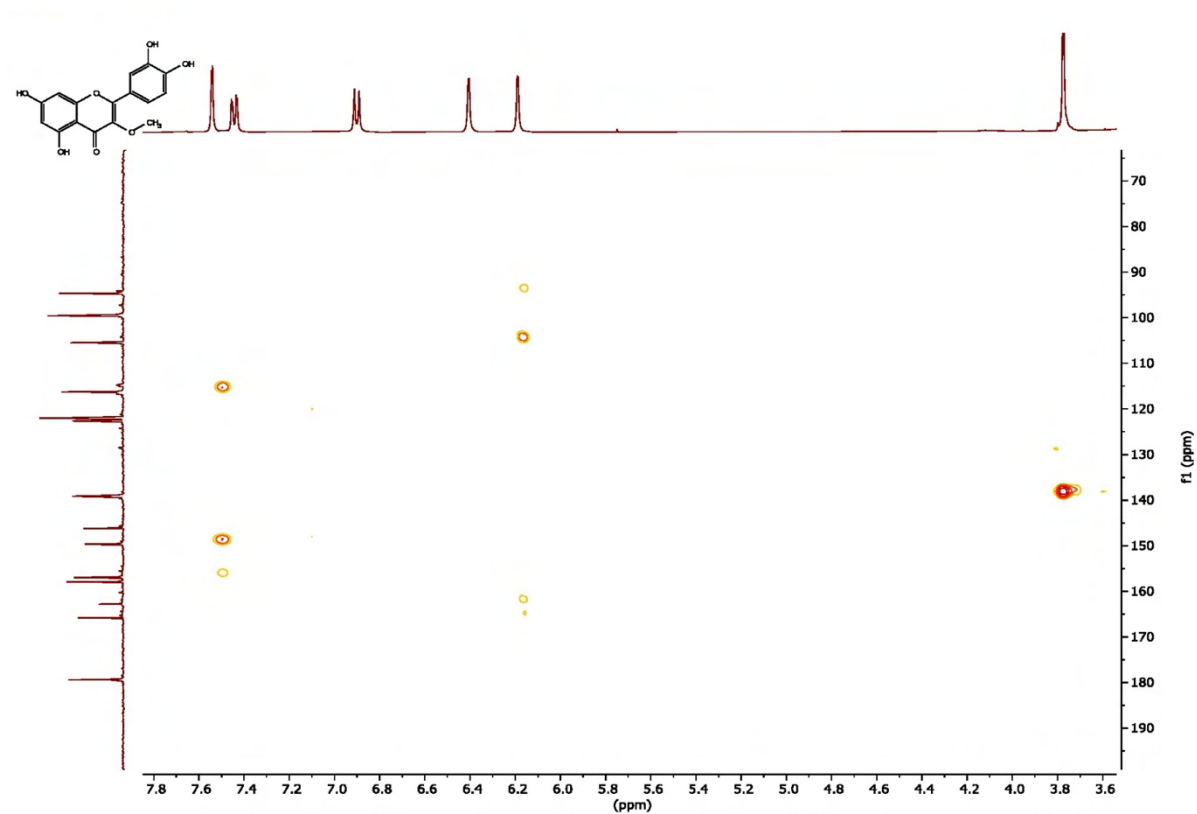
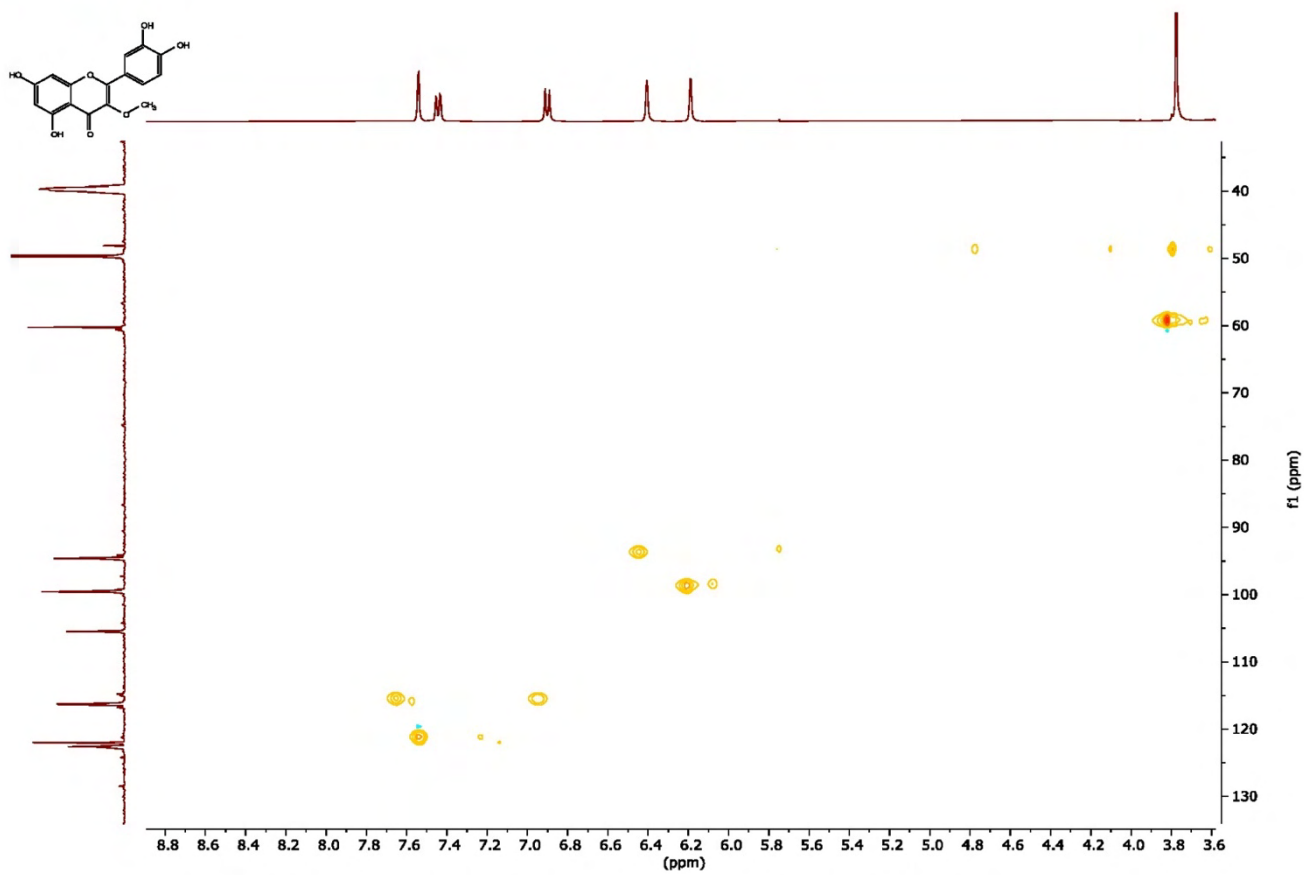


Figure 4.34: DEPT spectrum for compound C3



The structure was identified as 3',4',5,7-tetrahydroxy-3-methoxyflavone (3-O-methylquercetin) by comparison of ¹H NMR and UV (methanol λ_{\max}) data from the literature (Wang et al., 2010). The compound **C3** (figure 4.30) has been previously isolated from various plants such as *Halimodendron halodendron* (Wang et al., 2010), *Carex folliculate* seeds (Li et al., 2009), and Sudanese *Albizia zygia*. Interestingly, **C3** was found to exhibit high antimalarial activity (Abdalla & Laatsch, 2012) and has also been previously isolated from South African *H. kraussii* and *H. odoratissimum*, exhibiting an antioxidant DPPH free radical scavenging activity of 40.7 % at concentration 1 mg/mL (Legoalea et al., 2013; Van Puyvelde et al., 1989).

4.5.4 Structure Elucidation of Compound C4

UV spectral data

The UV spectrum in methanol (figure 4.37, table 4.11) suggests the presence of a hydroxyl functional group on position 5 of the A-ring. UV data also confirmed the B-ring to be unsubstituted and by comparison with previously confirmed structures. After addition of AlCl_3 , a notable bathochromic shift in Band I is observed, and after addition to HCl remains unchanged, diagnostic of a stable aluminium complex formed between position 5-hydroxyl and position 4-keto functional groups (figure 4.37B). The presence of C-7 hydroxy group was confirmed by the 10 nm bathochromic shift in Band II of UV spectrum with the addition of NaOAc to the methanol solution (figure 4.37C).

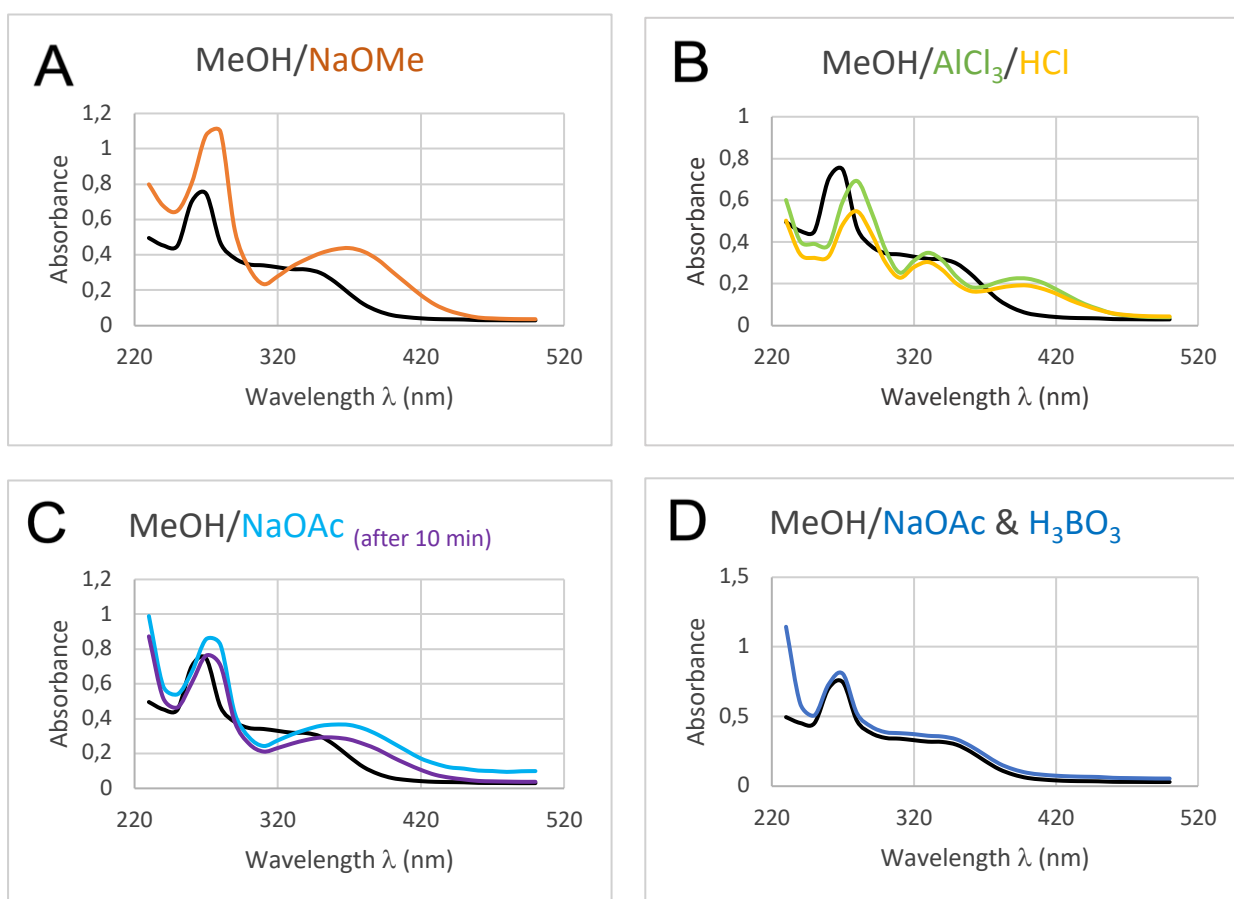


Figure 4.37: UV spectra of compound **C4** after addition of various reagents. Black lines represent the methanol spectra. Graph A: Spectrum obtained after addition of NaOMe (orange). Graph B: Spectrum obtained after addition of AlCl_3 (green), followed by the addition of HCl (yellow). Graph C: Spectrum obtained after addition of NaOAc. Measured at two intervals, first immediately (light blue) and second after 10 min (purple) to observe degradation of the flavonoid structure. Graph D: Spectrum obtained after addition of NaOAc and H_3BO_3 (blue)

NMR data

^1H NMR (400 MHz, $(\text{CD}_3)_2\text{CO}$): 8.09-8.06 (*m*, 2H, H-2', H-6'), 7.56 (*m*, 3H, H-3', H-4', H-5'), 6.49 (*d*, $J = 2$ Hz, 1H, 8-H), 6.26 (*d*, $J = 2$ Hz, 1H, 6-H), 3.88 (*s*, 3H, 3-OMe). ^{13}C NMR (100 MHz, $(\text{CD}_3)_2\text{CO}$) and DEPT-135: δ 179.8 (C=O, C-4), 166.3 (C-7), 163.3 (C-5), 158.3 (C-9), 156.5 (C-2), 140.4 (C-3), 131.9 (C-4'), 129.7 (C-3', C-5'), 129.4 (C-2', C-6'), 105.9 (C-10), 100.0 (C-6), 95.0 (C-8), 60.8 (CH_3 , 3-OMe).

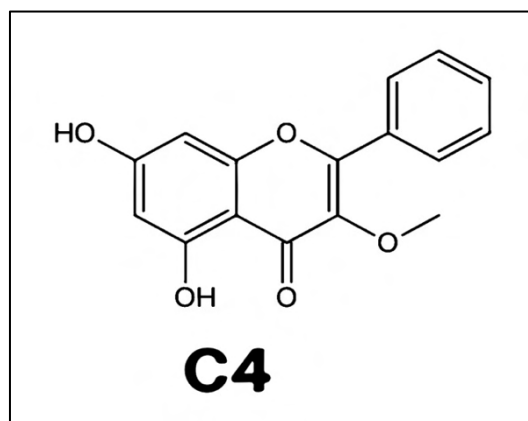


Figure 4.38: Structure of 5,7-dihydroxy-3-methoxyflavone

The proton spectrum (figure 4.39) showed the methoxy peak as a singlet at 3.88 ppm. The protons at positions 2' and 6' in the ring B showed a multiplet (8.02-7.99 ppm). The other unsubstituted protons at 3', 4' and 5' also displayed a multiplet. The unsubstituted protons at positions 6' and 8' in the ring showed a doublet at 6.26 and 6.49 ppm respectively with $J = 2$ Hz, indicating a meta coupling.

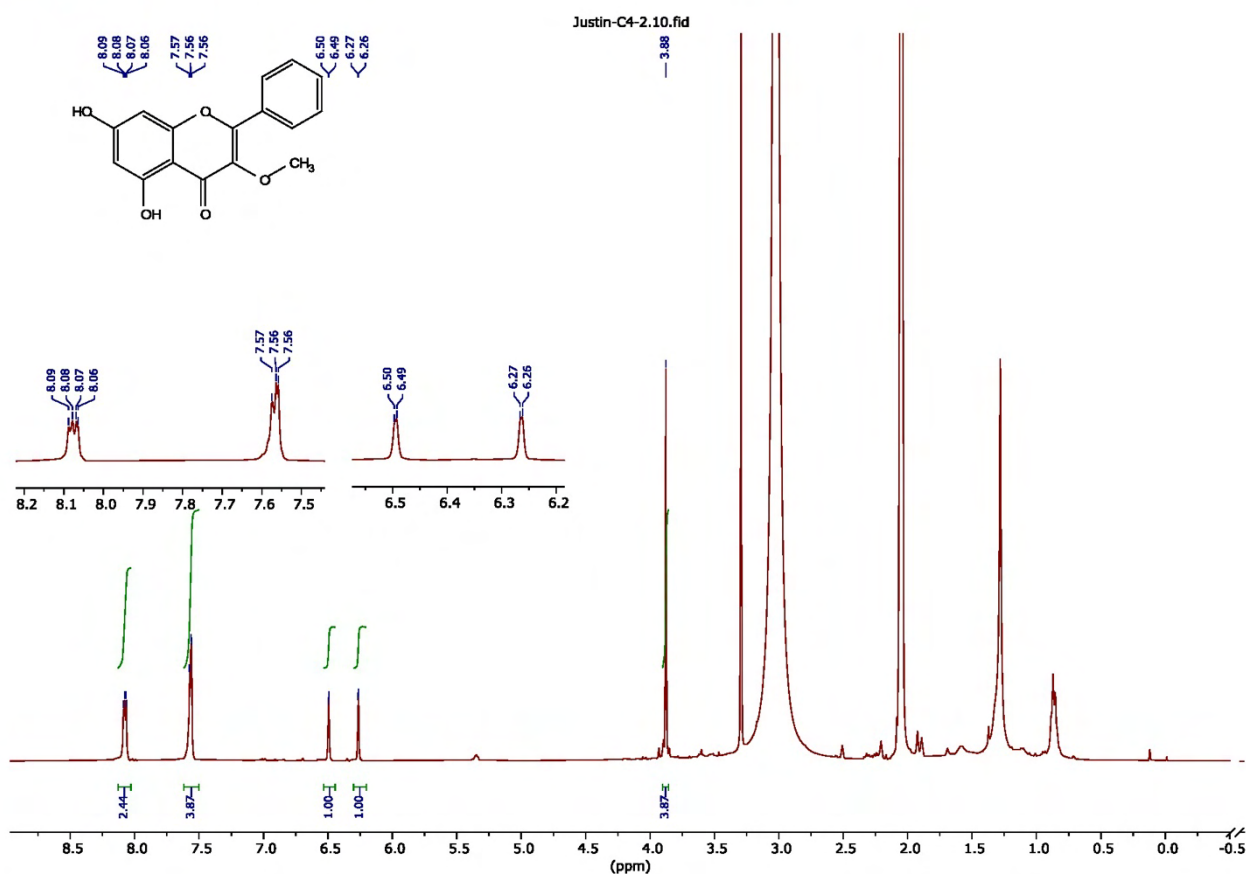


Figure 4.39: ^1H NMR spectrum of compound **C4**

In the ^{13}C spectrum (figure 4.40), the keto peak at C-4 appears at 179.8 ppm and peak for methoxy appeared at 60.8 ppm. An analysis of the HSQC spectrum (figure 4.41) indicated that the protons at the positions 8 and 6 showed correlation with the carbons at 95.0 and 100.0 ppm respectively. In the ring B, the protons at *o*-, *m*- and *p*- positions showed correlation with carbons at 129.4, 129.7 and 131.9 ppm respectively. The methoxy protons correlated with carbon at 60.8 ppm. In the HMBC spectra (figure 4.42), the methoxy protons showed a three bond correlation with C-3 at 140.4 ppm. The H-6 proton displayed a three bond correlation with C-8 and C-10 at 95.0 ppm and 105.9 ppm respectively. It also showed a weaker two bond correlation with C-5 and C-7 at 163.3 and 166.3 ppm respectively. The H-8 proton also showed similar trend with two each three bond (with C-6 and C-10) and two bond (with C-5 and C-7) correlations.

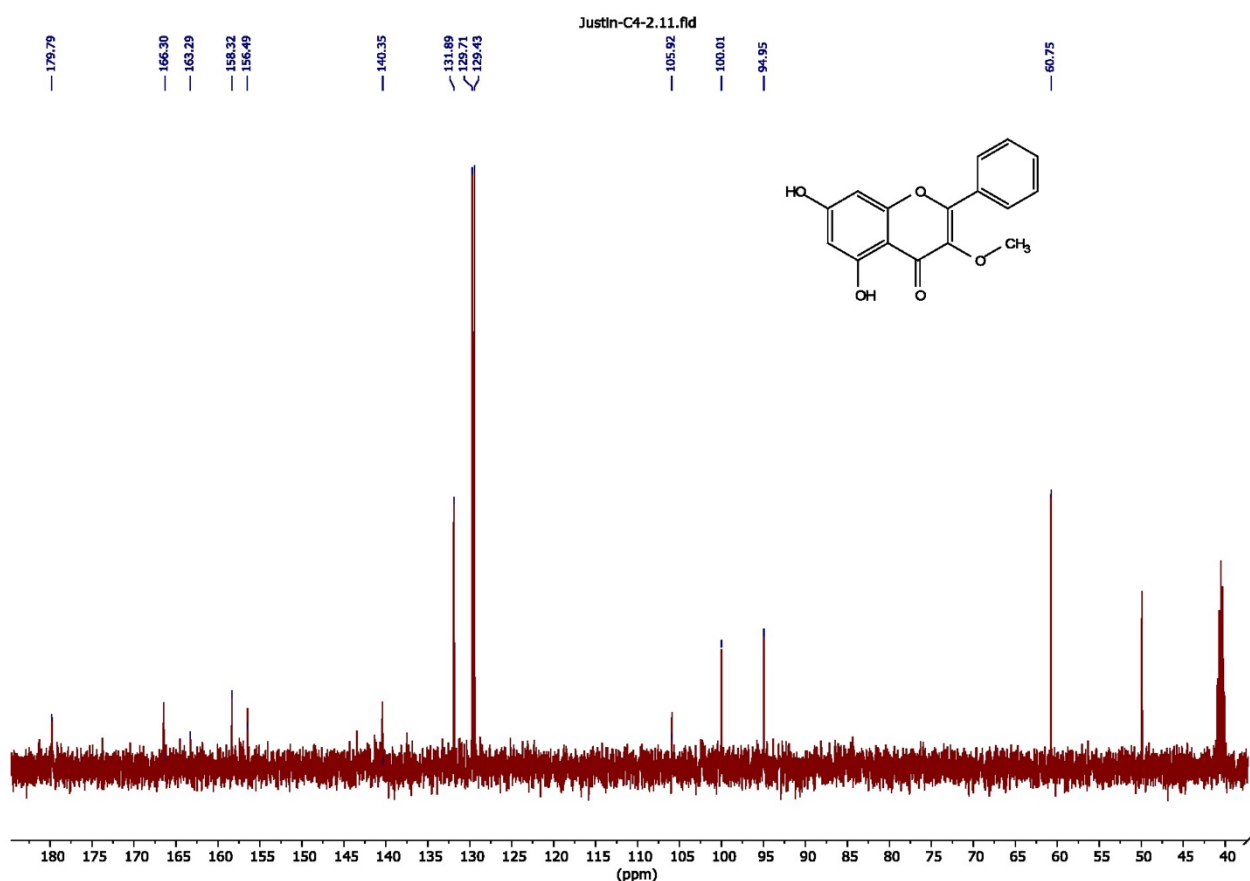


Figure 4.40: ^{13}C NMR of compound **C4**

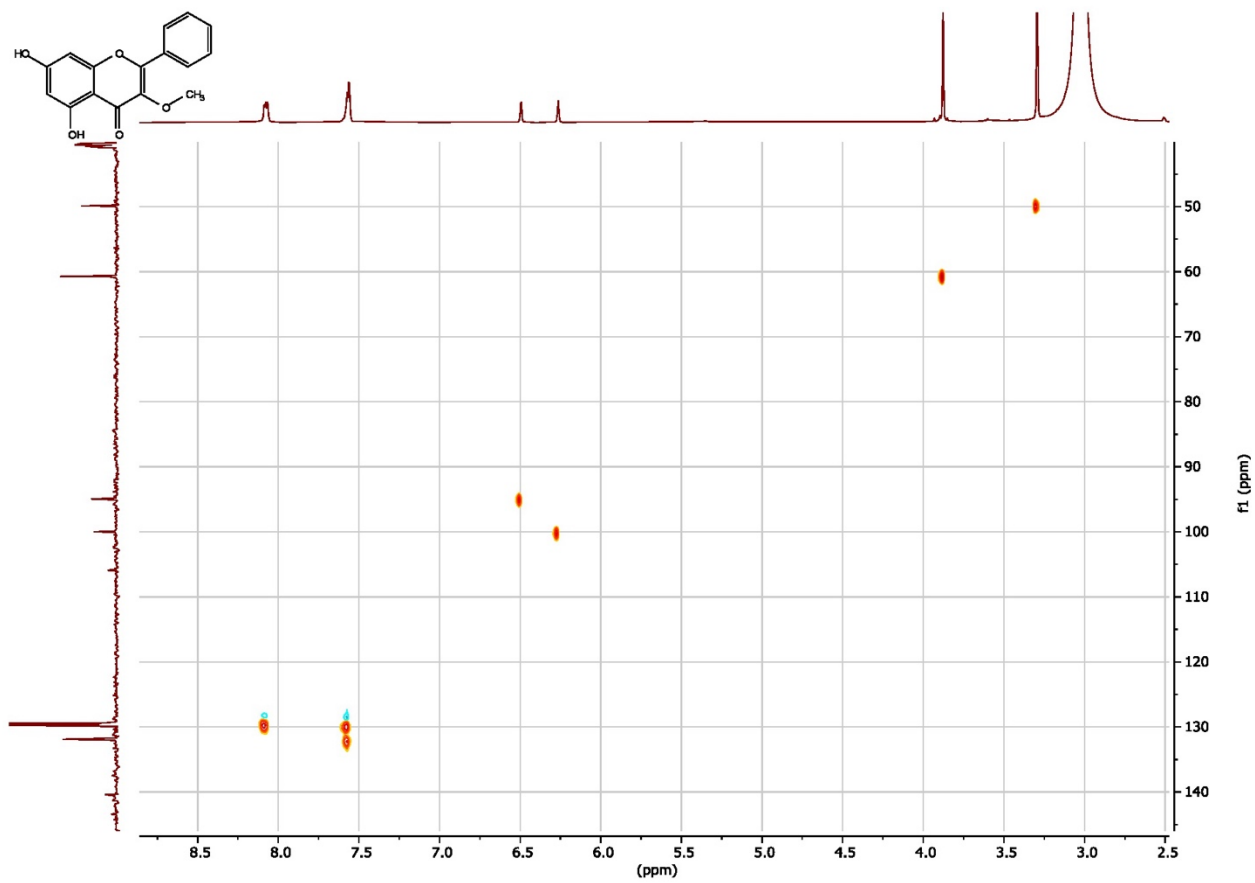


Figure 4.41: HSQC spectrum of **C4**

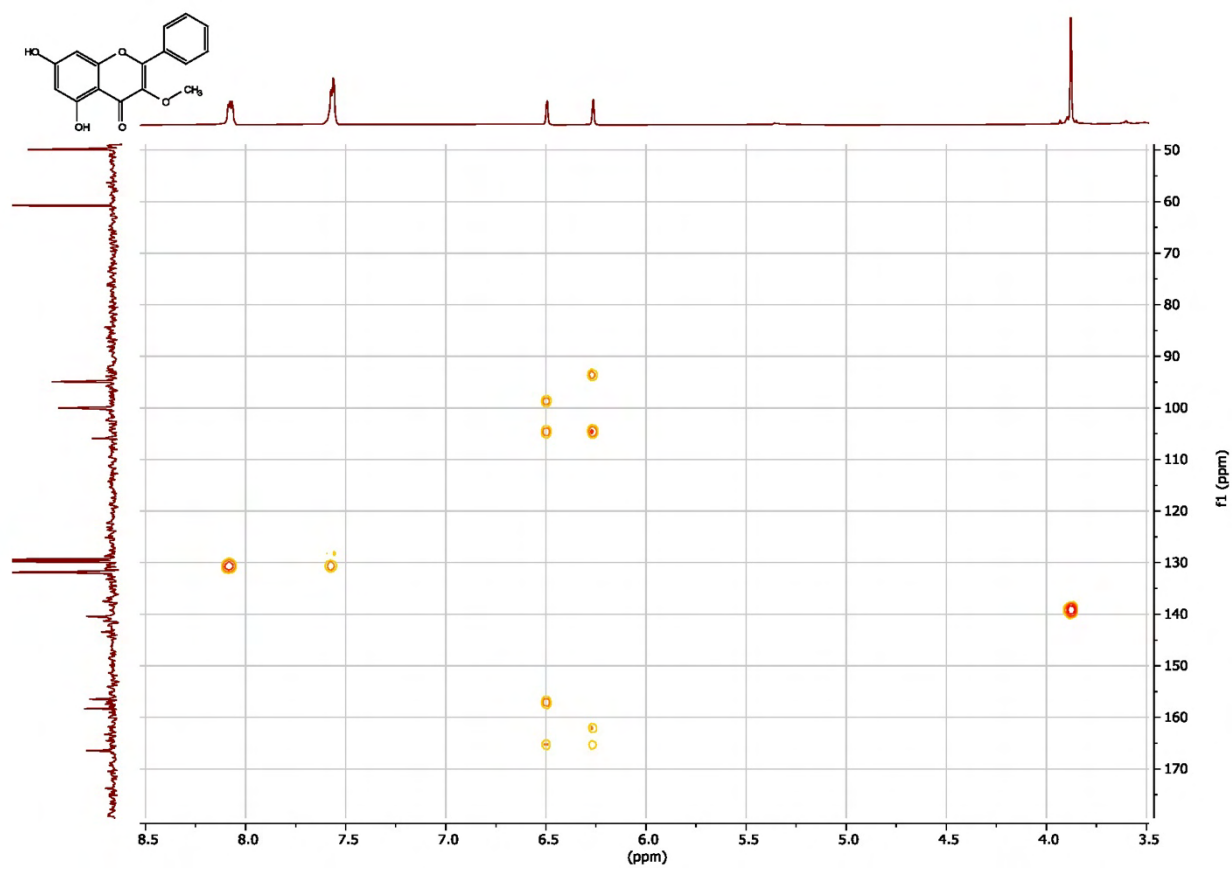


Figure 4.42: HMBC spectrum for compound **C4**

The structure of **C4** (figure 4.38) was identified as 5,7-dihydroxy-3-methoxyflavone (3-methylethergalangin) by comparison of ¹H NMR and ¹³C NMR data from literature (Shin et al., 2003). **C4** has been previously isolated from *Alpinia officinarum*, *H. picardii*, and South African *H. kraussii*, where it was found to exhibit an antioxidant DPPH free radical scavenging activity of 41,3 % at concentration 1 mg/mL (Legoalea et al., 2013; De La Puerta et al., 1990).

4.6 Conclusion

The total extract was obtained with a yield of 11,27% (total of 42,20 g), which was then subjected to column chromatography and yield four pure flavonoids. The compounds have flavonol basic skeleton and were identified as 5-hydroxy-3,7-dimethoxyflavone (**C1**, 60 mg), 3,5-dihydroxy-6,7,8-trimethoxyflavone (**C2**, 118 mg), 3',4',5,7-tetrahydroxy-3-methoxyflavone (**C3**, 132 mg) and 5,7-dihydroxy-3-methoxyflavone (**C4**, 20 mg), using a combination of analytical spectroscopic techniques.

CHAPTER 5: BIOLOGICAL CHARACTERIZATION OF HELICHRYSUM PANDURIFOLIUM CONSTITUENTS

“There is no such thing as applied sciences, only applications of science.”

– Louis Pasteur

5.1 Chapter Overview

The following chapter investigates the antioxidant activity and anti-diabetic potential of four isolated flavonoids and the total methanolic extract of *H. pandurifolium*. Included in this investigation is the total phenolic content of *H. pandurifolium*, which gives an estimation of the plants` total reducing capacity. The FRAP and TEAC antioxidant activities are evaluated *in vitro* to better determine the antioxidant activity of *H. pandurifolium* and the four isolated flavonoids. α -Glucosidase and α -amylase biological studies are quantified for *H. pandurifolium* total extract and the four isolated flavonoids to identify whether any anti-diabetic potential exists.

5.2 Biological Evaluations: Results and Discussion

The *in vitro* studies of the total methanolic extract of *H. pandurifolium* and its four isolated flavonoids were carried out to determine the antioxidant capacities of the plant material and its pure components. The antioxidant activities were explored for two possible mechanisms by using the FRAP and TEAC assays (3.4.2.2 and 3.4.2.3), whereas the Folin-Ciocalteu assay (3.4.2.1) was used to determine the total polyphenolic content. L-ascorbic acid (vitamin C), Trolox (water-soluble analogue of vitamin E), and gallic acid were used as reference standards for the FRAP, TEAC, and Folin-Ciocalteu assays respectively. An anti-diabetic investigation was performed by analysing the ability of the total extract (methanolic), and its four purely isolated flavonoids, to inhibit α -glucosidase and α -amylase enzymes following the procedures mentioned in the earlier chapter (3.4.3.1 and 3.4.3.2).

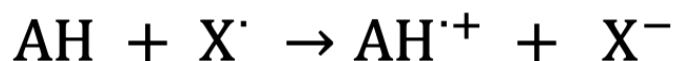
5.2.1 Evaluating the Total Polyphenolic Content of *H. pandurifolium* (Folin-Ciocalteu assay)

Phenolic compounds are considered to have the highest potential to neutralise free radicals. The total phenolic content (TPC) of the Folin-Ciocalteu assay finds wide use in the food and beverage industry being a quick determination for antioxidant properties or total reducing capacity in food products (Magalhães et al., 2007; Sánchez-Rangel et al., 2013). The total

phenolic content of *H. Pandurifolium* (reported as milligram gallic acid equivalents per gram) was found to be 108.3 ± 18.9 mg GAE/g. Interestingly, the total phenolic content was found to be greater than that for most of the methanolic extracts of *Helichrysum* species (table 2.2).

5.2.2 Evaluating the FRAP and TEAC Activity of the Isolated Compounds

Phenolic antioxidants from natural sources have become an increasingly popular topic of study due to their chemoprotective effects against oxidative stress-mediated disorders. The mechanisms by which these effects occur are attributed to their ability to scavenge free radicals, chelate metals, and their effects on cell signaling pathways on gene expression (Soobrattee et al., 2005). These two methods detect the antioxidant's capability to transfer an electron via the mechanism given in equation 5.1. The ability of flavonoids to inhibit free radicals and chelate metals can be related to their chemical features, namely the type of substitutions on the flavonoid backbone, their positions, and the number of substitutions. There is a substantial amount of evidence correlating antioxidant potency with chelating ability due to multiple hydroxyl groups on the structure, on the other hand methoxy groups generally result in unfavorable steric effects. Increased activity also occurs as a function of increased conjugation and electron delocalisation, due to a more stable flavonoid radical being formed (Heim et al., 2002).



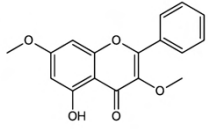
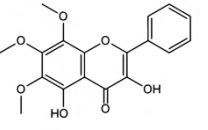
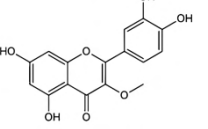
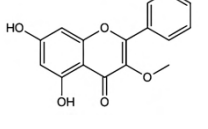
Equation 5.1: Free radical scavenging mechanism

Table 5.1 presents the antioxidant capacities measured for four isolated flavonoids and the total extract of *H. pandurifolium*. A graphical comparison of the antioxidant abilities among the extract and the flavonoids (**C1-C4**) from both FRAP and TEAC assays are presented in figures 5.1 and 5.2 respectively.

Compound **C3** was found to be the phytochemical with the greatest antioxidant capacity of the four isolated compounds. This result is in accordance with the theory that more hydroxyl functional groups on the flavan backbone structure lead to greater antioxidant activity, as described in chapter 2. This also confirms the significance of the 3'- and 4'- hydroxy groups (catechol) on the B-ring. Compound **C1** on the other hand, having only one free OH at position 5, showed no significant activity in the FRAP antioxidant assay and relatively low activity in the TEAC antioxidant assay when compared to the other compounds. Compound **C4** showed similar (low) antioxidant activity in the FRAP assay due to the methylated hydroxyl functional group at position 3. The significance of the free hydroxy on the C-3 is evident in the FRAP assay results, where compound **C2** (only compound with a free 3-OH) yields significantly

greater antioxidant effect compared to the others (excluding **C3**), even though the positions C-6, C-7, and C-8 are all methoxylated. The total methanolic extract of *H. pandurifolium*, when compared to other methanolic extracts of *Helichrysum* (table 2.2), showed FRAP antioxidant activity (43.7 ± 0.1 mg AAE/g) being less than those of the various other *Helichrysum* species summarised in chapter 2. Epigallocatechingallate (EGCG) was used as a reference standard.

Table 5.1: Total antioxidant capacities of isolated flavonoids and total extract of *H. pandurifolium*

Sample	Structure	FRAP		TEAC	
		$\mu\text{mol AAE/g}$	mg AAE/g	$\mu\text{mol TE/g}$	mg TE/g
C1		No significant activity	No significant activity	$246,8 \pm 2,9$	43.5 ± 0.7
C2		272.8 ± 7.1	48.0 ± 1.3	799.8 ± 8.6	200.2 ± 2.1
C3		1183.6 ± 69.7	208.5 ± 12.7	952.9 ± 1.5	238.5 ± 0.4
C4		17.6 ± 2.8	3.1 ± 0.5	486.6 ± 3.7	121.8 ± 0.9
Total extract	N/A	248.2 ± 0.1	43.7 ± 0.1	722.4 ± 16.6	180.8 ± 4.1
EGCG	N/A	7525.0 ± 4.9	1325.3 ± 0.9	4146.4 ± 19.8	1037.8 ± 1.0

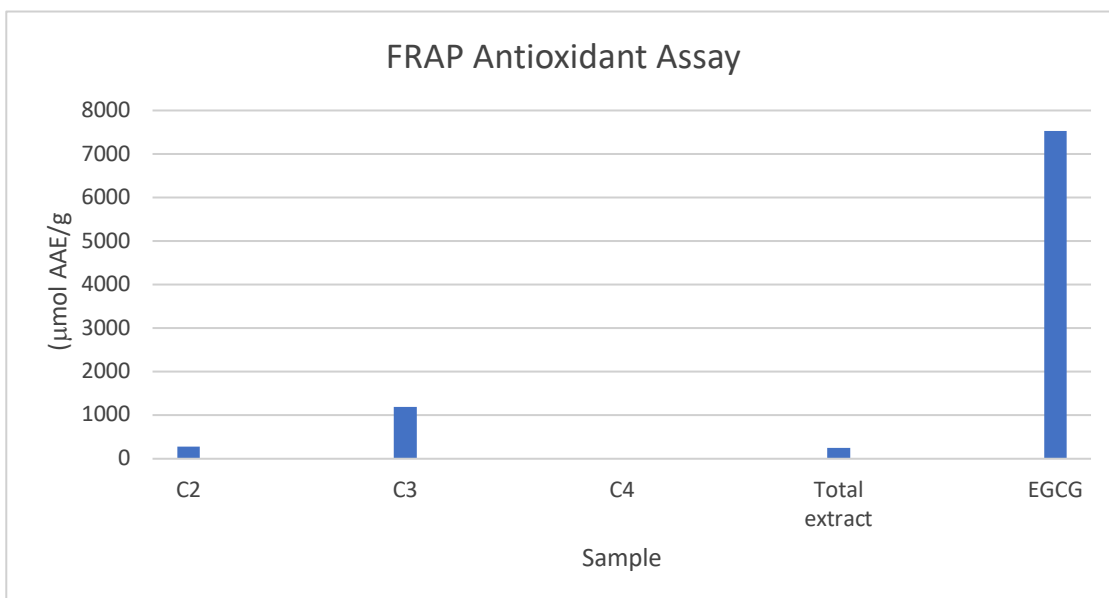


Figure 5.1: Visual comparison of FRAP antioxidant assay results

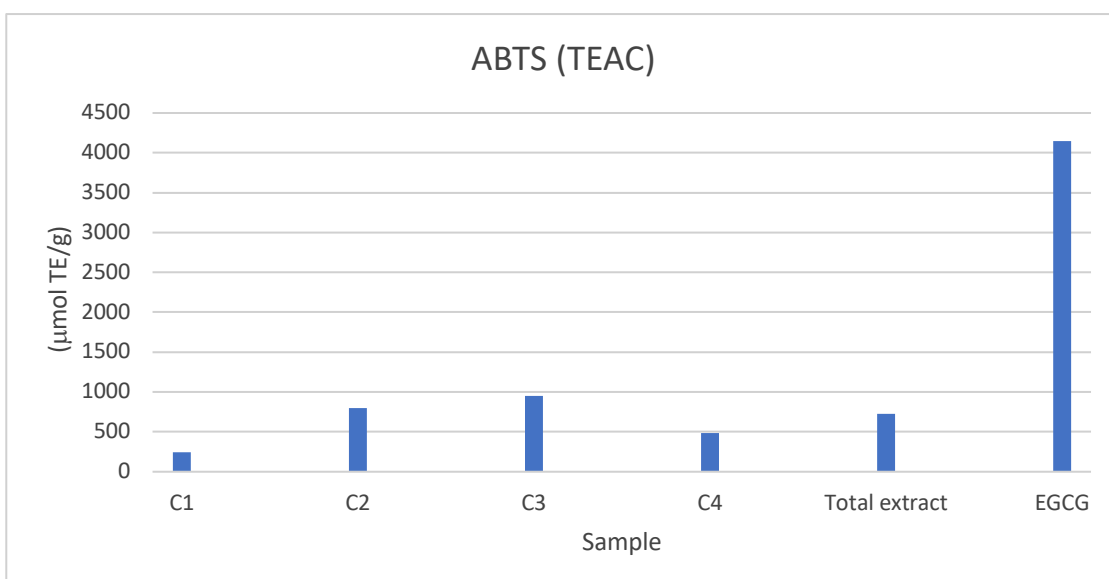


Figure 5.2: Visual comparison of ABTS (TEAC) antioxidant assay results

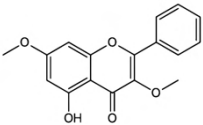
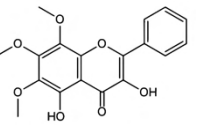
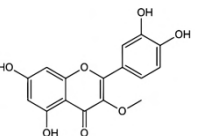
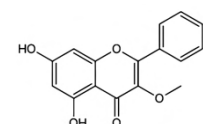
5.2.3 Evaluating the α -glucosidase Inhibition of Isolated Compounds

When it comes to the effective management of non-insulin-dependent diabetes mellitus, many researchers have been looking to natural sources in search of effective enzyme inhibitors in hope of developing functional foods to be used to combat diabetic disorders such as hyperglycaemia. This is done by identifying naturally occurring compounds that retard the absorption of glucose into the bloodstream by the inhibition of the carbohydrate hydrolysing α -glucosidase and α -amylase key digestive enzymes. α -Glucosidase is involved in the final step of the breakdown of carbohydrates in the digestive system. An inhibition of α -glucosidase

activity can lead to a delay in the rate of glucose uptake, thus leading to the suppression of postprandial hyperglycaemia. Many α -glucosidase phytochemical inhibitors have been isolated from plants, particularly flavonoids (Kumar et al., 2011).

Table 5.2 presents the IC_{50} values for α -glucosidase inhibition by four isolated flavonoids (**C1-C4**) and the total methanolic extract of *H. pandurifolium*. Typically, lower the IC_{50} value the greater the inhibition, meaning that a lower concentration of the flavonoid is needed to obtain a 50% inhibition of the enzyme. It should be noted that an experimental IC_{50} for compound **C4** was not obtained, although results show that **C4** had 82.10 % α -glucosidase inhibition at 8.33 μ g/mL. This value is a surprisingly low concentration for a relatively high percentage of inhibition, and as reference the percent inhibition for **C3** at 8.33 μ g/mL was included in table 5.2 (see appendix 7 for α -glucosidase inhibition curve). Acarbose was used as positive control.

Table 5.2: α -Glucosidase inhibition (IC_{50}) for isolated flavonoids and total extract

Sample	Structure	α -Glucosidase IC_{50} (μ g/mL)
C1		18.7 \pm 2.4
C2		40.5 \pm 11.6
C3		3.3 \pm 0.4 (84% inhibition at 8.33 μ g/mL)
C4		Not quantified (82% inhibition at 8.33 μ g/mL)
Total extract	N/A	126.5 \pm 14.3
Acarbose	N/A	610.4 \pm 1.0

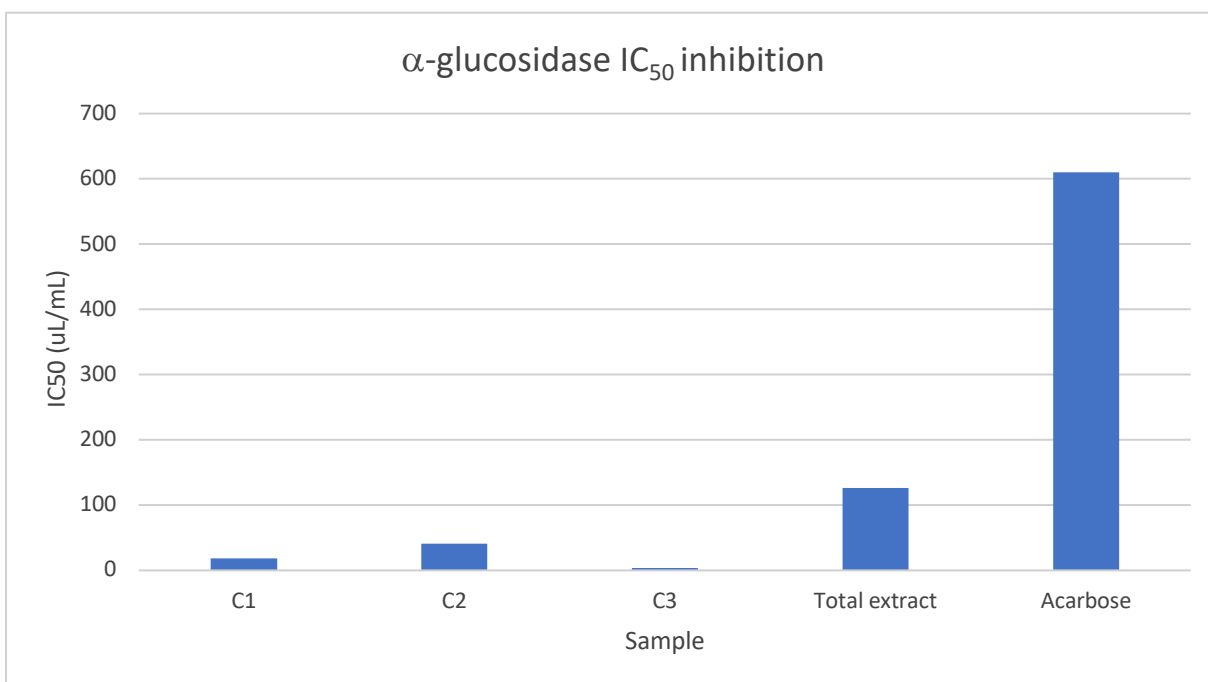


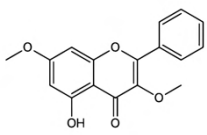
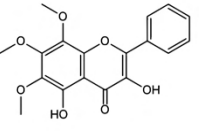
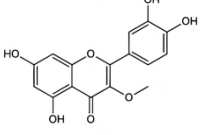
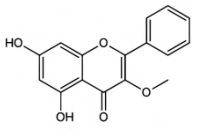
Figure 5.3: Graphical comparison of IC₅₀ values from α-glucosidase inhibition assay

5.2.4 Evaluating the α-amylase Inhibition of the Isolated Compounds

α-Amylase is the enzyme involved in the breakdown of carbohydrates (starch) into maltose, maltotriose, oligoglucans, and small amounts of glucose which can then be further broken down by α-glucosidase and absorbed by the body (Naveen & Baskaran, 2018). For type-2 diabetic patients, inhibiting α-amylase can be an alternate strategy in the management of blood glucose levels (Tundis et al., 2010).

Table 5.3 presents the IC₅₀ values for α-amylase inhibition by four isolated flavonoids (**C1-C4**) and the total methanolic extract of *H. pandurifolium*. Only the flavonoid 3',4',5,7-tetrahydroxy-3-methoxyflavone (compound **C3**) showed α-amylase inhibition with an IC₅₀ of 166.2 ± 15.8 µg/mL. Compounds **C1** and **C4** showed no inhibition up to concentrations of 133 µg/mL, whilst compounds **C2** and the total extract gave results from a negative straight-line plot (appendix 10 and 12), and therefore were not included as a positive result for α-amylase inhibition. Acarbose positive control was found to have an inhibition of 10.2 ± 0.6 µg/mL. The negative straight-line plot may in fact represent an enhancement of enzyme activity at low concentrations, and further investigation into this is advised. The positive result for compound **C3** is in accordance with the structure-activity relationship stated in section 2.6.6. Equipped with functional hydroxy groups at optimal positions (with the exception of the 3-OMe), compound **C3** exhibits good overall anti-diabetic activity. For reference purposes, quercetin showed 41.70% α-amylase inhibition in a study for structure-activity relationships (Proença et al., 2019).

Table 5.3: α -amylase inhibition for isolated flavonoids and total extract (IC_{50})

Sample	Structure	α -Amylase IC_{50} ($\mu\text{g/mL}$)
C1		No inhibition
C2		5.7 ± 1.0 (negative curve)
C3		166.2 ± 15.8
C4		No inhibition
Total extract	N/A	482.1 ± 387.6 (negative curve)
Acarbose	N/A	10.2 ± 0.6

5.3 Conclusion

The total phenolic content of *H. pandurifolium* was found to be greater than majority of the many other *Helichrysum* species mentioned in the chapter 2 literature (table 2.2, page 21), and the plant species and its four isolated flavonoids were revealed to possess measurable antioxidant activities. Additionally, the isolated flavonoids of *H. pandurifolium* showed anti-diabetic potential via *in vitro* studies.

CHAPTER 6: GENERAL DISCUSSION, CONCLUSION AND RECOMMENDATIONS

“Every single day you`re the result of what you did on the days prior.”

– Chris Hadfield

Medicinal plants, such as *Helichrysum*, provide an everlasting range of secondary metabolites, such as flavonoids, terpenoids, phloroglucinols, phenolics, and vitamins which possess valuable bioactivities within the human body such as antioxidant, anti-diabetic, antibacterial, anti-inflammatory, anti-carcinogenic, antitumor and antimutagenic effects (Jain et al., 2019; Velu et al., 2018). Significantly, although *Helichrysum* spp. have been thoroughly studied both biologically and chemically worldwide, there are still many species within Southern Africa that have not yet been investigated – *H. pandurifolium* being one of them. This investigation is a first scientific report to conclude on some of the phytochemicals found in *H. pandurifolium*, as well as documentation pertaining to their antioxidant and anti-diabetic properties.

Oxidative stress is the result of the excess accumulation of bioactive oxidative products, free radicals, and reactive oxygen species within the body such that they overwhelm the capacity of the cellular antioxidant defence system (Basu, 2010; Schrader & Fahimi, 2006). Oxidative stress is often associated with an increased risk of chronic diseases such as diabetes, carcinogenesis, and atherosclerosis. Additionally, oxidative stress increases inflammation, damage to DNA, cells, and organs which can lead to the progression of various degenerative diseases and ultimately accelerate the ageing process (Adom & Liu, 2002; Albayrak et al., 2010; Carocho & Ferreira, 2013; Rufino et al., 2009). Flavonoids, being one of the major class constituents of *Helichrysum* spp., have time and time again, demonstrated antioxidant and oxidative stress modulatory properties. Possessing significant antioxidant and chelating properties, flavonoids may be one of the most underrated classes of natural phytochemicals. Flavonoids achieve their antioxidant effects by acting as acceptors of free radicals, chelating with metals to form complexes, or breaking down chain reactions caused by oxidative stress.

Diabetes mellitus is a metabolic condition whereby the body is persistently affected by hyperglycaemia, which is caused by defects in insulin secretion, insulin action, or the latter two combined (Rees et al., 2017). In 2019, it was announced that 463 million people were diagnosed with diabetes worldwide (Wass et al., 2014; International Diabetes Federation, 2019). In this manner, the ongoing search for cheaper, natural alternatives to diabetic treatment proves useful as global statistics continue to increase annually. Flavonoids have proven to be *in vitro* anti-diabetic agents through the inhibition of key digestive enzymes, namely α -amylase and α -glucosidase. Additionally, flavonoids have also been shown to help

regulate glucose metabolism (Ren et al., 2016), improve glucose tolerance and insulin resistance (Oza & Kulkarni, 2018), reduce blood glucose levels and slow the production of glucose in the liver (Xu et al., 2018), regulate lipid metabolism, protect against hepatic inflammation and lipid accumulation (Minxuan et al., 2019), down-regulate oxidative stress and inflammation, lower levels of pro-inflammatory cytokines (Samie et al., 2018) and even exhibit *in vivo* renoprotective effects (Y. J. Chen et al., 2019).

This investigation was initiated with a preliminary TLC analysis of *H. pandurifolium* total methanolic extract which revealed a multitude of interesting phytochemical components. After developing and staining the TLC plate with vanillin/H₂SO₄, it exhibited a unique spectrum of yellow, orange, red, purple, and blue spots. *H. pandurifolium* is a species which contains not only flavonoids (yellow/orange/red spots), but also a variety of other phytochemical classes such as phloroglucinols (often purple spots) and terpenoids (usually blue spots). Further separation of phytochemicals was carried out using column chromatographic methods employing silica gel and sephadex as stationary phases, and hexane, ethyl acetate, methanol, ethanol, acetic acid and water in various ratios as mobile phases via gradient elution methods. Information was gathered from subsequent sub-fraction TLC analysis, allowing for the identification of worthy phytochemical targets and the required solvent polarity for their adequate separation. Further purifications resulted in the isolation of four pure flavonoids namely; 5-hydroxy-3,7-dimethoxyflavone (**C1**), 3,5-dihydroxy-6,7,8-trimethoxyflavone (**C2**), 3',4',5,7-tetrahydroxy-3-methoxyflavone (**C3**) and 5,7-dihydroxy-3-methoxyflavone (**C4**) identified using NMR and UV spectroscopic analysis described in table 6.1.

The antioxidant activities of the isolated flavonoids were carried out *in vitro* using Ferric-ion reducing antioxidant power (FRAP) and Trolox equivalent absorbance capacity (TEAC) assays, as well as the determination of the total phenolic content (TPC) of the *H. pandurifolium* total extract using the Folin-Ciocalteu assay. The anti-diabetic properties were evaluated *in vitro* by the studying the inhibition of key digestive enzymes α -glucosidase and α -amylase by the total extract and four isolated flavonoids. The biological activities of isolated flavonoids and *H. pandurifolium* total extract are summarised in table 6.2.

Table 6.1: Isolated flavonoids from *H. pandurifolium*

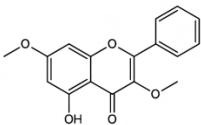
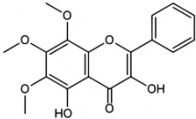
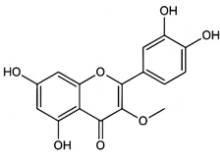
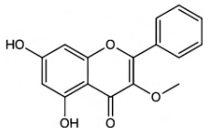
Compound	Name	Structure	Mass isolated
C1	5-hydroxy-3,7-dimethoxyflavone		60 mg
C2	3,5-dihydroxy-6,7,8-trimethoxyflavone		118 mg
C3	3',4',5,7-tetrahydroxy-3-methoxyflavone		132 mg
C4	5,7-dihydroxy-3-methoxyflavone		20 mg

Table 6.2: Summary of biological activities of isolated flavonoids and total extract from *H. pandurifolium*

Compound	TPC (mg GAE/g)	FRAP ($\mu\text{mol AAE/g}$)	TEAC ($\mu\text{mol TE/g}$)	α -glucosidase ($\mu\text{g/mL}$)	α -amylase ($\mu\text{g/mL}$)
C1	N/A	No activity	246.8 \pm 2.9	18.7 \pm 2.4	No inhibition
C2	N/A	272.8 \pm 7.1	799.8 \pm 8.6	40.5 \pm 11.6	5.7 \pm 0.1 (negative curve)
C3	N/A	1183.6 \pm 69.7	952.9 \pm 1.5	3.3 \pm 0.4	116.2 \pm 15.8
C4	N/A	17.6 \pm 2.8	486.6 \pm 3.7	82% inhibition at 8.33 $\mu\text{g/mL}$	No inhibition
Total extract	108.3 \pm 18.9	248.2 \pm 0.1	722.4 \pm 16.6	126.5 \pm 14.3	482.1 \pm 387.6 (negative curve)
EGCG	N/A	7525.0 \pm 4.9	4146.4 \pm 19.8	N/A	N/A
Acarbose	N/A	N/A	N/A	610.4 \pm 1.0	10.2 \pm 0.6

The antioxidant assays used in this study determine the ability of phytochemicals to scavenge free radicals via the transfer of an electron. The total phenolic content (TPC) of *H. pandurifolium* was found to be 108.3 ± 18.9 mg GAE/g, which interestingly enough, is greater than that for most of the other *helichrysum* species described earlier (blue bars, figure 6.1). Yet, *H. pandurifolium* total extract simultaneously showed significantly lower FRAP antioxidant activity (43.7 ± 0.1 mg AAE/g, table 5.1) than all other *Helichrysum* species described in the literature review (orange bars, figure 6.1). One reason for this observation may be due to the total extract being stored for a period of 12-18 months prior to FRAP antioxidant analysis, resulting in the total phenolic content remaining constant, but total antioxidant capacity of the total extract decreasing due to oxidation and degradation with time. Many *Helichrysum* species are still being used as a traditional medicine in South Africa today, and *H. pandurifolium* could be one of the more effective antioxidant species of local *Helichrysum* spp. due to its relatively high phenolic content. The FRAP antioxidant activity should however be measured directly after extraction to obtain a more accurate measurement. The main fractions chosen to isolate flavonoids in this study were relatively non-polar compared to the rest of the main fractions, and thus due to the nature of the extraction methods used, it is proposed that even more highly polar flavonoids exist in the main fractions which are predicted to be adding to the total antioxidant power and relatively high TPC observed by the *H. pandurifolium* total extract. Of the isolated phytochemicals 3',4',5,7-tetrahydroxy-3-methoxyflavone (**C3**) showed the highest antioxidant activity among all the other isolated flavonoids for both the FRAP and TEAC assays (1183.6 ± 69.7 μ mol AAE/g and 952.9 ± 1.5 μ mol TE/g respectively), which is in agreement with the antioxidant structure-activity relationship proposed for flavonoids. This is considered moderate activity when compared to the reference antioxidant epigallocatechingallate (EGCG). Compound 3',4',5,7-tetrahydroxy-3-methoxyflavone (**C3**) was also isolated in the largest quantity from *H. pandurifolium* (132 mg) and may be adding significantly to the total extracts' antioxidant activity, although again, it is believed that more polar main fractions may contain more potent flavonoids, possibly in even higher concentrations. Therefore, *H. pandurifolium* ultimately requires further investigation into its more polar fractions and may contain compounds with even more effective antioxidant properties.

The anti-diabetic properties of the total extract and four isolated flavonoids were evaluated by studying their *in vitro* inhibitory properties for key digestive enzymes α -glucosidase and α -amylase. Compounds **C3** and **C1** showed the highest positive inhibitory activity and exhibited the lowest IC₅₀ values for the inhibition of α -glucosidase being 3.3 ± 0.4 and 18.7 ± 2.4 μ g/mL respectively. Unfortunately, the IC₅₀ α -glucosidase inhibition for compound **C4** was not obtained due to a lack of experimental data, although experimental results showed that **C4** had a significant 82,10% α -glucosidase inhibition at 8,33 μ g/mL concentration. As a reference, **C3** had 84,39% α -glucosidase inhibitions at that same concentration. This indirectly means

that compound **C4** may in fact have an IC_{50} similar, but not quite as potent as **C3**, yet still greater anti-diabetic effects than **C1**. Compound **C3** was the only flavonoid that showed any significant α -amylase inhibition with an IC_{50} value of $116.2 \pm 15.8 \mu\text{g/mL}$. Again, this was expected as the inhibition followed suit in accordance with the structure-activity relationship discussed in chapter 2, where the catechol group on ring-B, hydroxy functional groups at 5-, 7- or 8-position of ring-A and $C2=C3$ double bond in ring-C are all crucial for flavonoid α -glucosidase and α -amylase activity (Proença et al., 2017). Interestingly, compound **C2** and the total extract showed somewhat significant α -amylase inhibition, 5.7 ± 1.0 and $482.1 \pm 387.6 \mu\text{g/mL}$ respectively, although from negative straight-line curves (see appendix 10 and 12). This could mean that these present an enhancement of enzyme activity at low concentrations and should be further investigated. It was observed that the α -glucosidase inhibition of *H. pandurifolium* total extract is not as effective as that of its pure phytochemical components, probably due to the dilution of active phytochemicals by various non-active components. It is therefore probably necessary to chemically process the plant and its total extracts to obtain a highly effective anti-diabetic extract for therapeutic application. The total extract may be useful as an antioxidant health supplement, but this is only recommended after further cytotoxicity studies have been done on the plant.

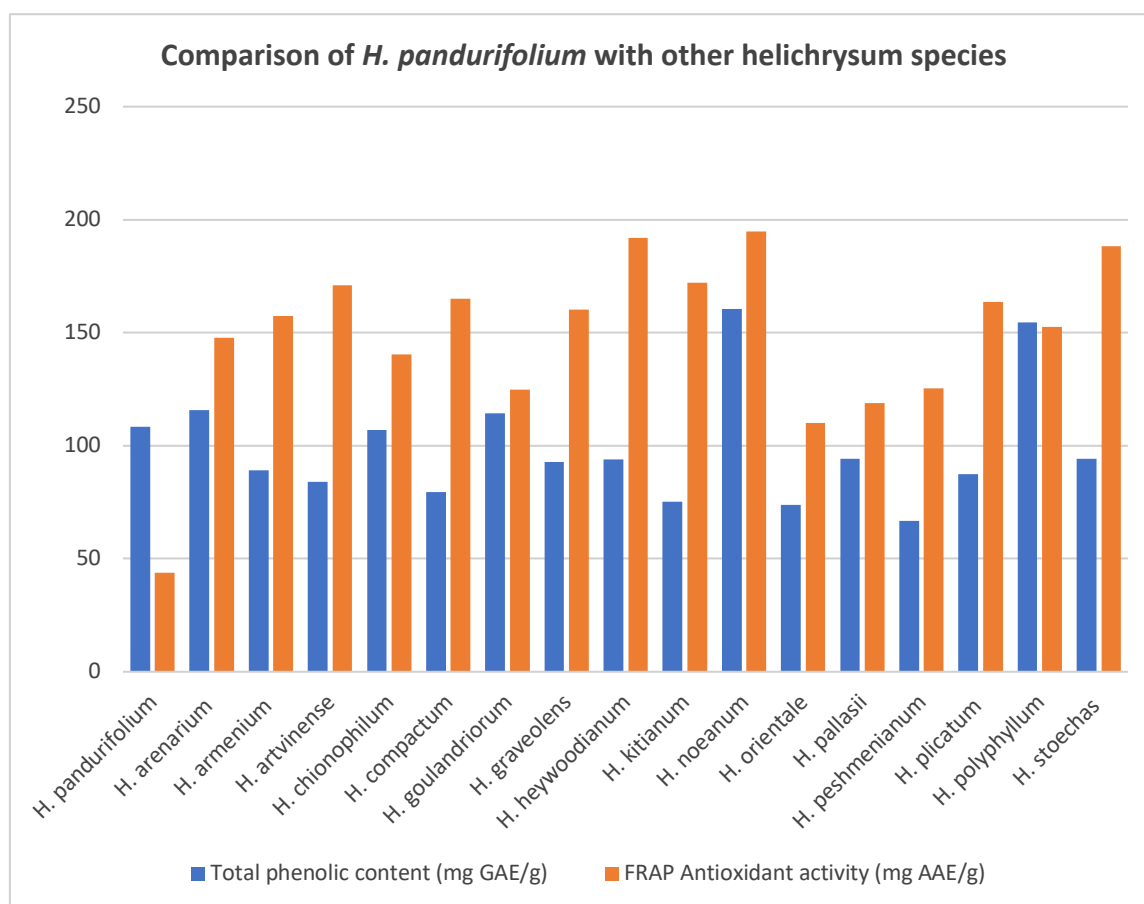


Figure 6.1: Comparison of TPC and FRAP results of *H. pandurifolium* with other *Helichrysum* species

Conclusion

Four known flavonoids were isolated for the first time from *H. pandurifolium* Schrank. All of the isolated compounds (including total extract) were revealed to have moderate to good antioxidant activity (according to both the TEAC and FRAP assays), and were shown to have the ability to inhibit α -glucosidase enzymes. Compound **C3** was able to inhibit α -amylase enzyme. The research findings in this study establish that *H. pandurifolium* has the potential be an important medicinal plant which is rich in flavonoids, and may be beneficial in the prevention of diseases caused by free radical damage. *H. pandurifolium* extracts may find use as a viable strategy in the management of high blood glucose levels for diabetics.

Recommendations

The following recommendations can be made based on research findings in this study:

1. As this study included the separation of flavonoids from comparatively non-polar fractions of the total extract, further exploration of more polar fractions of the total extract is recommended for a complete study of the phytochemistry of *H. pandurifolium* Schrank.
2. It is recommended that the essential oil of *H. pandurifolium* be analysed in the future.
3. The isolated compounds can be further derivatised to improve the biological activities.
4. It is recommended that further cytotoxicity studies be performed for *H. pandurifolium* before approaching it as a natural supplement.

References

- Abdalla, M.A. & Laatsch, H. 2012. Flavonoids from Sudanese *Albizia Zygia* (Leguminosae, subfamily *mimosoideae*), a plant with antimalarial potency. *The African Journal of Traditional, Complementary and Alternative medicines*, 9(1): 56–58.
- Van Acker, S.A.B.E., Van Den Berg, D.J., Tromp, M.N.J.L., Griffioen, D.H., Van Bennekom, W.P., Van Der Vijgh, W.J.F. & Bast, A. 1996. Structural aspects of antioxidant activity of flavonoids. *Free Radical Biology and Medicine*, 20(3): 331–342.
- Adom, K. & Liu, R. 2002. Antioxidant Activity of Grains. *Journal of Agricultural and Food Chemistry*, 50(21): 6182–6187.
- Afolayan, A.J. & Meyer, J.J. 1997. The antimicrobial activity of 3,5,7-trihydroxyflavone isolated from the shoots of *Helichrysum aureonitens*. *Journal of Ethnopharmacology*, 57(3): 177–181.
- Afoulous, S., Ferhout, H., Raelison, E.G., Valentin, A., Moukarzel, B., Couderc, F. & Bouajila, J. 2011. *Helichrysum gymnocephalum* essential oil: chemical composition and cytotoxic, antimalarial and antioxidant activities, attribution of the activity origin by correlations. *Molecules*, 16(10): 8273–8291.
- Ahmed, D., Kumar, V., Sharma, M. & Verma, A. 2014. Target guided isolation, in-vitro antidiabetic, antioxidant activity and molecular docking studies of some flavonoids from *Albizzia Lebbeck* Benth. bark. *BMC Complementary and Alternative Medicine*, 14.
- Aiyegoro, O.A., Afolayan, A.J. & Okoh, A.I. 2010. Interactions of antibiotics and extracts of *Helichrysum pedunculatum* against bacteria implicated in wound infections. *Folia Microbiologica*, 55(2): 176–180.
- Aiyegoro, O.A. & Okoh, A.I. 2009. Phytochemical screening and polyphenolic antioxidant activity of aqueous crude leaf extract of *Helichrysum pedunculatum*. *International Journal of Molecular Sciences*, 10(11): 4990–5001.
- Al-Rehaily, A.J., Albishi, O.A., El-Olemy, M.M. & Mossa, J.S. 2008. Flavonoids and terpenoids from *Helichrysum forskahlii*. *Phytochemistry*, 69(9): 1910–1914.
- Albayrak, S., Aksoy, A., Sağdıç, O. & Hamzaoğlu, E. 2010. Compositions, antioxidant and antimicrobial activities of *Helichrysum (Asteraceae)* species collected from Turkey. *Food Chemistry*, 119: 114–122.
- Anderberg, A.A. 1994. Tribe Inuleae. In: Bremer K. (ed.). *Asteraceae: Cladistics and Classification*: 273–291.
- Anderson, R.A., Evans, M.L., Ellis, G.R., Graham, J., Morris, K., Jackson, S.K., Lewis, M.J., Rees, A. & Frenneaux, M.P. 2001. The relationships between post-prandial lipaemia, endothelial function and oxidative stress in healthy individuals and patients with type 2 diabetes. *Atherosclerosis*, 154(2): 475–483.
- Anon. 2017. International Diabetes Federation. *IDF Diabetes Atlas*. <https://diabetesatlas.org/en/> 29 January 2020.
- Antunes Viegas, D., Palmeira-De-Oliveira, A., Salgueiro, L., Martinez-De-Oliveira, J. & Palmeira-De-Oliveira, R. 2014. *Helichrysum italicum*: From traditional use to scientific data. *Journal of Ethnopharmacology*, 151(1): 54–65.
- Arnold, T.H., Prentice, C.A., Hawker, L.C., Snyman, E.E., Tomalin, M., Crouch, N.R. & Pottas-

- Bircher, C. 2002. Medicinal and Magical Plants of Southern Africa: an Annotated Checklist. *National Botanical Institute, Pretoria.*: 32–34.
- Asekun, O.T., Grierson, D.S. & Afolayan, A.J. 2007. Characterization of essential oils from *Helichrysum odoratissimum* using different drying methods. *Journal of Applied Sciences*, 7(7): 1005–1008.
- Aslan, M., Orhan, D.D., Orhan, Nilufer & Sezik, E. 2007. In vivo antidiabetic and antioxidant potential of *Helichrysum plicatum* ssp. *plicatum* capitulums in streptozotocin-induced-diabetic rats. *Journal of Ethnopharmacology*, 109(1): 54–59.
- Aslan, M., Orhan, D.D., Orhan, Nilüfer, Sezik, E. & Yeşilada, E. 2007. A study of antidiabetic and antioxidant effects of *Helichrysum graveolens* capitulums in streptozotocin-induced diabetic rats. *Journal of Medicinal Food*, 10(2): 396–400.
- Baena-Díez, J.M., Peñafiel, J., Subirana, I., Ramos, R., Elosua, R., Marín-Ibañez, A., Guembe, M.J., Rigo, F., Tormo-Díaz, M.J. & Moreno-Iribas, C. 2016. Risk of cause-specific death in individuals with diabetes: a competing risks analysis. *Diabetes Care*, 39(11): 1987–1995.
- Bailey, C. & Day, C. 1989. Traditional Plant Medicines as Treatments for Diabetes. *Diabetes Care*, 12(September): 553–564.
- Balunas, M.J. & Kinghorn, A.D. 2005. Drug discovery from medicinal plants. *Life Sciences*, 78(5): 431–441.
- Basu, S. 2010. Fatty acid oxidation and isoprostanes: Oxidative strain and oxidative stress. *Prostaglandins, Leukotrienes and Essential Fatty Acids*, 82(4–6): 219–225.
- Bhat, R.B. 2014. Medicinal plants and traditional practices of Xhosa people in the Transkei region of Eastern Cape, South Africa. *Indian Journal of Traditional Knowledge*, 13(2): 292–298.
- Bohlmann, F. & Mahanta, P.K. 1979. Further phloroglucinol derivatives from *Helichrysum gymnoconum*. *Phytochemistry*, 18(2): 348–350.
- Bohlmann, F. & Misra, L.N. 1984. New prenylflavanones and chalcones from *Helichrysum rugulosum*. *Planta Medica*, 50(3): 271–272.
- Bohlmann, F. & Zdero, C. 1980. Naturally occurring coumarins. 18. New obliquin derivatives from *Helichrysum serpyllifolium*. *Phytochemistry*, 19(2): 331–332.
- Bohlmann, F., Zdero, C., Hoffmann, E., Mahanta, P.K. & Dorner, W. 1978. Naturally occurring terpene derivatives. Part 166. New diterpenes and sesquiterpenes from South African *Helichrysum* species. *Phytochemistry*, 17(11): 1917–1922.
- Bohm, B.A. & Stuessy, T.F. 2001. *Flavonoids of the Sunflower Family (Asteraceae)*.
- Brown, J.E., Khodr, H., Hider, R.C. & Rice-evans, C.A. 1998. Structural dependence of flavonoid interactions with Cu²⁺ ions- implications for their antioxidant properties. , 1178: 1173–1178.
- Buckingham, J. & Munasinghe, V.R.N. 2015. *Dictionary of Flavonoids with CD-ROM*.
- Buettner, G.R. 1993. The Pecking Order of Free Radicals and Antioxidants: Lipid Peroxidation, α -Tocopherol, and Ascorbate. *Archives of Biochemistry and Biophysics*, 300(2): 535–543.
- Carocho, M. & Ferreira, I. 2013. A review on antioxidants, prooxidants and related controversy:

Natural and synthetic compounds, screening and analysis methodologies and future perspectives. *Food and Chemical Toxicology*, 51: 15–25.

- Cerretani, L. & Bendini, A. 2010. *Olives and Olive Oil in Health and Disease Prevention*.
- Chabert, P., Auger, C., Pincemail, J. & Schini-Kerth, V.B. 2014. Overview of Plant-Derived Antioxidants. *Systems Biology of Free Radicals and Antioxidants*: 4005–4022.
- Chatterjee, S., Khunti, K. & Davies, M.J. 2017. Type 2 diabetes. *The Lancet*, 389(10085): 2239–2251.
- Chaudhury, A., Duvoor, C., Reddy Dendi, V.S., Kraleti, S., Chada, A., Ravilla, R., Marco, A., Shekhawat, N.S., Montales, M.T., Kuriakose, K., Sasapu, A., Beebe, A., Patil, N., Musham, C.K., Lohani, G.P. & Mirza, W. 2017. Clinical Review of Antidiabetic Drugs: Implications for Type 2 Diabetes Mellitus Management. *Frontiers in Endocrinology*.
- Chen, Y.J., Kong, L., Tang, Z.Z., Zhang, Y.M., Liu, Y., Wang, T.Y. & Liu, Y.W. 2019. Hesperetin ameliorates diabetic nephropathy in rats by activating Nrf2/ARE/glyoxalase 1 pathway. *Biomedicine and Pharmacotherapy*, 111(209): 1166–1175. <https://doi.org/10.1016/j.biopha.2019.01.030>.
- Chen, Y.L., Weng, S.F., Yang, C.Y., Wang, J.J. & Tien, K.J. 2019. Diabetic ketoacidosis further increases risk of Alzheimer's disease in patients with type 2 diabetes. *Diabetes Research and Clinical Practice*, 147(901): 55–61. <https://doi.org/10.1016/j.diabres.2018.11.013>.
- Cho, N.H., Shaw, J.E., Karuranga, S., Huang, Y., da Rocha Fernandes, J.D., Ohlrogge, A.W. & Malanda, B. 2018. IDF Diabetes Atlas: Global estimates of diabetes prevalence for 2017 and projections for 2045. *Diabetes Research and Clinical Practice*, 138: 271–281. <https://doi.org/10.1016/j.diabres.2018.02.023>.
- Correlation, T.H.E., Active, B., Scavenging, O., Effects, A., Flavonoids, O.F., Hanasaki, Y., Ogawa, S. & Fukui, S. 1994. The Correlation Between Active Oxygens Scavenging and Antioxidative Effects Of Flavonoids. *Free radical biology & medicine*, 16(6): 845–850.
- Coşar, G. & Çubukçu, B. 1990. Antibacterial activity of *Helichrysum* species growing in Turkey. *Fitoterapia*, 61: 161–164.
- Cowling, R.M., MacDonald, I.A.W. & Simmons, M.T. 1996. The Cape Peninsula, South Africa: physiographical, biological and historical background to an extraordinary hot-spot of biodiversity. *Biodiversity & Conservation*, 5(5): 527–550. <https://doi.org/10.1007/BF00137608>.
- Cragg, G.M., Newman, D.J. & Snader, K.M. 1997. Natural products in drug discovery and development. *Journal of Natural Products*, 60(1): 52–60.
- Cunningham, A. 1988. *An Investigation of the Herbal Medicine Trade in Natal/KwaZulu. Institute of Natural Resources Investigational Report 29*.
- Cushnie, T., Hamilton, V., Chapman, D., Taylor, P. & Lamb, A. 2007. Aggregation of *Staphylococcus aureus* following treatment with the antibacterial flavonol galangin. *Journal of Applied Microbiology*, 103(5): 1562–1567.
- Czinner, E., Hagymási, K., Blázovics, A., Kéry, Á., Szóke, É. & Lemberkovics, É. 2000. In vitro antioxidant properties of *Helichrysum arenarium* (L.) Moench. *Journal of Ethnopharmacology*, 73: 437–443.
- Davies, K.J. 1995. Oxidative stress: the paradox of aerobic life. *Biochemical Society symposium*, 61: 1–31.

- Dekker, T.G., Fourie, T.G., Snyckers, F.O. & Van der Schyf, C.J. 1983. Studies of South African medicinal plants. Part 2. Caespitin, a new phloroglucinol derivative with antimicrobial properties from *Helichrysum caespitium*. *South African Journal of Chemistry*, 36(4): 114–116.
- Delli, A.J. & Lernmark, Å. 2015. *Type 1 (Insulin-Dependent) Diabetes Mellitus: Etiology, Pathogenesis, Prediction, and Prevention*. Seventh Ed. Elsevier Inc. <http://dx.doi.org/10.1016/B978-0-323-18907-1.00039-1>.
- Drewes, S.E., Mudau, K.E., Van Vuuren, S.F. & Viljoen, A.M. 2006. Antimicrobial monomeric and dimeric diterpenes from the leaves of *Helichrysum tenax var tenax*. *Phytochemistry*, 67(7): 716–722.
- Drewes, S.E. & van Vuuren, S.F. 2008. Antimicrobial acylphloroglucinols and dibenzyloxy flavonoids from flowers of *Helichrysum gymnocomum*. *Phytochemistry*, 69(8): 1745–1749.
- Duckworth, W.C. 2001. Hyperglycemia and cardiovascular disease. *Current atherosclerosis reports*, 3(5): 383–391.
- Duthie, G.G., Gardner, P.T. & Kyle, J.A.M. 2003. Plant polyphenols: are they the new magic bullet? *Proceedings of the Nutrition Society*, 62(3): 599–603.
- Eichler, H.G., Korn, A., Gasic, S., Pirson, W. & Businger, J. 1984. The effect of a new specific α -amylase inhibitor on post-prandial glucose and insulin excursions in normal subjects and Type 2 (non-insulin-dependent) diabetic patients. *Diabetologia*, 26: 278–281.
- Elgorashi, E.E., van Heerden, F.R. & van Staden, J. 2008. Kaempferol, a mutagenic flavonol from *Helichrysum simillimum*. *Human & Experimental Toxicology*, 27(11): 845–849.
- Errico, J.P. 2018. *Insulin Resistance, Glucose Metabolism, Inflammation, and the Role of Neuromodulation as a Therapy for Type-2 Diabetes*. Second Edi. Elsevier Ltd. <https://doi.org/10.1016/B978-0-12-805353-9.00133-9>.
- Farhadi, F., Khameneh, B., Iranshahi, M. & Iranshahi, M. 2019. Antibacterial activity of flavonoids and their structure–activity relationship: An update review. *Phytotherapy Research*, 33(1): 13–40.
- Finnan, D. 2020. Artemisia: Madagascar's coronavirus cure or Covid-19 quackery? <http://www.rfi.fr/en/africa/20200505-artemisia-madagascar-s-coronavirus-cure-or-covid-19-quackery-covid-organics-malaria> 13 May 2020.
- Forbes, J.M. & Cooper, M.E. 2013. Mechanisms of diabetic complications. *Physiological Reviews*, 93(1): 137–188.
- Forkmann, G. 1989. *Gene-enzyme relations and genetic manipulation of anthocyanin biosynthesis in flowering plants*. D. E. Styles, G. A. Gavazzi, & M. L. Racchi, eds.
- Geissman, T.A., Mukherjee, R. & Sim, K.Y. 1967. Constituents of *Helichrysum viscosum var bracteatum*. *Phytochemistry*, 6(11): 1575–1581.
- Ghani, U. 2020. Introduction, rationale and the current clinical status of oral α -glucosidase inhibitors. *Alpha-Glucosidase Inhibitors*: 1–15.
- Giacco, F. & Brownlee, M. 2010. Oxidative Stress and Diabetic Complications A. M. Schmidt, ed. *Circulation Research*, 107(9): 1058–1070. <https://www.ahajournals.org/doi/10.1161/CIRCRESAHA.110.223545>.

- Giuliani, C., Bucci, I., Di Santo, S., Rossi, C., Grassadonia, A., Piantelli, M., Monaco, F. & Napolitano, G. 2014. The flavonoid quercetin inhibits thyroid-restricted genes expression and thyroid function. *Food and Chemical Toxicology*, 66: 23–29. <http://dx.doi.org/10.1016/j.fct.2014.01.016>.
- Goldblatt, P. & Manning, J.C. 2002. Plant diversity of the Cape region of Southern Africa. *Annals of the Missouri Botanical Garden*, 89(2): 281–302. http://cdiac.esd.ornl.gov/oceans/GLODAP/glodap_pdfs/Thermohaline.web.pdf.
- Gouda, H., Charlson, F., Sorsdahl, K., Ahmadzada, S., Ferrari, A., Erskine, H., Leung, J., Santamauro, D., Lund, C., Aminde, L., Mayosi, B., Kengne, A., Harris, M., Achoki, T., Wiysonge, C., Stein, D. & Whiteford, H. 2019. Burden of non-communicable diseases in sub-Saharan Africa, 1990–2017. Results from the Global Burden of Disease Study. *Thee Lancet Global Health*, 7(10): 1375–1387.
- Halliwell, B. & Gutteridge, J.M.C. 1998. *Free Radicals in Biology and Medicine*. Oxford: Oxford University Press.
- Harman, D. 1956. Aging: A Theory on Free Radical Radiation Chemistry. *J. Gerontol.*, 11: 298–300.
- Heim, K.E., Tagliaferro, A.R. & Bobilya, D.J. 2002. Flavonoid antioxidants: Chemistry, metabolism and structure-activity relationships. *Journal of Nutritional Biochemistry*, 13(10): 572–584.
- Heyman, H.M., Maharai, V. & Meyer, J.J.M. 2013. *Identification of anti-HIV compounds in Helichrysum species (Asteraceae) by means of NMR-based metabolomic guided fractionation*. Pretoria.
- Hilliard, O.M. 1983. Asteraceae, Inuleae, Gnaphaliinae. *Flora of Southern Africa*, 33.
- Hodnick, W.F., Mlilosavljević, E.B., Nelson, J.H. & Pardini, R.S. 1988. Electrochemistry of flavonoids. Relationships between redox potentials, inhibition of mitochondrial respiration, and production of oxygen radicals by flavonoids. *Biochemical Pharmacology*, 37(13): 2607–2611.
- Hudson, J. & Vimalanathan, S. 2011. Echinacea-A source of potent antivirals for respiratory virus infections. *Pharmaceuticals*, 4(7): 1019–1031.
- International Diabetes Federation. 2019. IDF Diabetes Atlas. <https://diabetesatlas.org/en/> 19 December 2019.
- Jain, C., Khatana, S. & Vijayvergia, R. 2019. Bioactivity of secondary metabolites of various plants: A review. *International Journal of Pharmaceutical Sciences and Research*, 10(2): 494–504.
- Jakupovic, J., Zdero, C., Grenz, M., Tschritzis, F., Lehmann, L., Hashemi-Nejad, S.M. & Bohlmann, F. 1989. Twenty-one acylphloroglucinol derivatives and further constituents from South African *Helichrysum* species. *Phytochemistry*, 28(4): 1119–1131.
- Jovanovic, S. V, Steenken, S., Hara, Y. & Simic, M.G. 1996. Which Ring in Flavonoids Is Responsible for Antioxidant Activity? *J. Chem. Soc. Perkins Trans.*, 2: 2497–2504.
- Jung, M., Park, M., Lee, H.C., Kang, Y.-H., Kang, E.S. & Kim., S.K. 2006. Antidiabetic Agents from Medicinal Plants. *Current Medicinal Chemistry*, 13(10): 1203–1218.
- Knekt, P., Järvinen, R., Seppänen, R., Heliövaara, M., Teppo, L., Pukkala, E. & Aromaa, A. 1997. Dietary Flavonoids and the Risk of Lung Cancer and Other Malignant Neoplasms.

American Journal of Epidemiology, 146(3): 223–230.

- Kumar, S., Narwal, S., Kumar, V. & Prakash, O. 2011. α -glucosidase inhibitors from plants: A natural approach to treat diabetes. *Pharmacognosy Reviews*, 5(9): 19–29.
- Kutluka, I., Aslanbl, M., Orhan, I.E. & Özçelika, B. 2018. Antibacterial, antifungal and antiviral bioactivities of selected *Helichrysum* species. *South African Journal of Botany*, 119: 252–257.
- De La Garza, A.L., Etxeberria, U., Lostao, M.P., San Román, B., Barrenetxe, J., Alfredo Martínez, J. & Milagro, F.I. 2013. *Helichrysum* and grapefruit extracts inhibit carbohydrate digestion and absorption, improving postprandial glucose levels and hyperinsulinemia in rats. *Journal of Agricultural and Food Chemistry*, 61(49): 12012–12019.
- De La Puerta, R., Garcia, M.D., Saenz, M.T. & Gil, A.M. 1990. Phytochemistry of *Helichrysum picardii* Boiss. & Reuter. *Plantas Medicinales et Phytotherapie*, 24(4): 258-263.
- Laishram, S., Sheikh, Y., Moirangthem, D.S., Deb, L., Pal, B.C., Talukdar, N.C. & Borah, J.C. 2015. Anti-diabetic molecules from *Cycas pectinata* Griff. traditionally used by the Maiba-Maibi. *Phytomedicine*, 22(1): 23–26. <http://dx.doi.org/10.1016/j.phymed.2014.10.007>.
- Lall, N., Hussein, A.A. & Meyer, J.J.M. 2006. Antiviral and antituberculous activity of *Helichrysum melanacme* constituents. *Fitoterapia*, 77: 230–232.
- Legoalea, P.B., Mashimbyeb, M.J. & van Reec, T. 2013. Antinflammatory and Antioxidant Flavonoids from *Helichrysum kraussii* and *H. odoratissimum* Flowers. *Natural Product Communications*, 8(10): 1403–1404.
- Li, L., Henry, G.E. & Seeram, N.P. 2009. Identification and bioactivities of resveratrol oligomers and flavonoids from carex folliculata Seeds. *Journal of Agricultural and Food Chemistry*, 57(16): 7282–7287.
- Lin, C., Zhu, C., Hu, M., Wu, A., Zerendawa, B. & Suolangqimei, K. 2014. Structure-activity Relationships of Antioxidant Activity in vitro about Flavonoids Isolated from Pyrethrum Tatsienense. *Journal of Intercultural Ethnopharmacology*, 3(3): 123.
- Liu, H.-Y., He, H.-P., Yang, X.-W., Chen, M.-W. & Hao, X.-J. 2007. Chemical constituents of the flowers of *Helichrysum bracteatum*. *Tianran Chanwu Yanjiu Yu Kaifa*, 19(3): 423–426.
- Liu, L., Tang, D., Zhao, H., Xin, X. & Aisa, H.A. 2017. Hypoglycemic effect of the polyphenols rich extract from Rose rugosa Thunb on high fat diet and STZ induced diabetic rats. *Journal of Ethnopharmacology*, 200(October 2016): 174–181. <http://dx.doi.org/10.1016/j.jep.2017.02.022>.
- Lourens A, Van Vuuren S, Viljoen A, Davids H, V.H.F. 2011. Antimicrobial activity and in vitro cytotoxicity of selected South African *Helichrysum* species. *South African Journal of Botany*, 77(1): 229–235.
- Lourens, A.C.U., Reddy, D., Başer, K.H.C., Viljoen, A.M. & Van Vuuren, S.F. 2004. In vitro biological activity and essential oil composition of four indigenous South African *Helichrysum* species. *Journal of Ethnopharmacology*, 95(2–3): 253–258.
- Lourens, A.C.U., Viljoen, A.M. & van Heerden, F.R. 2008a. South African *Helichrysum* species: A review of the traditional uses, biological activity and phytochemistry. *Journal of Ethnopharmacology*, 119(3): 630–652.
- Lourens, A.C.U., Viljoen, A.M. & van Heerden, F.R. 2008b. South African *Helichrysum* species: A review of the traditional uses, biological activity and phytochemistry. *Journal of*

Ethnopharmacology, 119(3): 630–652.

- Lubbe, A., Seibert, I., Klimkait, T. & Van Der Kooy, F. 2012. Ethnopharmacology in overdrive: The remarkable anti-HIV activity of *Artemisia annua*. *Journal of Ethnopharmacology*, 141(3): 854–859. <http://dx.doi.org/10.1016/j.jep.2012.03.024>.
- Mabry, T.J., Markham, K.R. & Thomas, M.B. 1970. *The Systematic Identification of Flavonoids*.
- Mabry, T.J. & Ulubelen, A. 1980. Chemistry and Utilization of Phenylpropanoids Including Flavonoids, Coumarins, and Lignans. *Journal of Agricultural and Food Chemistry*, 28(2): 188–196.
- MacGregor, J.T. & Jurd, L. 1978. Mutagenicity of plant flavonoids: structural requirements for mutagenic activity in *Salmonella typhimurium*. *Mutation Research*, 54(3): 297–309.
- Magalhães, L.M., Segundo, M.A., Reis, S., Lima, J.L.F.C., Tóth, I. V. & Rangel, A.O.S.S. 2007. Automatic flow system for sequential determination of ABTS{radical dot}+ scavenging capacity and Folin-Ciocalteu index: A comparative study in food products. *Analytica Chimica Acta*, 592(2): 193–201.
- Malunga, L.N., Eck, P. & Beta, T. 2016. Inhibition of Intestinal α -Glucosidase and Glucose Absorption by Feruloylated Arabinoxylan Mono- and Oligosaccharides from Corn Bran and Wheat Aleurone. *Journal of Nutrition and Metabolism*, 2016.
- Manning, J. & Goldblatt, P. 2012. *Plants of The Greater Cape Floristic Region 1: The Core Cape Flora*.
- Manthey, J.A. & Buslig, B.S. eds. 1998. *Flavonoids in the living system*.
- Maridass, M. & De Britto, A.J. 2008. Origins of Plant Derived Medicines. *Ethnobotanical Leaflets*, 12: 373–387.
- Maroyi, A. 2019. Medical uses, biological and phytochemical properties of *Helichrysum Foetidum* (L.) Moench. (Asteraceae). , 12(7): 63–68.
- Mashigo, M., Combrinck, S., Regnier, T., Du Plooy, W., Augustyn, W. & Mokgalaka, N. 2015. Chemical variations, trichome structure and antifungal activities of essential oils of *Helichrysum splendidum* from South Africa. *South African Journal of Botany*, 96: 78–84. <http://dx.doi.org/10.1016/j.sajb.2014.10.006>.
- Merxmüller, H., Leins, P. & Roessler, H. 1977. Inuleae - systematic review. In: Heywood V. H., Harborne J. B., Turner B. L. (eds.). *The Biology and Chemistry of the Compositae*, 1: 577–602.
- Meyer, J.J.M. & Afolayan, A.J. 1995. Antibacterial activity of *Helichrysum aureonitens* (Asteraceae). *Journal of Ethnopharmacology*, 47: 109–111.
- Mezzitti, T., Orzalesi, G., Rossi, C. & Bellavita, V. 1970. New triterpenoids lactone, α -amyrin and uvaol from *Helichrysum italicum*. *Planta Medica*, 18(4): 326–331.
- Mhlongo, L.S. & Van Wyk, B.E. 2019. Zulu medicinal ethnobotany: new records from the Amandawe area of KwaZulu-Natal, South Africa. *South African Journal of Botany*, 122: 266–290. <https://doi.org/10.1016/j.sajb.2019.02.012>.
- Minaian, M., Ghassemi-Dehkordi, N. & Ahmadi, N. 2004. Anti-inflammatory effect of *Helichrysum oligocephalum* DC extract on acetic acid — Induced acute colitis in rats. *Advanced Biomedical Research*, 3(87).

- Minxuan, X., Sun, Y., Dai, X., Zhan, J., Long, T., Xiong, M., Li, H., Kuang, Q., Tang, T., Qin, Y., Chenxu, G. & Jun, T. 2019. Fisetin attenuates high fat diet-triggered hepatic lipid accumulation: A mechanism involving liver inflammation overload associated TACE/TNF- α pathway. *Journal of Functional Foods*, 53(August 2018): 7–21. <https://doi.org/10.1016/j.jff.2018.12.007>.
- Mmamoshedi, E. & Sibanda, M. 2016. African Traditional Medicine: South African Perspective. *Intech*: 5. <https://www.intechopen.com/books/advanced-biometric-technologies/liveness-detection-in-biometrics>.
- National Aids Treatment Advocacy Project. 2019. The absurdly high cost of insulin. http://www.natap.org/2019/HIV/052819_02.htm 19 December 2019.
- National Institute of Diabetes and Digestive and Kidney Diseases. 2016. Symptoms & Causes of Diabetes.
- Naveen, J. & Baskaran, V. 2018. Antidiabetic plant-derived nutraceuticals: a critical review. *European Journal of Nutrition*, 57(4): 1275–1299. <http://dx.doi.org/10.1007/s00394-017-1552-6>.
- Neuwinger, H.. 1996. Poisons and Drugs: Chemistry, Pharmacology, Toxicology . *African Ethnobotany*: 253–255.
- Njagi, J.M., Ngugi, M.P., Kibiti, C.M., Ngeranwa, J., Njue, W., Gathunmbi, P. & Njagi, E. 2015. Hypoglycemic Effect of *Lippia javanica* in Alloxan Induced Diabetic Mice. *Journal of Diabetes & Metabolism*, 6(11): 30–33.
- Odendaal, L.J., Haupt, T.M. & Griffiths, C.L. 2008. The alien invasive land snail *Theba pisana* in the West Coast National Park: Is there cause for concern? *Koedoe*, 50(1): 93–98.
- Oza, M.J. & Kulkarni, Y.A. 2018. Biochanin A improves insulin sensitivity and controls hyperglycemia in type 2 diabetes. *Biomedicine and Pharmacotherapy*, 107(August): 1119–1127. <https://doi.org/10.1016/j.biopha.2018.08.073>.
- Patel, D.K., Prasad, S.K., Kumar, R. & Hemalatha, S. 2012. An overview on antidiabetic medicinal plants having insulin mimetic property. *Asian Pacific Journal of Tropical Biomedicine*, 2(4): 320–330.
- Pietta, P.G. 2000. Flavonoids as antioxidants. *Journal of Natural Products*, 63(7): 1035–1042.
- Pooley, E. 2003. *Mountain Flowers: A Field Guide to the Flora of the Drakensberg and Lesotho*. 1st Editio. The Flora Publications Trust, Durban.
- Pratt, D.E. 1992. Antioxidants from Plant Material. In *Phenolic Compounds in Food and Their Effects on Health II*. 54–71.
- Proença, C., Freitas, M., Ribeiro, D., Oliveira, E.F.T., Sousa, J.L.C., Tomé, S.M., Ramos, M.J., Silva, A.M.S., Fernandes, P.A. & Fernandes, E. 2017. α -Glucosidase inhibition by flavonoids: an in vitro and in silico structure–activity relationship study. *Journal of Enzyme Inhibition and Medicinal Chemistry*, 32(1): 1216–1228. <https://doi.org/10.1080/14756366.2017.1368503>.
- Proença, C., Freitas, M., Ribeiro, D., Tomé, S.M., Oliveira, E.F.T., Viegas, M.F., Araújo, A.N., Ramos, M.J., Silva, A.M.S., Fernandes, P.A. & Fernandes, E. 2019. Evaluation of a flavonoids library for inhibition of pancreatic α -amylase towards a structure–activity relationship. *Journal of Enzyme Inhibition and Medicinal Chemistry*, 34(1): 577–588. <https://doi.org/10.1080/14756366.2018.1558221>.

- Van Puyvelde, L., De Kimpe, N., Costa, J., Munyjabo, V., Nyirankuliza, S., Hakizamungu, E. & Schamp, N. 1989. Isolation of flavonoids and a chalcone from *Helichrysum odoratissimum* and synthesis of helichrysetin. *Journal of Natural Products*, 52(3): 629–633.
- Randriaminahy, M., Proksch, P., Witte, L. & Wray, V. 1992. Lipophilic phenolic constituents from *Helichrysum* species endemic to Madagascar. *Journal of Bioscience*, 47(1–2): 10–16.
- Reeg, S. & Grune, T. 2015. Protein Oxidation in Aging: Does It Play a Role in Aging Progression? *Antioxidants and Redox Signaling*, 23(3): 239–255.
- Rees, A., Levy, M. & Lansdown, A. 2017. *Clinical Endocrinology and Diabetes at a Glance*. John Wiley & Sons.
- Rekha, S.S., Pradeepkiran, J.A. & Bhaskar, M. 2019. Bioflavonoid hesperidin possesses the anti-hyperglycemic and hypolipidemic property in STZ induced diabetic myocardial infarction (DMI) in male Wistar rats. *Journal of Nutrition and Intermediary Metabolism*, 15(December 2018): 58–64. <https://doi.org/10.1016/j.jnim.2018.12.004>.
- Ren, B., Qin, W., Wu, F., Wang, S., Pan, C., Wang, L., Zeng, B., Ma, S. & Liang, J. 2016. Apigenin and naringenin regulate glucose and lipid metabolism, and ameliorate vascular dysfunction in type 2 diabetic rats. *European Journal of Pharmacology*, 773(201010267636): 13–23. <http://dx.doi.org/10.1016/j.ejphar.2016.01.002>.
- Ross, J.A. & Kasum, C.M. 2002. DIETARY FLAVONOIDS : Bioavailability, Metabolic Effects, and Safety. *Annual Review of Nutrition*, 22(1): 19–34.
- Rufino, M., Fernandes, F., Alves, R. & E, B. 2009. Free radical-scavenging behaviour of some north-east Brazilian fruits in a DPPH system. *Food Chemistry*, 114(2): 693–695.
- Saeedi, P., Petersohn, I., Salpea, P., Malanda, B., Karuranga, S., Unwin, N., Colagiuri, S., Guariguata, L., Motala, A., Ogurtsova, K., Shaw, J., Bright, D. & Williams, R. 2019. Global and regional diabetes prevalence estimates for 2019 and projections for 2030 and 2045: Results from the International Diabetes Federation Diabetes Atlas, 9th edition. *Diabetes Research and Clinical Practice*, 157: 107843.
- Sala, A., Recio, M., Giner, R.M., Máñez, S., Tournier, H., Schinella, G. & Ríos, J.L. 2002. Anti-inflammatory and antioxidant properties of *Helichrysum italicum*. *Journal of Pharmacy and Pharmacology*, 54(3): 365–371.
- Samie, A., Sedaghat, R., Baluchnejadmojarad, T. & Roghani, M. 2018. Hesperetin, a citrus flavonoid, attenuates testicular damage in diabetic rats via inhibition of oxidative stress, inflammation, and apoptosis. *Life Sciences*, 210(March): 132–139. <https://doi.org/10.1016/j.lfs.2018.08.074>.
- Sánchez-Rangel, J.C., Benavides, J., Heredia, J.B., Cisneros-Zevallos, L. & Jacobo-Velázquez, D.A. 2013. The Folin–Ciocalteu assay revisited: improvement of its specificity for total phenolic content determination. *Analytical Methods*, (21).
- Sarian, M.N., Ahmed, Q.U., Mat So'Ad, S.Z., Alhassan, A.M., Murugesu, S., Perumal, V., Syed Mohamad, S.N.A., Khatib, A. & Latip, J. 2017. Antioxidant and antidiabetic effects of flavonoids: A structure-activity relationship based study. *BioMed Research International*, 2017.
- Schrader, M. & Fahimi, H.D. 2006. Peroxisomes and oxidative stress. *Biochimica et Biophysica Acta (BBA) - Molecular Cell Research*, 1763(12): 1755–1766.

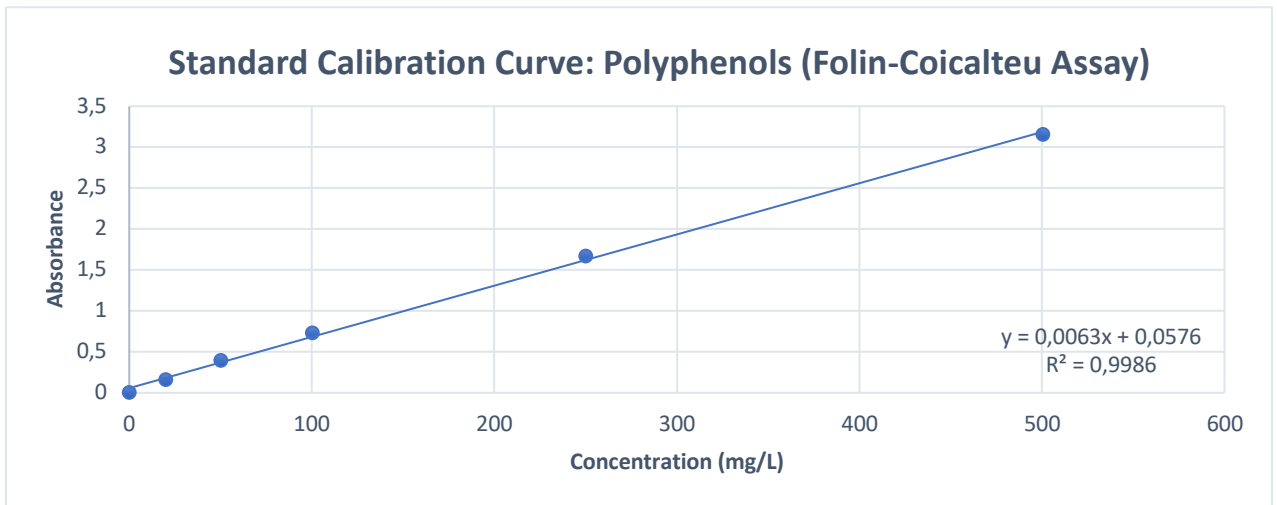
- Scott, G. & Hewett, M.L. 2008. Pioneers in ethnopharmacology: The Dutch East India Company (VOC) at the Cape from 1650 to 1800. *Journal of Ethnopharmacology*, 115: 339–360.
- Sechi, M., Syed, D.N., Pala, N., Mariani, A., Marceddu, S., Brunetti, A., Mukhtar, H. & Sanna, V. 2016. Nanoencapsulation of dietary flavonoid fisetin: Formulation and in vitro antioxidant and α -glucosidase inhibition activities. *Materials Science and Engineering C*, 68: 594–602. <http://dx.doi.org/10.1016/j.msec.2016.06.042>.
- Sell, P. & Murrell, G. 2006. *Flora of Great Britain and Ireland*.
- Shahidi, F., Janitha, P.K. & Wanasundara, P.D. 1992. Phenolic Antioxidants. *Critical Reviews in Food Science and Nutrition*, 32(1): 67–103.
- Shin, J., Han, M.J. & Kim, D. 2003. 3-Methylethergalangin Isolated from *Alpinia officinarum* Inhibits Pancreatic Lipase. *Biological and Pharmaceutical Bulletin*, 26(6): 854–857.
- Soobrattee, M.A., Neergheen, V.S., Luximon-Ramma, A., Aruoma, O.I. & Bahorun, T. 2005. Phenolics as potential antioxidant therapeutic agents: mechanism and actions. *Mutation Research/Fundamental and Molecular Mechanisms of Mutagenesis*, 579(1–2): 200–213.
- Stupar, M., Milica, L.G., Dzamic, A., Unković, N., Mihailo, R. & Vukojevic, J. 2014. Antifungal activity of *Helichrysum italicum* (Roth) G. Don (Asteraceae) essential oil against fungi isolated from cultural heritage objects. *Archives of Biological Sciences*, 66: 1539–1545.
- Subramoniam, A. 2016. *Plants with Anti-Diabetes Mellitus Properties*.
- Sutthanut, K., Sripanidkulchai, B., Yenjai, C. & Jay, M. 2007. Simultaneous identification and quantitation of 11 flavonoid constituents in *Kaempferia parviflora* by gas chromatography. *Journal of Chromatography A*, 1143(1–2): 227–233.
- Süzgeç-Selçuk, S. & Birteksöz, A.S. 2011. Flavonoids of *Helichrysum chasmolycicum* and its antioxidant and antimicrobial activities. *South African Journal of Botany*, 77(1): 170–174. <http://dx.doi.org/10.1016/j.sajb.2010.07.017>.
- Süzgeç, S., Meriçli, A.H., Houghton, P.J. & Çubukçu, B. 2005. Flavonoids of *Helichrysum compactum* and their antioxidant and antibacterial activity. *Fitoterapia*, 76(2): 269–272.
- Szmulowicz, E.D., Josefson, J.L. & Metzger, B.E. 2019. Gestational Diabetes Mellitus. *Endocrinology and Metabolism Clinics of North America*.
- Szymanska, R., Pospíšil, P. & Kruk, J. 2018. Plant-Derived Antioxidants in Disease Prevention 2018. *Oxidative Medicine and Cellular Longevity*, 2018: 2.
- Tagliatalata-Scafati, O., Pollastro, F., Chianese, G., Minassi, A., Gibbons, S., Arunotayanun, W., Mabebie, B., Ballero, M. & Appendino, G. 2013. Antimicrobial phenolics and unusual glycerides from *Helichrysum italicum* subsp. *microphyllum*. *Journal of Natural Products*, 76(3): 346–353.
- Tamokou, J. de D., Mbaveng, A.T. & Kuete, V. 2017. *Antimicrobial Activities of African Medicinal Spices and Vegetables*. Elsevier Inc. <http://dx.doi.org/10.1016/B978-0-12-809286-6/00008-X>.
- Tomas-Barberan, F.A., Msonthi, J.D. & Hostettmann, K. 1988. Antifungal epicuticular methylated flavonoids from *Helichrysum nitens*. *Phytochemistry*, 27(3): 753–755.
- Tomás-Lorente, F., Iniesta-Sanmartín, E., Tomás-Barberán, F.A., Trowitzsch-Kienast, W. & Wray, V. 1989. Antifungal phloroglucinol derivatives and lipophilic flavonoids from

- Helichrysum decumbens*. *Phytochemistry*, 28(6): 1613–1615.
- Tundis, R., Loizzo, M.R. & Menichini, F. 2010. Natural products as alpha-amylase and alpha-glucosidase inhibitors and their hypoglycaemic potential in the treatment of diabetes: an update. *Mini-Reviews in Medicinal Chemistry*, 10(4): 315–331.
- Turner, R.C., Holman, R.R., Matthews, D., Hockaday, T.D.R. & Peto, J. 1979. Insulin deficiency and insulin resistance interaction in diabetes: estimation of their relative contribution by feedback analysis from basal plasma insulin and glucose concentrations. *Metabolism*, 28: 1086–1096.
- Ursini, F., Maiorino, M., Morazzoni, P., Roveri, A. & Pifferi, G. 1994. A novel antioxidant flavonoid (IdB 1031) affecting molecular mechanisms of cellular activation. *Free Radical Biology and Medicine*, 16(5): 547–553.
- Velu, G., Palanichamy, V. & Rajan, A.P. 2018. Bioorganic Phase in Natural Food: An Overview. In pp.135-156.
- Vrkoc, J., Dolejs, L. & Budesinsky, M. 1975. Methylene-bis-2H-pyran-2-ones and phenolic constituents from the root of *Helichrysum arenarium*. *Phytochemistry*, 14(5–6): 1383–1384.
- van Vuuren, S.F., Başerd, C., Viljoen, A.M., Hüsnü, K., van Zyl, R.L. & van Heerden, F.R. 2006. The antimicrobial, antimalarial and toxicity profiles of helihumulone, leaf essential oil and extracts of *Helichrysum cymosum* (L.) D. Don subsp. *cymosum*. *South African Journal of Botany*, 72(2): 287–290.
- Wahbeh, G.T. & Christie, D.L. 2011. *Pediatric Gastrointestinal and Liver Disease*. 4th Editio.
- Walker, J. 1996. *Wild Flowers of KwaZulu Natal*. Pinetown.
- Wang, J., Gao, H., Zhao, J., Wang, Q., Zhou, L., Han, J., Yu, Z. & Yang, F. 2010. Preparative separation of phenolic compounds from *Halimodendron halodendron* by high-speed counter-current chromatography. *Molecules*, 15(9): 5998–6007.
- Wang, Y., Chen, S. & Yu, O. 2011. Metabolic engineering of flavonoids in plants and microorganisms. *Applied Microbiology and Biotechnology*, 91(4): 949–956.
- Wass, J., Owen, K. & Turner, H. 2014. Oxford Handbook of Endocrinology and Diabetes. *Oxford Handbook of Endocrinology and Diabetes*: 684–687.
- Watt, J.M. & Breyer-Brandwijk, M.G. 1962. *The Medicinal and Poisonous Plants of Southern and Eastern Africa*. 2nd Editio. Livingstone, London.
- WHO. 2012. *WHO Position Statement: Effectiveness of Non-Pharmaceutical Forms of Artemisia annua against malaria*. http://www.who.int/malaria/publications/atoz/position_statement_herbal_remedy_artemisia_annua_/en/.
- Winde, A. 2020. Coronavirus COVID-19 Western Cape government approach. *South African Government*. <https://www.gov.za/speeches/premier-alan-winde-coronavirus-covid-19-western-cape-government-approach-7-may-2020-0000> 13 May 2020.
- Wubshet, S.G., Moresco, H.H., Tahtah, Y., Brighente, I.M.C. & Staerk, D. 2015. High-resolution bioactivity profiling combined with HPLC-HRMS-SPE-NMR: α -Glucosidase inhibitors and acetylated ellagic acid rhamnosides from *Myrcia palustris* DC. (Myrtaceae). *Phytochemistry*, 116(1): 246–252. <http://dx.doi.org/10.1016/j.phytochem.2015.04.004>.
- Van Wyk, B.E. & Gericke, N. 2000. *People's Plants. A guide to useful plants of Southern Africa*.

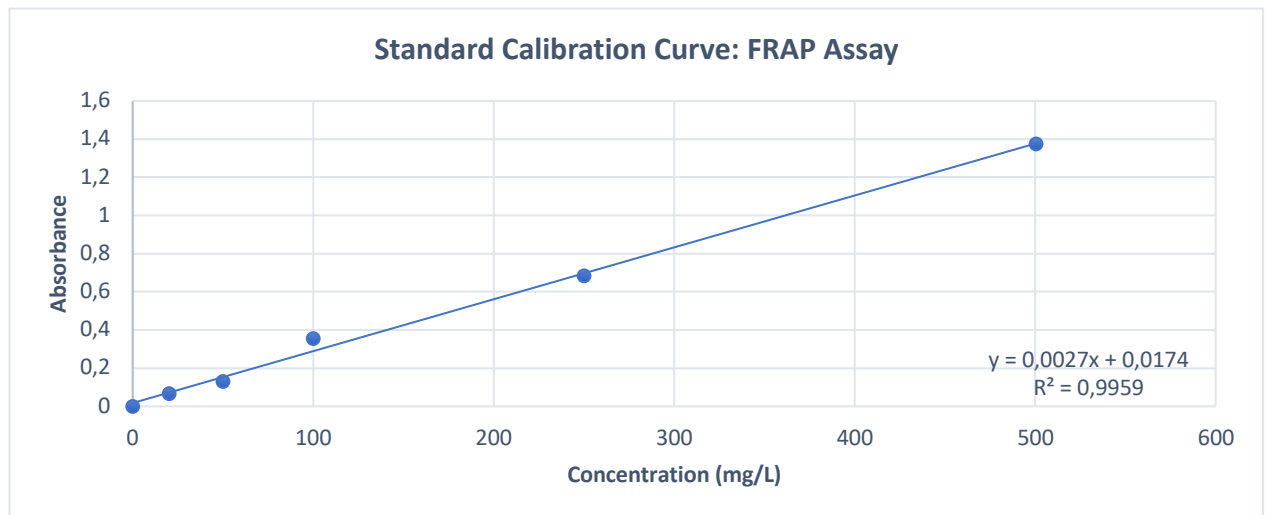
1st ed.

- Van Wyk, B.E., Van Oudtshoorn, B. & Gericke, N. 1997. *Medicinal Plants of South Africa*.
- Xie, Y., Yang, W., Tang, F., Chen, X. & Ren, L. 2015. Antibacterial activities of flavonoids: structure-activity relationship and mechanism. *Current Medicinal Chemistry*, 22(1): 132–149.
- Xu, D.-P., Li, Y., Meng, X., Zhou, T., Zhou, Y., Zheng, J., Zhang, J.-J. & Li, H.-B. 2017. Natural Antioxidants in Foods and Medicinal Plants: Extraction, Assessment and Resources. *International Journal of Molecular Sciences*, 19(1): 96.
- Xu, J., Li, Y., Lou, M., Xia, W., Liu, Q., Xie, G., Liu, L., Liu, B., Yang, J. & Qin, M. 2018. Baicalin regulates SirT1/STAT3 pathway and restrains excessive hepatic glucose production. *Pharmacological Research*, 136(August): 62–73.
- Yin, Z., Zhang, W., Feng, F., Zhang, Y. & Kang, W. 2014. α -Glucosidase inhibitors isolated from medicinal plants. *Food Science and Human Wellness*, 3(3–4): 136–174. <http://dx.doi.org/10.1016/j.fshw.2014.11.003>.
- Yoon, J.-W.Y. & Jun, H.-S.J. 2005. Autoimmune Destruction of Pancreatic β Cells. *American Journal of Therapeutics*, 12(6): 580–591.
- Zanetsie Kakam, A.M., Franke, K., Ndom, J.C., Dongo, E., Mpondo, T.N. & Wessjohann, L.A. 2011. Secondary metabolites from *Helichrysum foetidum* and their chemotaxonomic significance. *Biochemical Systematics and Ecology*, 39(2): 166–167. <http://dx.doi.org/10.1016/j.bse.2011.02.005>.
- Zeka, K., Alfa, H.H., Ruparelia, K.C. & Arroo, R.R.J. 2019. *Use of natural products in the prevention and management of type 2 diabetes*. 1st ed. Elsevier Inc. <http://dx.doi.org/10.1016/B978-0-12-817901-7.00007-1>.
- Zhong, Y. & Shahidi, F. 2015. Methods for the assessment of antioxidant activity in foods. *Food Science, Technology and Nutrition*: 287–333.
- Ziaratnia, S.M., Ohyama, K., Hussein, A.A.F., Muranaka, T., Lall, N., Kunert, K.J. & Meyer, J.J.M. 2009. Isolation and identification of a novel chlorophenol from a cell suspension culture of *Helichrysum aureonitens*. *Chemical and Pharmaceutical Bulletin*, 57(11): 1282–1283.

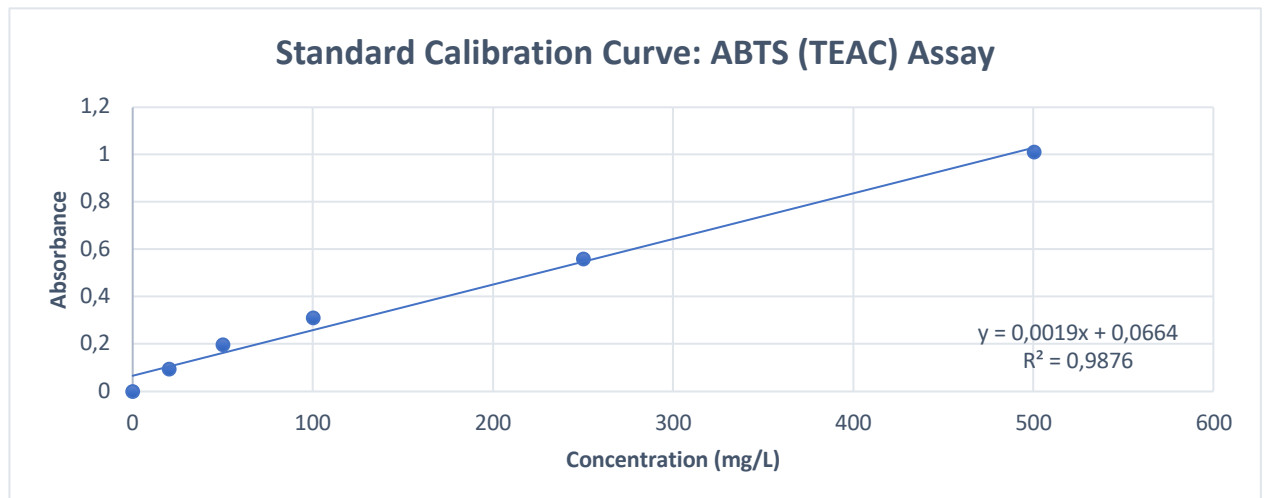
APPENDIX



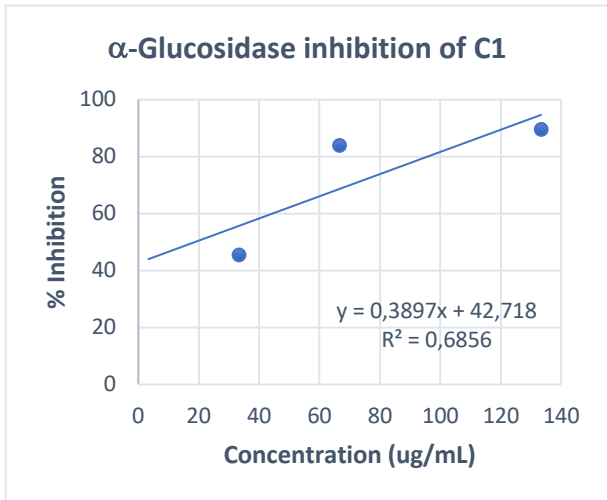
Appendix 1: Standard calibration curve - Polyphenols (Folin-Coicalteu assay)



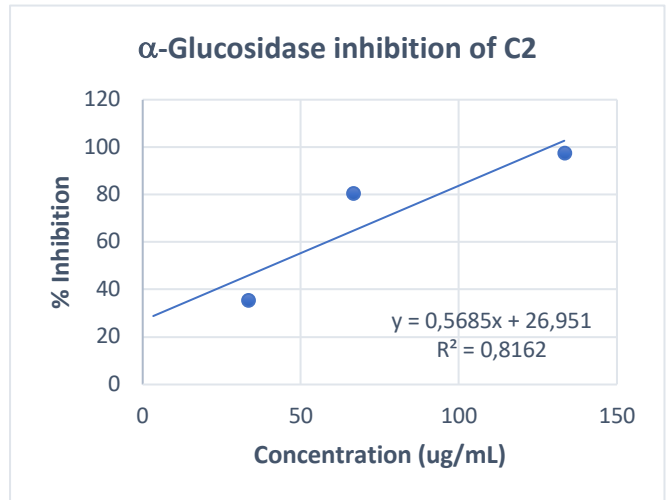
Appendix 2: Standard calibration curve - FRAP assay



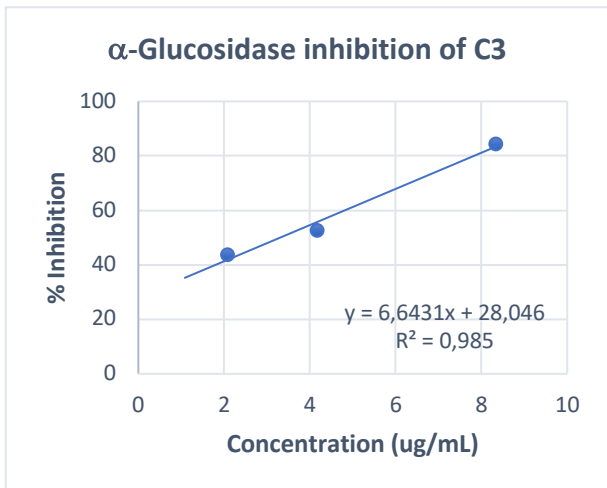
Appendix 3: Standard calibration curve - ABTS (TEAC) assay



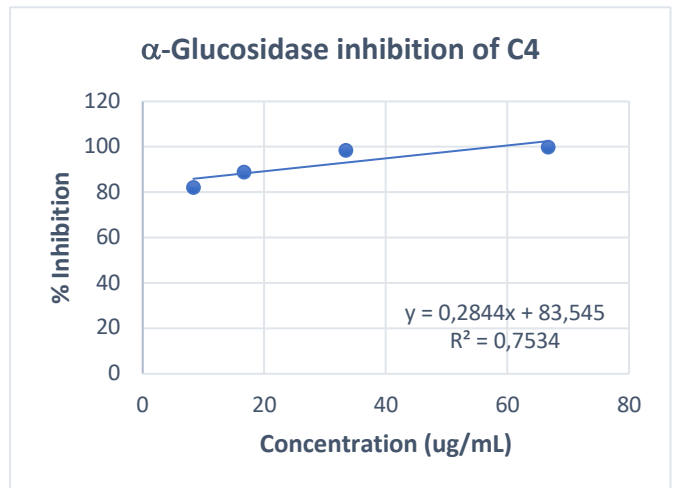
Appendix 4: α-Glucosidase inhibition curve of C1



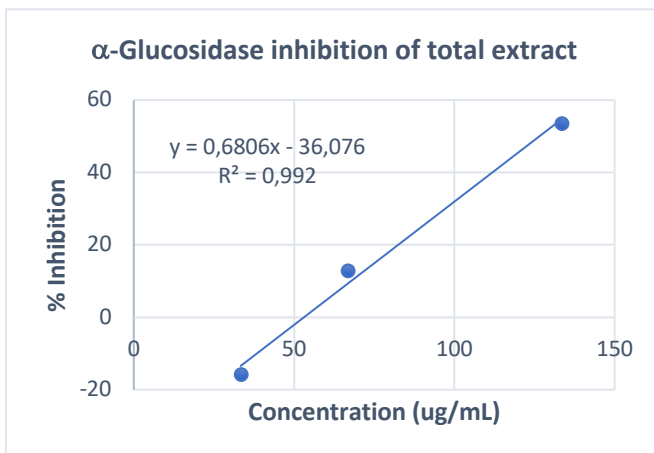
Appendix 5: α-Glucosidase inhibition curve of C2



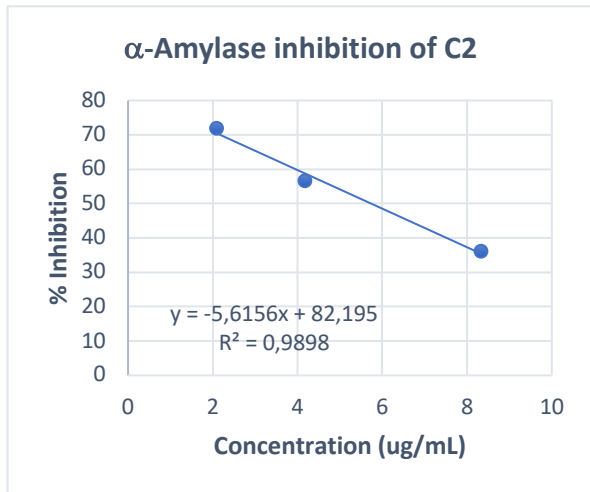
Appendix 6: α-Glucosidase inhibition curve of C3



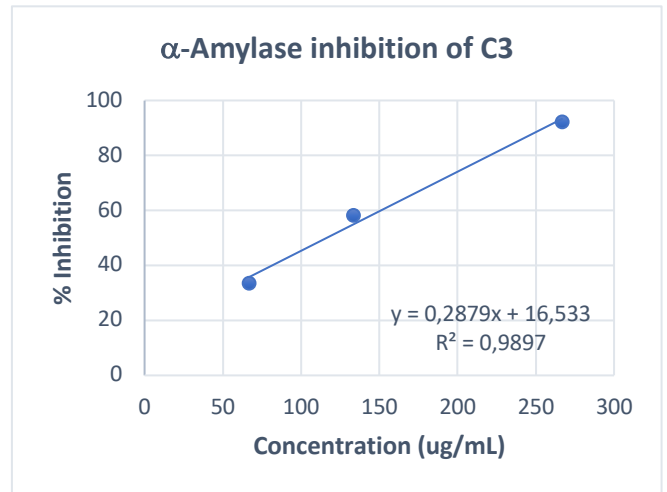
Appendix 7: α-Glucosidase inhibition curve of C4



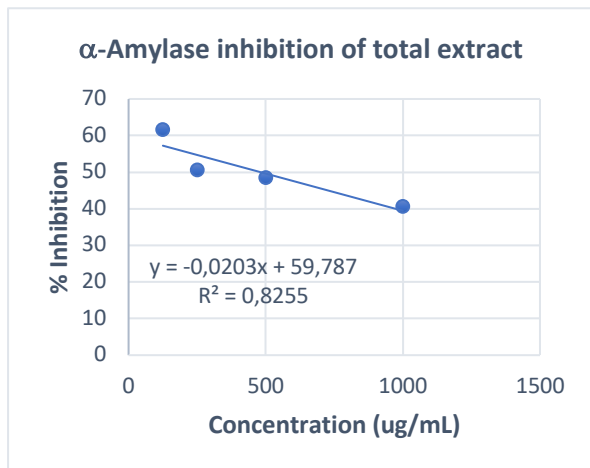
Appendix 9: α-Glucosidase inhibition curve of total extract



Appendix 10: α-Amylase inhibition curve of C2



Appendix 11: α-Amylase inhibition curve of C3



Appendix 12: α-Amylase inhibition curve of total extract